THE EFFECTS OF EARLY POSTNATAL ETHANOL INTOXICATION ON RETINA GANGLION CELL MORPHOLOGY AND THE DEVELOPMENT OF RETINO-GENICULATE PROJECTIONS IN MICE

A THESIS SUBMITTED TO

THE GRADUATE SCHOOL OF NATURAL AND APPLIED SCIENCES

OF

MIDDLE EAST TECHNICAL UNIVERSITY

BY

İLKNUR DURSUN

IN PARTIAL FULFILLMENT OF THE REQUIREMENTS
FOR
THE DEGREE OF DOCTOR OF PHILOSOPHY
IN
DEPARTMENT OF BIOLOGICAL SCIENCES

FEBRUARY 2011

Approval of the thesis:

THE EFFECTS OF EARLY POSTNATAL ETHANOL INTOXICATION ON RETINA GANGLION CELL MORPHOLOGY AND THE DEVELOPMENT OF RETINO-GENICULATE PROJECTIONS IN MICE

submitted by **İLKNUR DURSUN** in partial fulfillment of the requirements for the degree of **Doctor of Philosophy in Department of Biological Sciences, Middle East Technical University** by,

Prof. Dr. Canan Özgen _____
Dean, Graduate School of **Natural and Applied Sciences**

Prof. Dr. Musa Doğan _____
Head of Department, **Biological Sciences Dept., METU**

Assoc. Prof. Dr. Ewa Jakubowska Doğru _____
Supervisor, **Biological Sciences Dept., METU**

Examining Committee Members

Prof. Dr. Tayfun Uzbay _____
Medical Pharmacology Dept., GMMA

Assoc. Prof. Dr. Ewa Jakubowska Doğru _____
Biological Sciences Dept., METU

Prof. Dr. Hüseyin Avni Öktem _____
Biological Sciences Dept., METU

Prof. Dr. Emin Öztaş _____
Medical Histology & Embryology Dept., GMMA

Assoc. Prof. Dr. Sinan Canan _____
Physiology Dept., TÖU

Date: 11.02.2011

I hereby declare that all information in this document has been obtained and presented in accordance with academic rules and ethical conduct. I also declare that, as required by these rules and conduct, I have fully cited and referenced all material and results that are not original to this work.

Name, Last name: İLKNUR DURSUN

Signature:

ABSTRACT

THE EFFECTS OF EARLY POSTNATAL ETHANOL INTOXICATION ON RETINA GANGLION CELL MORPHOLOGY AND THE DEVELOPMENT OF RETINO-GENICULATE PROJECTIONS IN MICE

Dursun, İlknur

Ph.D., Department of Biological Sciences

Supervisor: Assoc. Prof. Dr. Ewa Jakubowska Doğru

February 2011, 149 pages

Experimental and clinical data have documented the adverse effects of perinatal ethanol intoxication on peripheral organs and the central nervous system. There is little known, however, about potential damaging effects of perinatal ethanol on the developing visual system. The purpose of this study was to examine the effects of neonatal ethanol intoxication on RGC morphology, estimate the total number of neurons in RGC layer and dorsolateral geniculate nucleus (dLGN), and on the eye-specific fiber segregation in the dLGN), in YFP and C57BL/6 mice pups. Ethanol (3 g/kg/day) was administered by intragastric intubation throughout postnatal days (PD) 3-20 or 3-10. Intubation control (IC) and untreated control (C) groups were included. Blood alcohol concentration (BAC) was measured in separate groups of pups on PD3, PD10, and PD20 at 4 different time points, 1, 1.5, 2 and 3 h after the second intubation. Numbers neurons in the RGCs and dLGN were quantified on PD10, PD20 using unbiased stereological procedures. The RGC images were taken using a confocal microscope and images were traced using Neurolucida software. On PD9, intraocular injections of cholera toxin-β (CTB) conjugated to Alexa 488 (green) or 594 (red) were administrated to the left and right eye, respectively. Measurements of the dLGN areas receiving projections from the

contralateral and ipsilateral eye were determined by using Image J (Image J, NIH). The early postnatal ethanol intoxication altered RGC morphology. Out of 13 morphological parameters examined in RGCs, soma area and dendritic field diameter were significantly reduced, while branch angles and dendrite tortuosity were increased. Additionally, a significant loss of RGCs and neurons in the dLGN was recorded at P20. The pixel intensity of total area and ipsilateral of retino-genuculate projection in the A group was significantly smaller as compared to the C group.

Keywords: early postnatal ethanol, mice, Retinal ganglion cell (RGC) morphology, stereological cell counts, Retino-Geniculate Projections

ÖZ

DOĞUM SONRASI DÖNEMDE ETANOLÜN RETİNA GANGLİON HÜCRELERİ VE RETİNA GENİKULAT PROJEKSİYONLARINI GELİŞİMİ ÜZERİNDEKİ TOKSİK ETKİLERİ

Dursun, İlknur

Doktora, Biyolojik Bilimler Bölümü

Tez Yöneticisi: Doç. Dr. Ewa Jakubowska Doğru

Şubat 2011, 149 sayfa

Deneysel ve klinik çalışmalar, doğum öncesi ve/veya sonrası dönemde alınan etanolün toksik etkilerinin periferal organlar ve merkezi sinir sistemi üzerindeki olumsuz etkilerini rapor etmiştir. Fakat, bu dönemde alınan etanolün, gelişmekte olan görme sistemi üzerindeki zarar verici etkileri hakkında az bilgi mevcuttur. Bu çalışmanın amacı, doğum sonrası dönemde etanole maruz kalmış YFP ve C57BL/6 farelerde etanolün toksik etkilerinin retina gangliyon hücre (RGC) morfolojisi ile retina ve lateral genikulat nükleusdaki (dLGN) toplam nöron sayısı ve retinadan gelen aksonların dorsal lateral genikulat nükleusa projeksiyoları üzerindeki etkilerini araştırmaktır. Etanol (A), intübasyon kontrol grubu (IC) ve hiçbir müdahaleye maruz kalmamış kontrol (C) grubu olmak üzere üç farklı grup bulunmaktadır. Etanol doğumdan sonra 3 ile 20 (PD3-20) ya da 3 ile 10 (PD3-10) günleri arasında 3g/ kg vücut ağırlığı/ gün dozunda alkol besleme hortumu yoluyla doğrudan mideye verilmiştir. Kandaki alkol konsantrasyonu ayrı bir grup üzerinde PD3,PD10 ve P20 günlerinde; 2. intübasyondan 1, 1.5, 2 ve 3 saat sonra ölçülmüştür. RGC tabakasındaki ve dLGN'deki toplam nöron sayısı tarafsız stereolojik yöntemi kullanarak PD10 ve PD20 günlerde hesaplanmıştır. RGC görüntüleri konfokal mikroskop kullanılarak çekilmiş ve çekilen görüntüler Neurolucida yazılımı ile değerlendirilmiştir. PD9 gününde kolera toksin-β (CTB) ile birleşmiş Alexa 488 (yeşil)

floresan boyası sol, Alexa 594 (kırmızı) floresan boyası sağ göz içine enjekte edilmiştir. Gözden gelen kontralateral ve ipsilateral projeksiyonların dLGN bölgesindeki uzantıları Image J (NIH) programı kullanılarak ölçülmüştür. Bu çalışmada, doğum sonrasında maruz kalınan etanolün RGC morfolojisini değiştirdiği gözlemlenmiştir. Araştırılan 13 morfolojik parametreden RGC soma alanında, dendritik bölge çapında istatistiksel olarak anlamlı azalma, dallanma açısı ve dendrit kıvrımlarında ise artma bulunmuştur. Ayrıca, P20 gününde bakılan RGC tabakasındaki ve dLGN'deki toplam nöron sayısında anlamlı azalma kaydedilmiştir. A grubundaki dLGN toplam alan piksel yoğunluğu ile ipsilateral projeksiyonunun piksel yoğunluğu C grubuna göre daha küçük olduğu gözlemlenmiştir.

Anahtar Kelimeler: doğum sonrası etanol, fare, retinal ganglion hücre (RGC) morfolojisi, stereolojik hücre sayımı, retino- genikulat projeksiyonu

Canım Annem'e

ACKNOWLEDGMENTS

I would like to express my deepest gratitude to my supervisor Assoc. Prof. Dr. Ewa Jakubowska Doğru for her guidance, advice, encouragement and patience.

I am very grateful to Prof. Dr. Leo M. Chalupa and Prof. Dr. Robert F. Berman for providing scientific guidance and for giving me an opportunity to use the facilities at UCDavis Department of Neurobiology, Physiology and Behavior, Center for Neuroscience & Department of Neurological Surgery to complete all of the experimental work related with this project.

I also want to say thank you to all the staff at Prof. Dr. Chalupa's and Prof. Dr. Berman's laboratory the great help, hospitality and friendship they provided me at all stages of these experiments.

I would like to thank to the members of my thesis examining committee, Prof. Dr. Tayfun Uzbay, Prof. Dr. Hüseyin Avni Öktem, Prof. Dr. Emin Öztaş and Assoc. Prof. Dr. Sinan Canan for their suggestions and constructive criticism.

I would like to thank Prof. Dr. Charles R. Goodlett for his assistance in assessment of BACs, and Prof. Dr. Sandra J Kelly for the help with the liquid diet formulation. I also thank Dr. Kyoungmi Kim for helpful advices concerning the statistical analysis of the data, and Dr. Jurgen Wenzel for his guidance on histology.

Very special thank to Münevver Gün and Evrim & Serdar Zeybek for their support, love and friendship.

Special thank to Margot & Marcus Clark, my all friends in Davis, CA and my labmates in METU for their support and frendship.

I am forever indebted to my family. I always felt their motivation at every stage of my life. I would like to send all my love and appreciation to my father Binali Dursun for his endless love, thrust and support. Mom, I miss you. You will always be with me in my hearth. I will always do my best to make you proud of me. I would like also to send my all love my nephew Uğur and my niece Zeynep.

This research was supported by grants from the National Eye Institute of the NIH EY003991 and P30EY12576 to Prof. Dr. Leo M. Chalupa and partially by the METU research fund BAP-08-11-DPT-2002-K120510.

TABLE OF CONTENTS

LIST OF TABLES

LIST OF FIGURES

LIST OF ABBREVIATIONS

A ..... Alcohol Group
ARBD..... Alcohol-Related Birth Defects
ARND ..... Alcohol-Related Neurodevelopmental Disorder
BAC..... Blood Alcohol Concentration
BC ..... Bipolar Cells
C ..... Control Group
°C ..... Degree Celsius
CNS ..... Central Nervous System
CTB ..... Cholera Toxin-β
$CuSO_4$ ..... Copper sulfate
DAPI ..... 4'-6-Diamidino-2-phenylindole
dLGN..... dorsal Lateral Geniculate Nucleus
E ..... Embryonic Day
EDC..... Ethanol Derived Calories
EtOH ..... Ethanol
$FeSO_4$ ..... Iron sulfate
FAE ..... Fetal Alcohol Effect
FAS ..... Fetal Alcohol Syndrome
FASD..... Fetal Alcohol Spectrum Disorders
GCL..... Ganglion Cell Layer
HC ..... Horizontal Cells
IC..... Intubation Control Group
INL ..... Inner Nuclear Layer
IP ..... Intraperitoneal
IPL..... Inner Plexiform Layer
g..... gram

GD ..... Gestational Day

h..... hour

H_2O..... Water

KCl ..... Potassium Chloride

M ..... Molar

MgCl ..... Magnesium Chloride

mg..... milligram

ml..... milliliter

µl ..... microliter

µm ..... micrometer

Na ..... Sodium

nm..... nanometer

ONL..... Outer Nuclear Layer

OPL ..... Outer Plexiform Layer

PB..... Phosphate Buffer

PBS..... Phosphate Buffered Saline

PFA ..... Paraformaldehyde

PD..... Postnatal Day

RGC..... Retina Ganglion Cell

RPC ..... Retinal Progenitor Cell

RPE ..... Retinal Pigment Epithelium

rpm ..... revolutions per minute

sec..... second

SEM..... Standard Error of Means

SPSS ..... Statistical Package for the Social Sciences

Thy-1 ..... Thymus Cell Antigen 1

YFP ..... Yellow Fluorescent Protein

$ZnSO_4$ ..... Zinc sulfate

CHAPTER 1

INTRODUCTION

1.1. Fetal Alcohol Syndrome

Several drugs and chemicals are identified to be teratogenic to the human embryo when administered during pregnancy, particularly during the period of organogenesis. Alcohol is a well-known human teratogen, have an effect on a variety of organ systems in both humans and laboratory animals. As a teratogen, alcohol is able of directly cause developmental abnormalities in a fetus. Alcohol is lipid soluble and thus rapidly absorbed from the stomach and gastrointestinal tract following ingestion, and is evenly distributed throughout the fluids and tissues of the body and brain. It is also able to freely cross the placental barrier producing approximately equal maternal and fetal blood alcohol concentrations (BACs) (Waltman and Iniquez, 1972). Birth defects due to maternal alcohol consumption during pregnancy have been first reported in the medical literature by Lemoine *et al.*, in 1968 and described as Fetal Alcohol Syndrome (FAS) by Jones and Smith, in 1973.

Maternal alcohol exposure during pregnancy results in a spectrum of growth and mental deficiences, structural anomalies, behavioral and neurocognitive disabilities, collectively termed fetal alcohol spectrum disorders (FASD). FAS is the most severe condition and clinically recognizable form of FASD and is characterized by a pattern of minor facial anomalies, prenatal and postnatal growth retardation, and functional or structural central nervous system (CNS) abnormalities (Hoyme *et al.*, 2005, Wattendorf and Muenke, 2005). The term fetal alcohol effects (FAE) has been previously used to describe cases

in which children exposed to alcohol prenatally do not meet all three of the diagnostic criteria of FAS. In 1996, the Institute of Medicine (IOM) replaced FAE with the terms alcohol-related neurodevelopmental disorder (ARND) and alcohol-related birth defects (ARBD) (Warren and Foudin, 2001). More recently, three terms have been developed to characterize children who were affected by alcohol prenatally but not meet all criteria for FAS. The term "partial FAS" refers to children with confirmed prenatal alcohol exposure and characteristic facial anomalies without full FAS. The term "alcohol-related birth defects" (ARBD) is used for children who have physical malformations or physiological abnormalities. Finally, the term "alcohol-related neurodevelopmental disorder" (ARND) describes children with either physical CNS abnormalities (i.e., smaller head size or structural brain abnormalities) or with behavioral and/or cognitive abnormalities, such as deficits in memory, language skills or learning abilities (Stratton *et al.,* 1996). Children exposed to prenatal alcohol abuse require special treatment. Therefore consumption of alcohol during pregnancy is an issue of widespread public concern. Today, FAS is considered the most common nonhereditary cause of mental retardation.

1.1.1. Animal Models of Human FAE /FAS

Legal and ethical constraints on research with humans create the need for animal models to determine the effects of perinatal (prenatal and early postnatal) alcohol exposure. Research on developmental and neurobehavioral effects of perinatal alcohol exposure aims better understanding the biological, molecular basis of the syndrome. Studies on alcohol effects using animal models are important for designing more effective therapies of alcohol related dysfunctions in humans. Animal models also provide an insight to the potential role of nutritional, environmental, and genetic factors in alcohol intoxication (Kelly *et al.,* 2009).

Among different animal species, rodents and particularly rats and mice have been most widely used in modeling fetal alcohol effects mainly because of the ease of handling, short gestation period and relatively low cost to purchase, house and feed (Keane and Leonard, 1989). The mechanisms of alcohol metabolism were shown to be similar in humans and rodents, with the exception that rodents as small endotherms have faster metabolic rate than human and, therefore, metabolize alcohol more quickly.

Several factors (independent variables) appear to contribute to the behavioral specificity of the neurotoxic effects of in utero or after birth alcohol exposure, including: alcohol dosage, timing and duration of gestational exposure, pattern and route of administration, gender and age of assessment of ethanol effects. It is also well known that genetic factors also play a considerable role in animals' susceptibility to ethanol effects. Kiianmaa and Tabakoff (1983) demonstrated that different strains of mice show different tolerance to the sedative effects of alcohol.

Neither the minimum alcohol dose required to produce deficits nor the amount, or period during which alcohol that can be "safely" consumed during pregnancy have been established. It was demonstrated, however, that BAC is more critical than the dose/duration of alcohol exposure in determining the degree of severity of ethanol effects. Thus, the pattern of alcohol intake is one of the critical factors. High dose binge-like drinking seems to be especially harmful to the brain of the developing fetus (Pierce and West, 1986; West *et al.,* 1989).

1.1.2. Critical Period of Exposure to Alcohol in Animals

The fetal development of humans and rats follow similar stages, but differ in the relative timing of birth. In human, the time of the fastest growth of the brain associated with the development of an intricate multi-cellular organization known as the brain growth-spurt period, coincides the last trimester of *in utero* gestation (Bayer *et al.,* 1993; Rice and

Barone, 2000). Conversely to this, the brain growth-spurt period in the rodents is restricted to the postnatal period that begins around birth and ends at approximately 2 weeks after birth (Dobbing and Sands, 1979). It is referred to as the human 3rd trimester equivalent.

As mentioned earlier, the severity of the deficits may involve the interaction of several risk factors, such as the amount of consumed alcohol, duration and pattern of alcohol consumption, the timing of alcohol consumption relative to critical windows of vulnerability, or the inherent differential vulnerability among the various brain regions to alcohol-induced brain injury.

The critical periods of alcohol exposure overlap with periods of greatest development and/or maturation of organ systems. For example, alcohol exposure in the first trimester is more often associated with organ and musculoskeletal anomalies including characteristic facial abnormalities, while exposure in the second and in the third trimester (the brain growth spurt period) is linked to growth retardation, and to the intellectual and behavioral deficits, respectively (Aronson and Olegard, 1987). Thus, if maternal alcohol consumption occurs during all three trimesters, the child is likely to show all the characteristic features of full FAS such as cranio-oral anomalies, growth deficits as well as and behavioral dysfunctions

1.1.3. Alcohol Exposure Protocols in Animals

Animals do not normally consume enough alcohol voluntarily to maintain chronically high blood alcohol concentrations (BAC) during pregnancy and postnatal period. Consequently, a variety of different methods has been developed to administer alcohol to the developing fetus or pups. They include injections, vapor inhalation, and intraoral / intragastric gavage (intubation). No method is ideal and each of these methods has advantages and disadvantages. An ideal method of alcohol administration to

experimental animals should ensure a control over the total daily dose of alcohol, as well as the time and pattern of alcohol intake, entail minimum stress during the alcohol delivery, allow to maintain high and stable blood alcohol concentrations over time, preferably should be technically easy to perform, and should provide a control for malnutrition associated with ethanol intoxication (Kelly and Lawrence, 2008).

In the literature, several alcohol administration methods used to establish FASD animal models has been described. They include continuous liquid diets and the binge-like drinking patterns of alcohol delivery. The liquid alcohol diet limits food and water consumption and serves as the animals' sole source of nutrition. Alcohol is added to this diet either at a low concentration usually equivalent ~18% ethanol derived calories (EDC) or at a higher concentration usually equivalent ~35% ethanol derived calories (EDC). These alcohol concentrations result in daily alcohol intake of ~12 and ~18 g/kg/day respectively. This method generally includes two control groups. The first is pair-fed to either 18 or 35% alcohol group and receives a similar liquid diet with a carbohydrate i.e. sucrose, substituted for the alcohol (Berman and Hannigan, 2000; Driscoll *et al.,* 1990). This procedure equates the total daily caloric intake across groups and therefore, serves as a control for reduced caloric intake which per se can affect fetus development. The second control group has continuous access to standard laboratory chow and water. If the alcohol group differs from both control groups, and the two control groups do not differ from each other, the effect may be attributed to alcohol intake. Alcohol administration with a liquid diet is more natural (Uzbay and Kayaalp, 1995), however, a basic disadvantage of this procedure is a great individual variation in the consumption of alcohol-containing solutions. The dose, duration, and pattern of alcohol exposure are determined by the animal, and thus the variation in the BAC among pregnant dams occurs.

Another frequently employed method involves direct intraoral or intragastric intubation of dams with alcohol solutions using PE10 Intramedic tubing attached to a 1-ml syringe.

Feeding needle is dipped in corn oil to provide lubrication. The alcohol is usually mixed with an artificial milk solution and delivered at the daily dose varying typically between 2-6 g/kg. To increase the portion of the day with elevated BACs, the total daily dose can be divided into two or three equal portions administered at even time intervals. This method also includes two controls. One control is pair-fed to alcohol group and receives via intubation the same volume of fluid as the alcohol group, except that carbohydrate is substituted isocalorically for alcohol. The other control group has continuous access to standard laboratory chow and water (Kelly and Lawrence, 2008). Intragastric intubation allows for more strict control of dosage and timing of alcohol administration. By administering alcohol via intragastric gavage, experimenter is able to administer the same amount of alcohol at approximately the same time to all animals, and is able to produce relatively high BAC over a sustained period of time, thus circumventing the problem of varying and fluctuating BACs due to individual differences in amount and pattern of alcohol consumption when provided with the liquid diet. The disadvantage of this method may be stress created by intubation. However, isocalloric control group provides also a control for the potential effect of stress related with animal manipulation during intubation. It might even be possible that, compared to the experimental group, control pair-fed animals are more stressed by the procedure since alcohol-treated subjects may be slightly sedated especially at time of second intubation. This method when applied to the new-born pups, allows the neonatal to stay with either biological or foster dam during the period of early neonatal alcohol administration. Administration of alcohol via intragastric intubation method does not need expensive equipment and is not technically demanding.

The third method employs a vapor inhalation system (Karanian *et al.*, 1986). Vapor inhalation chambers are commercially available (Gilpin *et al.*, 2008). In this method, pregnant dams or neonates are placed in an inhalation chamber filled with ethanol vapor for several hours. The dose, duration, and pattern of exposure of alcohol vapors can be easily controlled by the experimenter. This technique entails a rapid rise in blood alcohol

concentration and has been shown to produce reliable and consistent high BAC during exposure. Thus, the inhalation method has advantage of the precise control of BAC, and is less laborious than other techniques. However, vapor inhalation method needs purchasing expensive equipment and may be highly stressful to the pups due to maternal separation of pups which may interfere with normal brain development (Kuma *et al.*, 2004). Also, there is no efficient control group for the potential nutritional deficits of the ethanol-exposed pups.

Final method for administration of alcohol to neonates is called artificial rearing or pup-in-the-cup' method. The process requires surgically implanting a gastrostomy feeding tubes into the pups' stomach on postnatal day 4 under light ether anesthesia (West *et al.*, 1984). Liquid diet with or without alcohol is administered using a programmable pump that can release alcohol chronically or periodically. Pups are typically kept in a plastic cup supplied with nesting materials, floating in warm water, designed to mimic warm nesting and maternal interaction. This protocol also requires pups separation from the dam and litter. Moreover, a non-treated control group and a pair-fed control group that receives the same amount of calories in the same way as the alcohol-exposed group are necessary in order to correctly evaluate the effects of ethanol administration in this method. Although the dose, duration, and pattern of exposure of alcohol can be precisely controlled by the experimenter, the procedure is costly, labor intensive, and extremely invasive, involving potential health complications for the neonates.

1.2. Anatomy of the Mammalian Eye

1.2.1. The Structure of Eye Ball and the Eye Optics

The eyes work like a camera that collects focuses and transmits light to create an image of the visual world around us. There are several layers and structures; each plays an important role in vision (Figure 1.1).

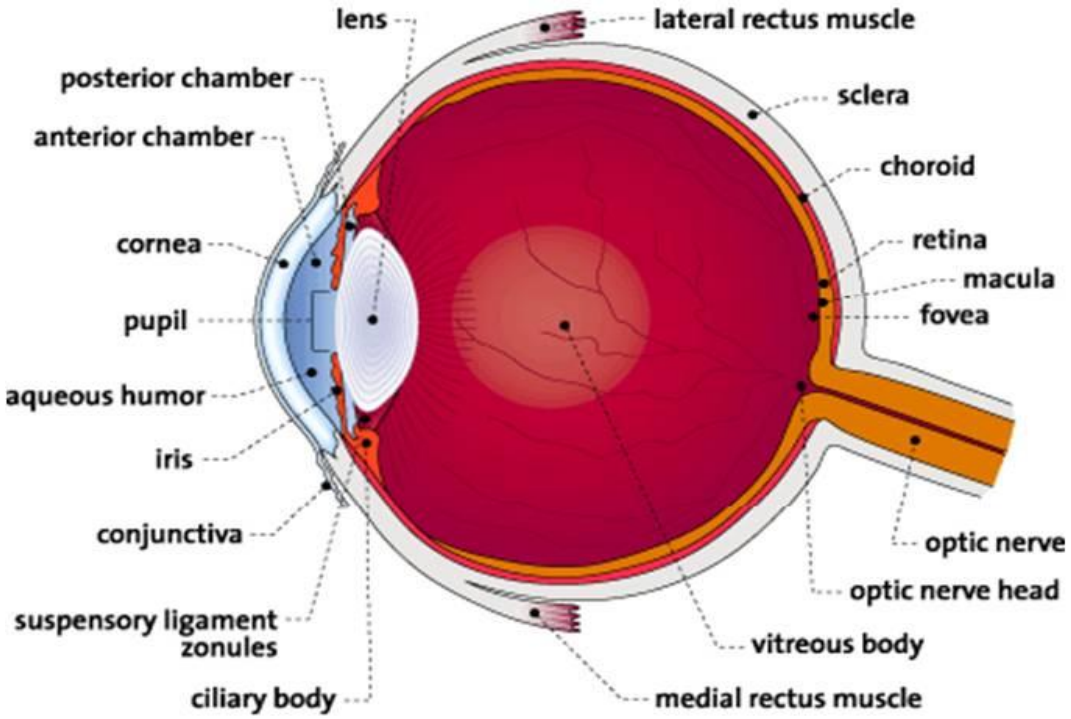

Figure 1.1 The structure of mammalian eye (http://www.allaboutvision.com).

The cornea is the outermost transparent layer of the eye coating the iris, pupil, and anterior chamber. The cornea is the first part in the eye's focusing system. The mean refractive index of the human cornea epithelium is approximately -1.40 diopters (D) and varying in the central (1.3970 (+/-0.001)), nasal (1.3946 (+/-0.001)), and temporal periphery (1.3940 (+/-0.001)) (Patel *et al.*, 1995; Vasudevan *et al.*, 2008). Next, the light passes through the lens. The lens which is not equally transparent to all colors, acts as a filter to block certain wavelengths of light. The curvature of the lens attached to the eye walls by cilliary muscle and suspensory ligaments is changing dependent on the distance of the focused object. Its refractive power in an emmetrope eye is controlled by the parasympathetic (oculomotor) nerve fibers and is changing between 10-26 dioptre (the

reciprocal value of the focal length of the lens in meter (m)) depending upon the age. The human eye in a relaxed state with the flat lens stretched by the suspensory ligaments is focusing distant objects (≥ 2.3-6 m) such that their images fall exactly onto retina. When the sight is shifted onto closer objects, automatic contraction of cilliary muscle reduces the pulling action of the suspensory ligament and the lens which is elastic takes more convex shape with increased refractive power ensuring focusing the image of a close object on the retina. This is an important component of so called eye accommodation. Two other components of eye accommodation is a papillary reflex (narrowing the pupil) responsible for the reduction of spherical aberration, and eye convergency reflex reducing retinal disparity (important for binocular vision). The lens also determines the overall size of the vertebrate eye such as; a small lens (microphakia) cause a small eye (microphthalmia) (Williams and Chalupa, 2008, pp 268). The space between the cornea and iris called the anterior chamber is filled with the aqueous humor nourishing nearby tissues. It is secreted by a gland called the ciliary body. The narrow gap between iris, zonule fibers and lens is called posterior chamber. The large gap between the lens and the retina is called vitreous chamber filled with the vitreous body. The vitreous body or vitreous humor is a thick, clear, and transparent gel-like liquid that fills the eyeball, behind the lens.

The retina is thin, delicate, light sensitive and multi layered tissue (Figure 1.2.) located at the back of the eye. The retina contains photoreceptors and several classes of nerve cell that communicate each other through synapses. The central retina is called macula lutea or the yellow spot due to high content of lutein and zeaxanthin (yellow xanthophyll carotenoids derived from the diet). In the human eye, it has a diameter of around 5 mm and is often histologically defined as having two or more layers of ganglion cells. Near its center is the fovea, a small pit that contains the largest concentration of cone cells in the eye and is responsible for central, high resolution vision (high visual acuity). Because of its yellow pigment macula absorbs excess of blue and ultraviolet light that enter the eye, and acts as a natural sun block for this area of the retina. The yellow color

comes from its content of lutein and zeaxanthin, which are yellow xanthophyll carotenoids derived from the diet. Zeaxanthin predominates at the macula, while lutein predominates elsewhere in the retina. There is some evidence that these carotenoids protect the pigmented region from some types of macular degeneration. The fovea contains the highest concentration of cone type photoreceptor cells. The eye from outside is surrounded by choroid and sclera. Choroid is a thin and highly vascularized membrane between the retina and sclera. It is composed of a dense pigment and numerous blood vessels that supplies oxygen and nourish to the internal tissues of the eye including retina. The iris is the visible portion of the choroid. It provides the eye's color that differs depending on the quantity of pigment present in the choroid. Sclera is the outermost membrane that main function is to provide mechanical strength to resist the intra-ocular pressure and to protect the delicate internal parts of eye from external trauma. The outside of sclera and the inside of eyelids are covered by the conjunctiva. It contains many glands that produce mucous to help lubrication of the eye. The conjunctiva is the first layer that protects eye from infections. Inside of sclera, there is choroid corresponding to arachnoid, the second of the brain meninges.

1.2.1.1. Comparison of Human and Small Rodent (mouse or rat) Eyes

The structure of mouse and rat eye is very similar to the eye structure in other mammalian spieces including human. In both humans and rats, the cornea lets the visible and ultraviolet light (down to 300 nm) to pass through (Hemmingsen and Douglas, 1970). Both in human and small rodents the pupilary reflexes are very efficient: pupil size variable (1,2–0,2 mm) (Block, 1969) and the changes very fast (a contraction from 2 mm to 0.5 mm takes around 500 ms) (Lashley, 1932). When comparing the small rodent and human lens, the rat's lens permits around 50% more of ultraviolet light (Gorgels and van Norren, 1992) but is less flexible and thus has poorer refractive power (Lashley, 1932). Interestingly rats and mice, with their small eyes and poor visual acuity, have much higher depth of focuse from 7 centimeters to infinity (Green *et al.*, 1980).

1.2.1.2. Retina Structure

The retina is a highly organized structure of the eye. Many types of retinal cells are distributed regularly across the retina (Cook and Chalupa, 2000). When the retina develops, neurons classify into a well organized laminar structure and form a complex neural circuitry communicating the visual signals initiated by photoreceptors to the brain through the axons of ganglion cells. Different retinal layer contain different retinal cells, their dendritic arbors and synaptic connections. Precise wiring amongst the major cell classes in the retina is fundamental to vision.

The mammalian retina is organized as follows (Figure 1.2):

1. The retinal pigment epithelium
2. The rod and cone photoreceptors in the outer nuclear layer (ONL)
3. The outer plexiform layer (OPL) contains connections between photoreceptors, the horizontal neurons, and bipolar neurons
4. The horizontal, bipolar and amacrine neurons and Müller glia in the inner nuclear layer (INL)
5. The inner plexiform layer (IPL) contains connections between RGC dendrites and projections from amacrine neurons and bipolar neurons
6. The ganglion and displaced amacrine cells in the ganglion cell layer (GCL)

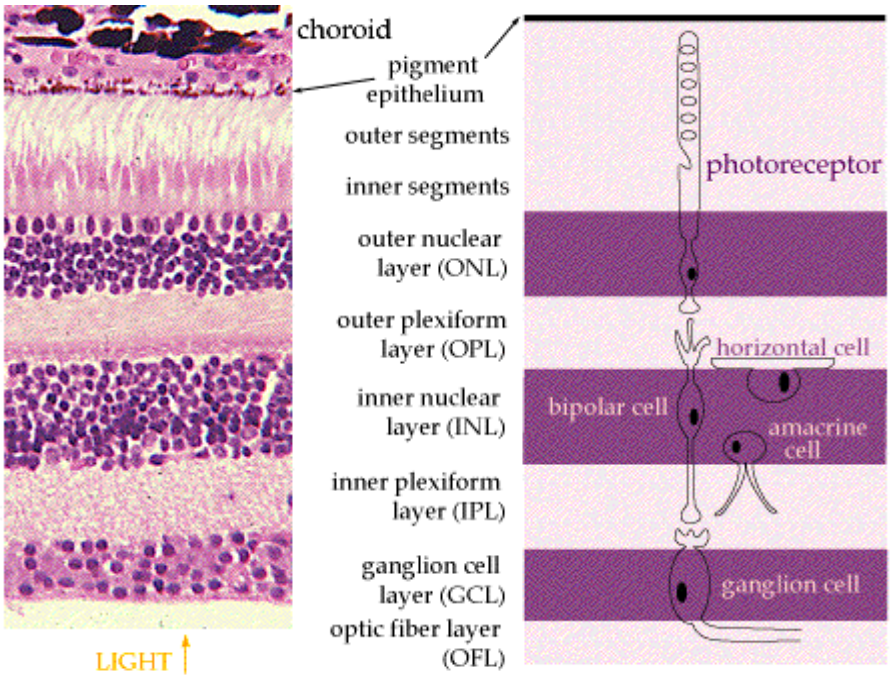

Figure 1.2 The structural organization the mammalian retina (http://thalamus.wustl.edu/course/eyeret.html)

There are two types of photoreceptor in the retina, cone and rod. Cone type photoreceptor cells are responsible for color perception and high resolution (high visual acuity) in photopic vision. When cones are densely packed in the central retina, rodes are located mainly in the peripheral retina and are responsible for low resolution scotopic (nocturnal) vision. Cones and rods cells have different shape outer segments that contain photopigments. Photopigments are light sensitive molecules and determine the spectral absorption characteristics of the cones. In human retina, three types of cone photoreceptors are identified (trichromatic vision). First one is the long-wavelength sensitive L or red cones with the mean wavelength of maximum absorption ~563 nm, second is the middle- wavelength sensitive M or green cones with the mean wavelength of maximum absorption ~534 nm and the last one is the short-wavelength sensitive S or blue cones with the mean wavelength of maximum absorption ~420 nm (Figure 1.3).

The absorption peak for rods' photopigment was found at the wavelength of ~520 nm (Bowmaker and Dartnall, 1980). In the human retina, S cones are more peripherally distributed and appear much less frequently than the M and L cones comprising only about 5%-7% of the total cone population. M-cones exist approximately two times more than L-cones and S -cones comprise only about 5% of the total cone population. L and M- cones are most intense in the fovea, however, S-cones are more peripherally distributed in the retina (Marc and Sperling, 1977; Roorda *et al.,* 2001). Normal color vision needs the presence of the S pigment and at least one from each of the L and M pigments. Red-green color vision deficiencies are caused by the absence of expression or function of either L or M pigment.

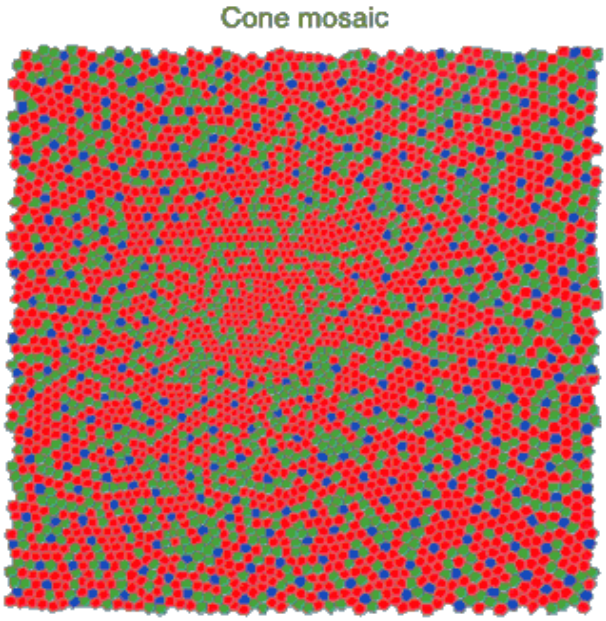

Figure 1.3 The diagram representing an area of human retina about 1° of visual angle showing the density of S (blue), M (green) and L (red) cones (http://www.cis.rit.edu/people/faculty/montag/vandplite/pages/chap_9/ch9p1.html)

Light signals from the photoreceptors are impinging on the bipolar cells (BCs) and then are transmitted to the dendrites of amacrine and ganglion cells. Two basic types of

bipolar cells are identified in all mammalian retinas: rod BCs and cone BCs. Despite the fact that rods highly outnumber cones, in most mammalian retinas, cone bipolars outnumber rod bipolars. The reason is that more rods converge onto a single rod bipolar than cones onto cone bipolar. This way rod system increases sensitivity to light at the expense of visual acuity.

One type of rod bipolar cell and at least nine types of cone bipolar cell have been reported in the mammalian retina. Bipolar cells are divided into two main classes: ON and OFF bipolar cells, occurring in approximately equal numbers (Masland, 2001; Wässle, 2004). When the retina is stimulated by light, OFF type of bipolar cell hyperpolarizes, and the ON type depolarizes. The classes of ON and OFF bipolars are further subdivided; to ON-transient (recovering from depolarization quickly), ON-sustained (recovering from depolarization slowly), OFF-transient (recovering from desensitization quickly) and OFF sustained BCs (recovering from desensitization slowly). Photoreceptors are not divided into once providing input only to ON bipolar cells or only to OFF bipolar cells. Each cone photoreceptor sends its signals into several bipolar cell types creating this way many parallel channels, each communicating a different version of the cone's output to the inner retina.

Horizontal cells (HCs) are second order inhibitory interneurons that contribute to the lateral interactions in the outer plexiform layer. Two morphological types of horizontal cells are known to exist in the majority of vertebrate retinas: A-type that are axonless and contacts cones, and B-type with axons that contact both cones and rods. However, there is only one morphological type of horizontal cell (B-type) in the mouse and rat retina (Peichl and González-Soriano, 1994). There are also two physiological types of HCs: luminosity (L-type) and chromaticity (C-type) horizontal cells. These cell types are distinguished on the basis of their responses to chromatic light stimuli. L-type horizontal cells always respond with hyperpolarization to light stimuli of any wavelength within the visible range of the spectrum, while C-type horizontal cells respond with different

polarity to light stimuli of different wavelengths (Dacey *et al.,* 1996). Horizontal cells are implemented in so called lateral inhibition responsible for "reading" contrast, but also movement and direction detection.

The second classes of inhibitory retinal interneurons are the amacrine cells (ACs). Their perikaryons are located in both, the inner nuclear and the GCs layers while their projections extend into the outer and/or inner sublamina (sublamina *a* and *b*, respectively) of the inner plexiform layer. Generally speaking, amacrine cells form an indirect link between the BCs and the GCs. Amacrine cells outnumber horizontal cells by amounts that range from 4:1 to 10:1 (depending on the species) and can outnumber ganglion cells by 15 to 1 and are very diverse. Several different types of amacrine cells have been classified in mammalian retina according to their structural, biochemical and functional properties (Wässle and Boycott, 1991). In the mammalian retina, the two important groups of ACs are the AI (wide – field GABAergic neurons) and AII (small – field glycinergic neurons) cells (Kolb, 1979). The AI amacrine cells receive input throughout the IPL from other types of amacrine cells (Nelson and Kolb, 1985). The AI cell has been called the reciprocal rod amacrine cell because the AI makes a reciprocal synapse back to the rod bipolar terminal. The AII cells have their bodies in the INL and their dendrites bistratify in both sublamine of the IPL. The greatest density of AII cells was noted in extra foveal central retina and it decreases with increasing eccentricity. Parallel to this, both dendritic fields of AII cells enlarge with eccentricity. AII cells transmits both rod and cone-driven signals within the ON- and OFF- retinal pathways to the inner retina and thus, participate more in the vertical flow of visual signals through the inner retina and less in lateral inhibitory pathways. In sublamina *a* of IPL layer, AII cells form contacts through sign-inverting inhibitory synapses with OFF-center cone bipolars, and in sublamine *b*, they form contacts via sign-conserving synapses with ON-center cone bipolars. Interestingly, the AII amacrine cells receiving excitatory input from rod bipolars relay them into cone bipolar cells (Kolb, 1979). By synapsing on the axon of the cone bipolar cell, the rod pathway gains access to the the cone circuitry,

Therefore, some ganglion cells retain their function in very dim light, even though they do not receive direct input from the rod BCs.

The most numerous amacrine cells found in species from turtles to macaques are 'starburst' ACs named so due to their regularly spaced, evenly radiating dendrites. Because they are richly represented in the retina and have expanded and widely overlapping dendritic fields (6 m of dendrite per mm of retinal surface in rabbit), starburst ACs occupy a substantial fraction of the volume of IPL. In the adult retina, the starburst ACs contain and release acetylcholine on their synapses with GCs and GABA on synapses with other ACs (O'Malley *et al.*, 1992). It has been postulated that they are strongly implemented in the process of lateral inhibition (Peters and Masland, 1996). The starburst amacrine belong to two paramorphic types: the OFF-starburst cells stratifying in sublamina *a*, and the displaced ON-starburst cells stratifying in sublamina *b* of the inner plexiform layer (Perry and Walker, 1980). The latter class of ACs extensively co-stratifies with both ON and ON-OFF directionally selective ganglion cells (DS GCs) and is known to provide a major synaptic input to these cells (Famiglietti, 2002). The displaced ON-starburst amacrine cells are thought to be important for the detection of moving stimuli and were shown to nondirectionally facilitate the responses of DS GCs (Chiao and Masland, 2002).

In addition to the previously described ACs' types there are also dopaminergic amacrine cells (DA ACc) representing the sparsest type of the retinal interneurons (Dacey 1990). DA ACs are thought to play role in a variety of visual processes associated with light adaptation and the transition from scotopic to photopic visual functions (Witkovsky, 2004).

The innermost retinal layers are formed by the bodies of ganglion cells (GCs) and their fibers. The retina of a macaque monkey contains approximately 1,500,000 retinal ganglion cells; a cat, 160,000; a rabbit, 380,000, and a mouse 120,000. RGCs are diverse

in morphological and functional properties, as well as their patterns of projections. Primates' retina contains a high number of small ganglion cells, the so-called midget cells. The second large classes of the primate GCs are parasol ganglion cells having bigger cell bodies and larger receptive fields (Polyak, 1941). Retinal ganglion cells are the exit cells projecting to the brain visual centers, superior colliculus (SC) and dorso-lateral geniculate nuclei (dLGN). Midget type ganglion cells project to the parvocellular layers of dLGN (P pathway), while parasol ganglion cells project to the magnocellulars layer of dLGN (M pathway). The midget GCs belonging to the predominating class of GCs in primate retina, have a simple center–surround organization with linear spatial summation in the receptive field center. Associated with midget ganglion cells is a special midget bipolar cell. In the fovea, an individual ganglion cell receives direct input from only a single cone. The fundamental advantage offered by a midget system is a high sampling density, which enables great spatial resolution. In the central fovea, the spatial resolution of this system is limited only by the cone packing density**.** Most of the retina ganglion cells are monostratified, ON or OFF. Dendrites of the ON ganglion cells stratify in the inner region (sublamina b), whereas OFF RGCs stratify in the outer sublamina (sublamina a) of the IPL (Famiglietti and Kolb, 1976). Small amount of cells are bistratified with arbors in both sublaminae and have ON and OFF responses. Bistratified ganglion cells project to the intercalated or the koniocellular layers (K) of the dLGN.

The distribution of different classes of GCs is as follow: Midget cells comprise about 90%, parasol cells about 5%, and small bistratified cells about 1% in the human fovea. Among the total of the RGC population in the periphery, midget cells constitute about 40-45%, parasol cells about 20% and small bistratified cells about 10% of the total of the RGC population (Dacey, 1994). The different morphological types of ganglion cell have been characterized by morphological properties such as cell soma size, dendritic arborization pattern, and dendritic stratification location in the different species including, monkey (Rodieck and Watanabe, 1993), cat (Stone and Fukuda, 1974), ferret

(Wingate *et al.,* 1992), rat (Sun *et al.,* 2002a) and mouse (Sun *et al.,* 2002b; Badea and Nathans, 2004; Kong *et al.,* 2005; Coombs *et al.,* 2006; Völgyi *et al.,* 2009). Sun *et al.,* (2002a) have been reported twelve subtypes of monostratified cells cluster and two subtypes of bistratified cells cluster in the mouse retina using the "DiOlistic" method. Moreover, Coombs *et al.,* (2006) have been shown ten subtypes of monostratified cells cluster and four subtypes of bistratified cells cluster in the mouse retina using three different techniques as follow; Lucifer Yellow injection, 'DiOlistics' and transgenic expression of yellow fluorescent protein.

In addition to photoreceptors and neurons, there are three types of glia cells in the mammalian retina. They maintain neuronal cells homeostasis. Müller cells remove glucose, glutamate and GABA from the extracellular space and convert glucose into lactose, and GABA and glutamate into glutamine. These products turn back to the extracellular space and are reused by neurons (Newman and Reichenbach, 1996). Astrocytes are mainly present in the retinal fiber layer mostly composed of ganglion cells axons. They cover these processes and the axon bundles that finally form the optic nerve. They also play role in synaptogenesis, nutrition, ionic homeostasis and the modulation of ganglion cells activity (Newman, 2003; Trivino *et al.,* 1992). Microglia cells localize in every layer of the retina. Microglial cells are responsible for the immune response against invading agents and the phagocytosis of endogenous waste (Langmann, 2007).

1.2.1.3. Neural Circuitry in the Retina

Visual information flow from the retina to brain is very complicated. Within the retina, visual information is conveyed by two different pathways. One of them, a vertical pathway, transmits visual signals from the photoreceptors to bipolar cells and from bipolar cells to the retina ganglion cells. Vision starts with the absorption of light by visual pigments in the retinal rod and cone photoreceptors and then the conversion into

an electrical signal, a process called phototransduction. Light triggers a cascade of intracellular biochemical reactions during the phototransduction which are nearly the same in rods and cones. A light sensitive chromophore called 11-*cis*-retinal is placed in the membranous folds or disks in the outer segments of rods and cones. Photopigment is bound to a protein, rhodopsin in rods, and iodopsin in cones. Light absorption by the photopigment molecule causes its dissociation from opsin which then activates a G-protein called transducine. Active transducine activates phosphodiesterase, an enzyme degrading cGMP, photoreceptor's second messenger molecule responsible for the gating (opening) cation (Ca^{2+} but mainly Na^{+}) channels in the outer segment membrane (Baylor, 1987). During darkness, due to the high activity of photoreceptors' guanylate cyclase (GC), the intracellular levels of cGMP stay high, and the cation channels open what ensures a continuous inward Na^{+} flow (so-called dark sodium current) depolarizing the receptor's membrane. Na^{+}, Ca^{2+} and K^{+} concentrations are regulated by a $4Na^{+}$-Ca^{2+}/K^{+} exchanger in the outer segment, and a $2K^{+}$-$3Na^{+}$ pump in the inner segment of membrane. Depolarized photoreceptors continuously release glutamate at their synapses with retina's first order neurons; bipolar and horizontal cells. Conversely, under the light stimulation, due to transducine and phosphodiesterase activation, cGMP concentration is reduced, channels close down, the receptor membrane is hyperpolarized, and neurotransmitter release reduced. Photoreceptors have developed specialized proteins that are involved in a series of inactivation steps and negative feedback reactions. They are frequently controlled by Ca^{2+}. These processes are responsible for shifting photoreceptors' operating range according to the basal light level and for adaptation to light (Baylor, 1987; Leskov *et al.*, 2000; Luo *et al.*, 2008).

Bipolar cells have concentrically organized ON-center/OFF-surround or OFF-center/ON-surround receptive fields. Under the equal stimulus conditions, when a light stimulus falls selectively on the center of BC's receptive field, some BCs become hyperpolarized (OFF-center bipolar cells) and some other BCs become depolarized (ON-center bipolar cells) (Joselevitch and Kamermans, 2007). Selective stimulation with

light of the surround gives the opposite effect. In a single BC, simultaneous stimulation with light of both center and surround of the receptive field produces very weak response (only a weak change in the cell membrane potential). These cells are arranged for reading contrast and enhancing the contours of visual objects. As shown in Figure 1.4. the axon terminal arborizations of OFF-type, cone-contacting bipolar cells lie in sublamina *a*, where they synapse with the dendrites of OFF-type ganglion cells, whereas the axon terminal arborizations of ON-type cone contacting bipolar cells lie in sublamina *b*, where they contact the dendrites of ON-center ganglion cells (Nelson *et al.*, 1978). OFF-center bipolar cells express the ionotropic glutamate receptors (iGluRs, both AMPA and kainite), whereas ON-center bipolar cells express both the metabotropic (mGluR6) and ionotropic glutamatergic receptors at their synaptic contacts with photoreceptors. Because of different types of glutamate receptors, OFF- and ON-center bipolar cells respond to light differently (Nakajima *et al.*, 1993; Nomura *et al.*, 1994; DeVries, 2000).

Depending on the stratification of their dendritic arbor GCs are classified as: (a) bi-stratified ON–OFF GCs among which there are direction-selective neurons; (b) mono-stratified medium field ON-type GCs which are also motion and direction detectors projecting to the superior colliculus and providing an error signal for eye velocity in optokinetic nystagmus (a vegetative function); (c) extremely small, mono-stratified GCs functioning as the edge detector.

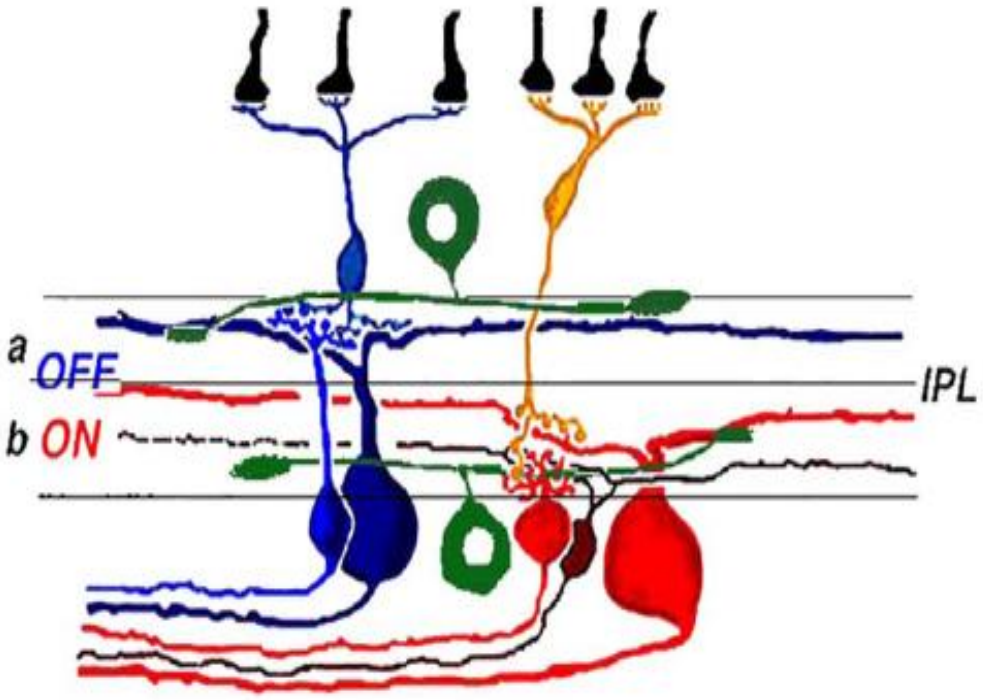

Figure 1.4 Organization of ON- and OFF- center ganglion cells into sublaminas *a* and *b* (after Chalupa and Günhan, 2004)

The axons of ganglion cells form optic nerve carrying visual signals from retina to its targets in the brain. Retina GCs express only ionotropic receptors and unlike the other retinal neurons respond to light with all-or-none action potentials.

The second pathway transmitting signals within retina is so-called lateral pathway including local feedback circuits from horizontal cells back to photopreceptors and from amacrine cells back to bipolar cells (Stell *et al.*, 1975; Tachibana and Kaneko, 1987; Kamermans *et al.*, 2001). Lateral interactions (including lateral inhibition) occur in both synaptic layers of the retina. Input coming from the photoreceptors and bipolar cells is collected and averaged by horizontal and amacrine cells. Depending on this average, they send feedback signals and adjust their output. Horizontal cells express and release GABA (Wu, 1992). Horizontal cells modulates the photoreceptor output by chemical

and electrical feedback mechanism (Kamermans *et al.,* 2001; Hirasawa and Kaneko, 2003; Vessey *et al.,* 2005). Because of the strength of the feedback signal different with the amount of light falling onto individual photoreceptors, horizontal cells amplify the gain the photoreceptor synapse in horizontal cell-cone feedback pathway (Skrzypek and Werblin, 1983; Kraaij *et al.,* 2000).

1.2.1.4. Comparison of Retina Structure and Functions in Human and Small Rodents (mouse and rat)

There is a great degree of similarity in retina structure between primates including human and small rodents such as laboratory mouse. Generally speaking, in primates as compared to other mammals, three new specializations emerged: a rod-free fovea, a large number of small bipolar and ganglion cells, the midget cells, and better color discrimination between long wavelengths due to evolution of red and green photopigments in cones (trichromatic vision).

Small rodents have both rods and cones, but there are only two types of cone photoreceptor responsible for dichromatic vision in these species. One of them is sensitive to ultraviolet (UV) light with absorption maximum at ~360 nm (S cones); the other is sensitive to medium wavelength light with absorption maximum at ~508 nm (M cones) (Nikonov *et al.,* 2006). Therefore, rats and mice are unable to see red colors but can discriminate between greens, blues and ultraviolets (Jacobs *et al.,* 2001). The sensitivity of small rodents to ultraviolet light provides important behavioral advantages. In wild, rats and mice are nocturnal, but they are also active during the twilight hours, when there is a significant increase in the ratio of ultraviolet to visible light. Ultraviolet vision would be then advantageous at these twilight hours. Sensitivity to ultraviolet light also substantially increases urine-mark visibility. Urine marking is an important way of communication in many species including small rodents.

The retina of mouse that is nocturnal animal consists of 97.2% of rods with an average density of 100.000/mm^2, and 2.8% of cones with an average density of 16.000 /mm^2 (Jeon *et al.,* 1998). Rodents, but also cats and lagomorphs do not have fovea with densely packed cones and high numbers of midget bipolar and ganglion cells what ensures high visual resolution. In small rodents like rat or mouse, the distribution of the cones and rods photoreceptors is different from foveate mammals. S-cones are dominantly distributed in the ventral retina and small amount of S-cones found in the dorsal retina. However, M-cones are found mainly in the dorsal half of the retina (Szel *et al.,* 1992). In strongly rod-dominated mouse retina rods outnumber cones by roughly 35:1 and highly converge on retinal neurons**.** Each neural cell in the rat retina is responsive to a much larger number of photoreceptors than in the human retina, which increases sensitivity to dim light at the expense of visual acuity. With these retinal properties and poor optics small rodents have poor visual acuity (Artal *et al.,* 1998). Visual acuity is measured in *cycles per degree* (cpd) that a measurement of the number of lines that can be seen as distinct within a degree of the visual field. Humans' acuity is about 20 times better than that of rats' (Wiesenfeld and Branchek, 1976, Birch and Jacobs, 1979, Artal *et al.,* 1998). The poor visual acuity in rats and mice was demonstrated in behavioral experiments. Prusky *et al.,* (2000, 2002) have shown that a normally pigmented rat has about 20/600 vision (1-1,5 cpd), and an albino has about 20/1200 vision (0.5 cpd) (see also Birch and Jacobs, 1979; Wiesenfeld and Branchek 1976).The average acuity of rats was approximately twice that of C57BU6 mice (0.50 to 0.56 cpd) (Prusky *et al.,* 2000; 2002). In albino rat and mouse species, the lack of pigment in the outer eye layer results in excessive scattering of light within the retina and thus impaired visual ability (Prusky *et al.,* 2002; Wong and Brown, 2006). Additionally, it has been shown that a melanin precursor, DOPA regulates mitosis in retina. As albino rats lack the pigment in their retina they have lower by 30% number of rods and also lower density of retinal neurons as compared to pigmented rats (Ilia and Jeffery, 2000). The retina of albino mice shows a reduction of photoreceptors and a decrease in uncrossed retinal fibers (Rachel *et al.,* 2002).

1.2.2. Development of Mouse Retina

The retina is a part of the central nervous system and derived from the neural tube (Pie and Rhodin, 1970).

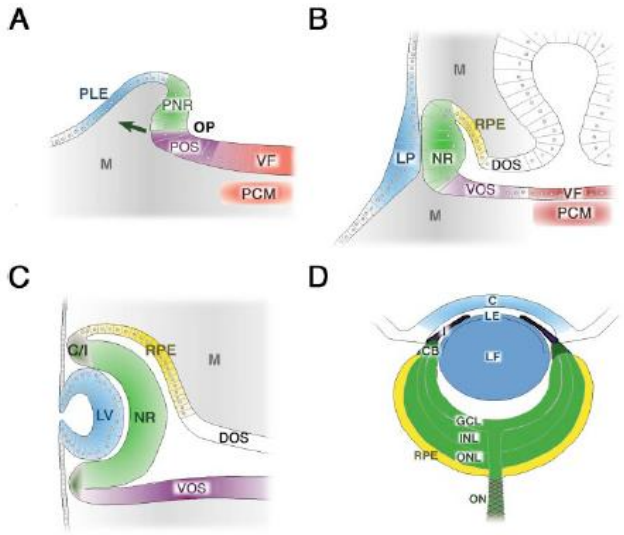

Figure 1.5 Schematic overview of vertebrate eye development
In panels *A–D*, presumptive or differentiated eye tissues are color-coded in the following manner: *blue*, lens/cornea; *green*, neural retina; *yellow*, retinal pigmented epithelium (RPE); *purple*, optic stalk; *red*, ventral forebrain/prechordal mesenchyme; *grey*, mesenchyme. (*A*) Formation of the optic vesicle is initiated by an evagination (*indicated by arrow*) of the presumptive forebrain region resulting in the formation of the optic pit (OP). The optic vesicle region is divided into dorso-distal region (*green*), which contains the presumptive neural retina (PNR) and RPE (not shown), and the proximo-ventral region, which gives rise to the presumptive ventral optic stalk (POS); PLE, presumptive lens ectoderm; M, mesenchyme; VF, ventral forebrain; PCM, prechordal mesoderm. (*B*) Continued growth of the optic vesicle culminates with a period of close contact between the lens placode (LP) and the presumptive neural retina (NR) during which important inductive signal likely exchange: RPE, presumptive retinal pigmented epithelium; VOS, ventral optic stalk; DOS, dorsal optic stalk. (*C*) Invagination of the optic vesicle results in formation of the lens vesicle (LV) and neural retina (NR) and establishes the overall structure of the eye. The point at which the neural retina and RPE meet gives rise to components of the ciliary body and iris (C/I). (*D*) Mature eye: C, cornea; LE, lens epithelium; LF, lens fiber cells; I, iris; CB, ciliary body; GCL, ganglion cell layer; INL, inner nuclear layer; ONL, outer nuclear layer; ON, optic nerve (after Chow and Lang, 2001).

The anterior edge of the neural plate is called the eye field that groups cells which differentiate into neuronal components of the eye. During embryogenesis, eye developes from three embryonic layers: retina and retinal pigment epithelium (RPE) arise from the neural ectoderm, the cornea and sclera are derived from the mesoderm, and the surface ectoderm gives rise to the lens. The optic vesicle is emerged from as an outgrowth on each side of the neural tube, and then develops into the eyes. These optic vesicles are joined to the developing central nervous system by a stalk that later give rise to the optic nerve. After the optic vesicles connect to the ectoderm, the epithelium forms a lens placode. The lens placode invaginates to form the lens vesicle and finally develops into lens. The cells in the posterior part of the lens vesicle quickly extent and become filled with proteins known as α, β, and γ crystalline that make them transparent. These densely packed elongating cells are known as transparent lens fibers or the primary lens fibers. Then, daughter cells move towards the bow of the lens and differentiate into secondary lens fibers.

In the course of these changes, the optic vesicle folds inwards and forms a double layered optic cup that gives the eye its shape. The outer layer of the optic vesicles turns into the pigmented epithelium, the inner layer becomes a single layered presumptive neural retina. The cells of the inner layer quickly proliferate and produce a variety of glia, ganglion neurons, interneurons, and photoreceptors. All these cells together constitute the multilayered neural retina. The iris and the ciliary body are developed from the peripheral edges of the optic cup where both inner and outer optic cup layer become conjugated. The connective tissue of the ciliary body, the smooth ciliary muscle, and the suspensory ligaments of the lens are derived from the mesenchyme at the edge part of optic cup that later invaginates and results in the lens. The formation of cornea is induces by the lens and the optic cup while the sclera is formed from a condensation of the mesenchyme outside of the optic cup. (Hollenberg and Spira, 1973; Beebe, 1986; Saha *et al.*, 1992; Chow and Lang, 2001; Wong, 2006; Graw, 1996, 2010).

1.2.2.1. Differentiation Time of Retinal Cells

Because of its well-known anatomy, physiology and cellular structure retina is a great system for studies of nervous system development. In the mouse, the multipotent retinal progenitor cells (RPCs) in the inner layer of the optic cup differentiates into the six main types of retinal neurons and Müller glia cells by following chronological order; the retinal ganglion cells, horizontal cells, cone photoreceptors, amacrine cells, rod photoreceptors, bipolar neurons, Müller glia cells (Young, 1985; Rapaport *et al.*, 2004). As shown in table 1.1, the retinal ganglion cells formation starts around Embryonic day 11 (E11), peaks on E13, and ends on E16, the horizontal cells formation also peaks around E13, the cone photoreceptors around E14, the amacrine cells around E15, the rod photoreceptors around PD2, and bipolar neurons peaks around PD4.

Retinogenesis starts after optic cup phase and continues throughout first two postnatal weeks. It has been postulated that already by PD13, around 97% of RGCs showed morphology comparable to one of the adult subtypes (Diao *et al.*, 2004). Coombs and colleagues (2006) in their studies showed that at postnatal PD1, the dendritic arbors of GCs largely overlap in the IPL while already on PD3-4, they separate and become confined to different IPL areas. Separation of dendritic fields of different types of GCs is thought to occur partially due to dendrite pruning and partially due to the vertical expansion of the IPL. On PD8, differentiation of GCs into different classes could be observed although the cells did not yet manifested their adult phenotypes. During early postnatal period, from PD1 through PD20, the morphological parameters of the cells such as soma area, dendritic field area, number of primary dendrites, the angle at which dendrites branch, number of branches, highest branch order, mean branch length, total dendrite length, the symmetry and tortuosity of the dendritic tree, spine density, dendrite and axon diameter undergo changes following different temporal patterns. According to Coombs et al. (2007), throughout the early postnatal period between PD1 and PD20, some morphological parameters of retinal GCs including dendrite number, branch angle,

symmetry, tortuosity, and axon diameter show almost no change. Some other parameters including soma area, dendritic field area, and mean branch length, remain unchanged during the first few days after birth, and then rapidly increase to reach the asymptotic value before PD20. Still other parameters such as total dendrite length, number of dendritic branches, highest branch order, dendrite diameter, and spine density first show linear increase and then regression to the adult values. Most (arount 97%) of retinal GCS was reported to show morphology close to that of mature cells approximately by the time of eye opening (PD11-12) (Diao *et al.,* 2004). Approximatelly by the same time mice' retina begin produce electrical responses to light (Chalupa and Williams, pp 195 2008)

Table 1.1. The Computed times of visual developmental events in mouse and human.

Neurodevelopment Event	**Mouse (PC days)**	**Human (PC days)**	**Structure**
RGCs generation - start of neurogenesis	10	38.1	Retina
superficial SC laminae- start of neurogenesis	10.7	41.9	Superior Colliculus
dLGN- start of neurogenesis	10.8	43	LGN
vLGN - peak of neurogenesis	11.7	47.9	LGN
axons in optic stalk	11.7	48.2	Optic Nerve
dLGN - peak of neurogenesis	12	49.9	LGN
optic axons at chiasm of optic tract	12.2	50.9	Optic Nerve
retinal horizontal cells - peak of neurogenesis	12.4	52.4	Retina
dLGN- end of neurogenesis	**12.8**	**54.4**	**LGN**
RGCs - peak of neurogenesis	**12.9**	**55.5**	**Retina**
optic axons reach dLGN and SC	**13.6**	**59.7**	**Optic Nerve**
optic axons invade visual centers	14.2	79.7	Cortex
superficial SC laminae - end of neurogenesis	14.2	62.8	Superior Colliculus
cones - peak of neurogenesis	14.7	66.3	Retina
retinal amacrine cells - peak of neurogenesis	15.2	69.2	Retina
RGCs - end of neurogenesis	**15.8**	**72.4**	**Retina**
LGN axons in subplate	16.2	94.6	Cortex
cortical axons reach dLGN	16.3	95.9	Cortex
optic nerve axon number - peak of neurogenesis	**17.2**	**80.9**	**Optic Nerve**
cortical axons innervate dLGN	18.4	111.4	Cortex
LGN axons in cortical layer IV	21.1	132.2	Cortex
superficial SC - start of lamination	21.2	104.6	Superior Colliculus
rods - peak of neurogenesis	21.6	106.9	Retina
visual cortical axons in SC	22.5	143.2	cortical
onset of retinal waves	20.6	101.2	Retina
retinal bipolar cells - peak of neurogenesis	23	115.5	Retina
rapid axon loss in optic nerve ends	**24.3**	**123**	**Optic Nerve**
ipsi/contra segregation in LGN and SC	**24.5**	**124.4**	**LGN and SC**
eye opening	29.7	155.3	eye opening

Table 1.1. presents the chronology of different visual developmental events in mouse and human. This table is provided from http://bioinformatics.ualr.edu/ttime/
Bold: developmental events addressed in the present study.

1.2.3. Development of Retinogeniculate Projection

The main output from retinal ganglion cell layer goes to eye-specific regions in dLGN of thalamus which projects through the optic radiation directly to the primary visual cortex (V1, or the striate cortex). In primates and human, the lateral geniculate nucleus has several layers, and the two eyes project to separate layers. In contrast to this, the lamination pattern is not obvious in rodents (De Courten and Garey, 1982; Garey and De Courten, 1983) although appropriate experimental methods revealed some pattern of lamination referred to as "hidden lamination" (Reese, 1988). Recent anatomical studies demonstrated several distinct ipsilateral projection areas within the rat dLGN (Discenza *et al.,* 2008). The ipsilateral projection fields showed bilateral symmetry and the same location in different animals. These data confirms the existence of multiple hidden laminas of both contra-and ipsilateral projections in rat.

In rodents, the anterograde labeling of retinal ganglion cells visualize the eye-specific patterns in LGN (Huberman *et al.*, 2003; Ziburkus and Guido, 2006). Retina ganglion axons originating from nasal and most of temporal retina cross at the optic chiasm and project contralaterally to the lateral and ventral regions of the LGN. In rodents such as rats and mice, crossed projections representing the contralateral eye predominate occupying aproximatelly 95% of the total area of LGN. The uncrossed (ipsilateral) projections originating from the temporal and ventral retina occupy the remaining 5% of the total area in the LGN (Dräger and Olsen, 1980). The nasal border of this bilaterally projecting region in the retina corresponds to the midline of the visual field. In primates including human, ipsilateral retinogeniculate projection occupies substantially larger

area within dLGN of about 20-25%. With laterally placed eyes and highly predominant contralateral retinogeniculate projection, rats and mice have poor binocular vision.

It has been shown that in rodents, the retinogeniculate fibers are site branches (collaterals) of retinocollicular axons (Linden and Perry, 1983; Martin, 1986). Contralaterally projecting ganglion cells were found to be generated from embryonic day E11 to about E19 in a crude concentric fashion with the oldest cells in central and youngest ones in peripheral retina. Ipsilaterally projecting cells were born from E11 to E16, that is, during the earlier part of the period in which the contralateral projection was born. In the adult retina, this bilateral projection system is preserved only in the large ganglion cells known to be the earliest ones formed in the mouse (E11-12) (Farah and Easter, 2005).

Crossed fibers start reaching the LGN at E16, while uncrossed fibers arrive at PD0. During the perinatal period (before and soon after the birth), crossed retinal fibers extend almost throughout the whole LGN. At PD0, uncrossed fibers start to innervate the LGN. Between PD2 and PD5, the projections from the two eyes still share a large amount of space. On PD7, a clear signs of segregation appear. In the period of natural eye opening around PD12–PD14, retinal projections coming from two eyes are well segregated and gave the same pattern found in the adult (Godement *et al.*, 1984; Jaubert-Miazza *et al.*, 2005).

It was demonstrated that segregation of retino-geniculate projections is accompanied by the high rate of death of retinal ganglion cells projectıng to inappropriate target areas in dLGN, and degeneration of their axons (Rakic, 1986; So *et al.*, 1990). It was however, also reported that some retinal output neurons may just retracte the axon collaterals invading inappropriate areas in LGN (Stanfield, 1984). The mechanism of refining the retino-geniculate projections is not quite clear. Some researchers suggest that the binocular projection system in the retina is established according to an early

developmental programme, rather than being the result of competition between the two eyes at later stages. However, it has been demonstrated that after unilateral removal of eye at birth, and thus removal of competing fibres, the transient synapses formed by the remaining eye in inappropriate dLGN regions with geniculate projection neurons and interneurons can survive (Robson *et al.,* 1978; Campbell *et al.,* 1985).

There is evidence that spontaneous activity such as retinal waves emerging during early postnatal period in the developing retina plays a role in the eye-specific segregation of retino-geniculate projections. Iwai and Kawasaki (2009) showed that when retinal waves were inhibited in both eyes, retinal projections from the two eyes remained intermingled in the LGN. Also, when neural activity was suppressed by intraocular administration of TTX, or when the same pattern of activity was delivered synchronously to both optic nerves the eye-specific fiber segregation was impaired (Shatz, 1990). It has been suggested that at early stage of postnatal development, between PD 0-8, the pattern of eye-specific segregation of retino-geniculate projections in the dLGN is modulated by cholinergic neurotransmission which then, by P10–P14, switches to glutamate signaling (Muir-Robinson *et al.,* 2002). On the other hand, however, stimulation by diffused light through the eyelids before eye opening seems not to play an important role in this process since the segregation of retino-geniculate fibers takes place in animals reared in darkness from birth (So *et al.,* 1982). Once the fiber segregation is almost complete before eye opening, patterned visual stimulation is probably not important either.

Interestingly, despite of the distinct eye-specific segregation of arriving retinal axons within dLGN, some of the target neurons give strong excitatory responses to stimulation of both eyes with receptive field organization similar for each eye (Grieve, 2005) which would suggest that, unlike in the other species (cats, monkeys), in small rodents binocular integration takes place already in the thalamus. Since, in the rat, a small number of RGCs has been reported to have bifurcating axons projecting to both ipsi- and contra-lateral dLGN (Jeffrey *et al.,* 1981; Kondo *et al.,* 1993), these neurons may be

responsible for the mentioned above binocular fusion. It is also possible that at least some binocular input to dLGN is not a direct input from the retina.

1.3. Effects of Perinatal Exposure to Alcohol on the Visual System Development

The effects of perinatal ethanol exposure on the developing brain have been extensively studied and well documented (Riley and McGee, 2005). Neuronal loss is one of the most common deleterious effects of perinatal exposure to alcohol on the CNS, and several studies have reported reduced numbers of neurons and fibers within different brain regions including the hippocampus (Barnes and Walker, 1981; Gonzalez-Burgos *et al.*, 2006; Livy *et al.*, 2003; Miki *et al.*, 2003; Moulder *et al.*, 2002) cerebellum (Goodlett *et al.*, 1998; Goodlett and Eilers, 1997; Miki *et al.*,1999; Thomas *et al.*, 1998), and corpus callosum (Qiang *et al.*, 2002; Riley *et al.*, 1995). Both human and animal research has shown reductions in brain weight and microencephaly resulting from prenatal exposure to alcohol (Jones *et al.*, 1973; Clarren *et al.*, 1978; Streissguth *et al.*, 1980; Pierce and West, 1986; Bonthius and West, 1990; Little *et al.*, 1990; Tran *et al.*, 2000). Several mechanisms have been reported to result in ethanol neurotoxicity including: oxidative stress, induction of apoptosis, excitotoxicity, disruption of cell–cell interaction, and interference with the activity of growth factors (Goodlett *et al.*, 2005). Neurons are more sensitive to ethanol-induced apoptotic cell death for the period of synaptogenesis, also known as the brain growth spurt (Ikonomidou *et al.*, 2000; Olney *et al.*, 2000).

Despite of substantial knowledge related to the adverse ethanol effects on the developing nervous system relatively less is known about the effects of prenatal ethanol exposure on the developing visual system.

1.3.1. Human Studies

Several studies have shown that ophthalmologic abnormalities are frequently observed in children with FAS or FASD. Perinatal alcohol exposure produces a variety of types of damage to the visual system. Ocular defects have been reported in about 90% of children with FAS suggesting that ocular structures are sensitive to alcohol exposure during their development (Strömland, 1987). Visual attention and higher visual processing impairment has been also reported in children born to alcoholic mother (Coles *et al.,* 2002; Connor *et al.,* 1999).

The optic nerve is the most commonly and seriously affected structure of the eye by ethanol intoxication. As reported by Strömland (1985), out of 30 FAS-related ocular anomalies 48% was due to hypoplasia of the optic nerve head. Another ophthalmology examination performed on the 25 children with FAS by Strömland and Hellström (1996) showed that 92% of the examined group had ophthalmologic abnormalities in ocular structure such as the eye balls (globes), anterior segments and media, and retina, with optic nerve hypoplasia found in 76% of the studied cases. In another clinical study by Hug *et al.,* (2000) optic nerve hypoplasia was found in 91% of the 11 children diagnosed with FAS. Additional ophthalmologic examinations reported similar results (Streissguth *et al.,* 1985; Strömland, 1987, 1990; Miller *et al.,* 1984; Chan *et al.,* 1991; Carones *et al.,* 1992; Strömland and Sundelin, 1996; Chan, 1999; Bruce *et al.,* 2009). The retinal fundus (the portion of the inner eye) examination in children with FAS showed increased tortuosity of the retinal vessels and malformation of the optic disks (Strömland, 1982, 1985, 1987; Miller *et al.,* 1981; Miller *et al.,* 1984; Chan *et al.,* 1991; Carones *et al.,* 1992; Strömland and Hellström 1996; Strömland and Sundelin, 1996; Strömland and Pinoza-Duran, 1994; Ribeiro *et al.,* 2007; Flanigan *et al.,* 2008).

However, the most often mentioned ocular defect linked to prenatal intoxication with alcohol is reduction in the eyes size known as microphthalmia (Jones *et al.,* 1973;

Strömland, 1982, 1985, 1987; Chan *et al.,* 1991; Little *et al.,* 1990; Hellström *et al.,* 1997; Strömland and Pinoza-Duran, 2002). It has been first reported by Lemonie *et al.,* (1968) and then accepted as one of the criteria for the diagnosis of FAS by the Fetal Alcohol Study Group of the US Research Society on Alcoholism (Rosett, 1980).

Strabismus is also a frequent finding in children with FAS. Esotropia (deviation of the eyes inward) is most common type of the strabismus reported in FAS, as well as exotropia (deviation of the eyes outward) (Jones *et al.,* 1973, 1974; Miller *et al.,* 1981, Miller *et al.,* 1984; Streissguth *et al.,* 1985; Strömland, 1985, 1987, 1990; Chan *et al.,* 1991; Strömland and Pinoza-Duran, 1994, 2002; Strömland and Hellström, 1996; Chan, 1999; Hug *et al.,* 2000; Ribeiro *et al.,* 2007; Bruce *et al.,* 2009).

These eye morphological anomalies related to FAS are accompanied by functional deficits. There are many reports on reduced visual acuity in children suffering from FAS (Miller *et al.,* 1981; Miller *et al.,* 1984; Strömland, 1985, 1987, 1990; Strömland and Pinoza-Duran, 1994, 2002; Strömland and Hellström, 1996; Strömland and Sundelin, 1996; Hug *et al.,* 2000; Carter *et al.,* 2005). There are also several clinical reports about significant refractive errors such as myopia, hyperopia, amblyopia and astigmatism observed in children with FAS (Miller *et al.,* 1981, 1984; Strömland, 1985; Chan *et al.,* 1991; Chan, 1999; Bruce *et al.,* 2009). In addition, defects in cornea, anterior chamber and iris (Peters' and Axenfeld's anomaly), cataract, glaucoma have been found in children exposed to chronic alcohol during gestation (Miller *et al.,* 1981, Miller *et al.,* 1984; Streissguth *et al.,* 1985; Strömland, 1985; Carones *et al.,* 1992; Strömland and Sundelin, 1996; Strömland and Hellström, 1996; Strömland and Pinoza-Duran, 1994, 2002; Ribeiro *et al.,* 2007).

In addition to ocular defects, short horizontal palpebral fissure (small opening of the eye) and ptosis (drooping eyelid) are very important indicator for FASD diagnosis (Jones *et al.,* 1973, 1974; Jones and Smith 1973; Clarren *et al.,* 1978; Miller *et al.,* 1981;

Streissguth *et al.,* 1985; Strömland, 1985; Chan *et al.,* 1991; Carones *et al.,* 1992; Little *et al.,* 1990; Strömland and Pinoza-Duran, 1994, 2002; Chan, 1999; Hug *et al.,* 2000; Bruce *et al.,* 2009).

1.3.2. Animal Studies

The adverse effects of fetal and perinatal ethanol intoxication on visual system development have been investigated in a number of animal species including, fish (Arenzana *et al.,* 2006; Matsui *et al.,* 2006; Dlugos and Rabin, 2007; Kashyap *et al.,* 2007), chick (Chmielewski *et al.,* 1997; Tufan *et al.,* 2007), mouse (Kennedy and Elliott, 1986; Cook *et al.,* 1987; Ashwell and Zhang, 1994; Parson *et al.,* 1995; Parson and Sojitra, 1995), rat (Philips *et al.,* 1991; Pinazo-Duran *et al.,* 1993, 1997; Strömland and Pinazo-Duran, 1994; Harris *et al.,* 2000) and monkey (Clarren *et al.,* 1990; Papia *et al.,* 2010). As a result of the marked similarity among the eyes of all vertebrates, it is not surprising that microphthalmia, retinal ganglion cell loss, optic nerve hypoplasia, delayed myelination, and/or reduced myelin thickness in the optic nerve fibers have all been observed after ethanol exposure during the embryonic development.

In the first publication related with the effects of ethanol intoxicatin on developing visual system (Stockard, 1910), the fish embryos were investigated. Later on, chicken and zebrafish embryos were used as a vertebrate model of ethanol teratogenicity. In these experiments, zebrafish embryos were exposed to different concentrations of ethanol (from 0.1% to 2.4%). The following examination of eyes morphology revealed a delay in the lamination of the neuronal retina, decreases in the volumes of the photoreceptor, inner nuclear, and ganglion cell layers, inhibition in the photoreceptor outer segment growth, reduced eye and lens size, and optic nerve hypoplasia. (Arenzana *et al.,* 2006; Matsui *et al.,* 2006; Dlugos and Rabin, 2007; Kashyap *et al.,* 2007) Observed deficits were proportional to ethanol dose used in the experiments.

Another successful model to investigate the potential effects of ethanol intoxication is a chick embryo. Fertilized chick embryos were exposed either to different concentrations of ethanol (10, 30, or 50% (v:v) in 0.9% NaCl) (Tufan *et al.,* 2007), or to a single high ethanol dose (50% (v:v)) (Chmielewski *et al.,* 1997). In these experiments too, ethanol caused dose-dependent deficits incuding retina degeneration, optic nerve hypoplasia, and decrease in the number of myelinated nerve fibers.

Among animal models used in the studies on ethanol effects on the developing visual system, the rodent model is most common. In mice, it has been shown that even a single exposure to ethanol, mimicking a 'binge' abuse of alcohol in human, when applied during a critical period of ocular ontogeny, was sufficient to cause adverse ocular changes and eye malformation (Sulik *et al.,* 1981; Sulik and Johnston, 1983; Kennedy and Elliott, 1986; Cook *et al.,* 1987). Several investigators demonstrated that a single intraperitonal ethanol injection on the gestation day (GD) 11 or 12 led to a decrease in the cross sectional area of the optic nerve and in the number of myelinated axon in addition to delayed myenilation of the optic axons (Parson *et al.,* 1995; Parson and Sojitra 1995; Dangata and Kaufman, 1997). Ashwell and Zhang, (1994) also observed reduction in the number of optic nerve axons, and deficient myelination. Despite of this no significant changes in the number of neuron in the dorsal lateral geniculate nucleus and superior colliculus were recorded after a single intraperitonal ethanol injection on the GD 8. Conversely to this, in the studies by other authors, a single ethanol intoxication episode during the early postnatal period was shown to trigger apoptosis of both retinal ganglion cells and the neurons at higher levels of visual system (Tenkova *et al*., .2003). Tenkova and colleagues observed a significant RGCs degeneration in rat pups after a single exposure to ethanol applied at various postnatal ages within the first postnatal weeks of life. The loss of RGCs was especially pronounced during a relatively narrow developmental time window from PD 1 to PD 4. The period of peak sensitivity for the higher order visual neurons was defined as postnatal days 4-7.

After the exposure of rat pups to 4% (v/v) ethanol in liquid diet on PD 5-9, morphological examination of the rats' optic nerve with electron microscopy carried out on the PD 10,16,22,29, and 90 revealed at P10 the reduced number of myelinated axons in the optic nerve but also delayed maturation of oligodendroglial cells (Philips, 1989; Philips and Kreuger, 1990). Subsequently, Philips and colleagues (1991, 1992) compared the effects of prenatal (GD1- untill birth) and early postnatal (PD 1-10) exposure to ethanol applied to the Sprague- Dawley rats (dams or pups) in a liquid diet containing 6% (v/v) or 3% (v/v) ethanol, the two doses resulting in intermediate BACs, 82 and 166 mg/dl, respectively. Alike other authors, they also reported reduction in the cross sectional area of the optic nerve, and a decrease in the thickness of the myelin sheath around the optic nerve fibers. These changes were observed at GD15, GD20, PD5, PD10, PD15, PD20, and PD90. Reduced number of optic nerve oligodendroglial cells was noted at PD15 and PD20 but not at PD90. Samorajski *et al.*, (1986) showed that administration of 30% EDC liquid diet through GD 4-19 to the Long Evans dams resulted in 15% reduction in the numbers of myelinated axons, however, this decrease was yielded insignificant. In contrast to this, the ratio of non-myelinated axons to myelinated axons was significantly greater in the pups exposed to ethanol on PD14. This deficit in the number of myelinated optic fibers became insignificant on PD28 what suggested some catch-up towards normal development. Similarly, in theWistar rat offspring exposed on PD4 -9 to either high or low ethanol ethanol dose (producing mean BAC of 171 mg/dl and 430 mg/dl, respectively) delivered by vapour chamber (Harris *et al.*, 2000) a decrease in the total number of optic nerve fibers and delayed myelination of the optic axons was observed when examined at PD10 and PD30.

Chronic alcohol intake prior to conception, and then throughout the whole gestation and lactation period was also shown to cause a decrease in the ocular globe weight, optic nerve size, the number of myelinated optic axons and in the thickness of myelin sheaths, as well as, the delay in the maturation of both oligodendroglial, and astrocytes were observed (Strömland and Pinoza-Duran, 1994; Pinoza-Duran *et al.*, 1997).

In primate experiments, Clarren *et al.,* (1990) reported ocular abnormalities, microphthalmia, and retinal ganglion cell loss after weekly binge like exposure to ethanol throughout pregnancy in different doses (0.3, 0.6, 1.2, 1.8, 2.5, 3.3, or 4.1 g/kg).

The presented survey of animal literature shows that up-to-date research of adverse effects of ethanol on the developing visual system mainly focused on the ocular changes and the optic nerve anomalies. There is very scarse information about alcohol effects on retinal cell morphology. However, ethanol effects on the cell morphology have been reported in other brain areas. For instance, Qiang *et al.,* (2002) reported abnormal dendritic arborization of corpus callosum projection neurons after ethanol exposue during the second trimester equivalent in rats. Most recently, Papia *et al.,* (2010) studying the effects of alcohol intake during the 3rd trimester of gestation on LGN structure in nonhuman primate found .significant reduction in the soma size of M neurons and no effect on the neuron numbers in the LGN's P and M regions

1.4. Aim of the Study

Most of the so far studies examining ethanol effects on the developing visual system focused on alcohol-induced ocular changes, the changes in the numbers of optic nerve fibers, and optic nerve myelination. Conversely, little is known about the potential effects of fetal and early postnatal ethanol exposure on the morphology of retinal neurons and their connection with higher order visual centers in the brain. Examination of the potential toxic effects of drugs including alcohol on the neuron architecture is important as it is well known that the neurons' dendritic arborization and the synapse distribution along the neurites have profound effects on the organization and functions of local neural circuits.

The results of many earlier animal studies suggest that in rodents, the visual system shows increased vulnerability to the adverse effects of ethanol during the first 10

postnatal days, the time corresponding to the third trimester in human and known as the brain growth-spurt period (Dobbing and Sands, 1979; Rice and Barone, 2000). On the other hand, in rodents, the RGCs development is not completed until PD20 when the dendritic arbor is finally shaped (Chalupa and Williams, 2008, pp194). Therefore, it is important to examine the potential adverse ethanol effects on developing retina over the extended postnatal period covering the whole process of RGCs maturation.

Having all these in view, the present study was designed to investigate the effect of the early postnatal exposure to ethanol on the morphology of RGCs, the numbers of neurons within the retinal GCs layer and dLGN, and the eye-specific segregation of optic nerve fibers in the dLGN in mice.

CHAPTER 2

MATERIALS AND METHODS

2.1. Subjects

Transgenic mice expressing Yellow Fluorescent Protein (YFP) controlled by a thymus cell antigen 1 (Thy-1) regulator on a C57 background (YFP-H line, Jackson Laboratory, Bar Harbor, ME, USA) were used in retina ganglion cell morphology study to visualize the whole structure of the retina ganglion cells including cell bodies, axons, nerve terminals, dendrites and dendtritic spines of retina ganglion cells (Feng *et al.*, 2000).

In anterograde labeling of retinogeniculate projections study and for neurons counting C57BL/6 mice from Charles River Laboratories (Wilmington, MA) were used.

In both studies, both male and female mice were used. All procedures were approved by the Institutional Animal Care and Use Committee of the University of California, Davis (IACUC). Animals were housed in the Sciences Laboratory Building, Animal Facilities room that was on a 12:12 h light:dark cycle (lights on 6 a.m. and off 6 p.m.) and maintained at 23°C and 50% humidity (Tecniplast,21020 Buguggiate VA, Italy).

2.2. Breeding

Female mice were housed in Plexiglas cages with commercial bedding material made from reclaimed cellulose pulp fiber (Carefresh). For mating, a male mice picked at random, was placed into a female's cage. Mice were mated nightly until a vaginal plug was observed on the following morning. The presence of a vaginal plug was used as evidence of successful fertilization and this day was marked as Gestational Day (GD) 0. Pregnant female mice were individually housed in its home cage with free access to laboratory chow and water.

2.3. Pups

Pregnant females were checked every day during the light cycle. The day of birth was determined as Postnatal Day (PD) 0. Each pup was weighted prior to the intubation throughout treatment. They remain with their natural mothers until treatment was completed.

2.4. Neonatal Treatment

The intubations were done starting from PD3 throughout PD 20. On PD3, one hour before the intubation all litter was taken from dam and put on a heating pad (GCA, Precision Scientific, Chicago, IL) maintained at 37 °C. Pups were weighed and marked with nontoxic marker for identification. Intubations were carried out using a PE-10 tubing (Clay Adams Brand, Becton Dickinson) lubricated with corn oil and attached to a 1cc insulin syringe (BD Ultra-Fine II) filled with milk with or without ethanol. The length of the tube was measured from the mouth to the stomach and marked. The PE-10 tube was carefully inserted down the esophagus into the stomach and a measured amount of solution was given immediately (Figure 2.1). Pups were weighed daily throughout the treatment. Pups in the alcohol group (A) were intubated with 3.0 g/kg

body weight ethanol (EtOH 200 proof, Sigma-Aldrich) in a volume (0.02 ml/g) of artificial enriched milk. The ethanol dose of 3.0 g/kg body weight was applied in earlier rodent studies by other authors and was shown to be effective in producing adverse effects on brain morphology and behavior (Tran *et al.,* 2000; Green *et al.,* 2006). This solution was divided into two equal doses given to pups two hours apart. Two hours after the second intubation, pups were intubated again with 0.02 ml/g of the milk solution alone. Between intubations, pups were returned back to the dams. Pups in the Intubation Control group (IC), a control for possible intubation-induced stress effects, were intragastrically intubated three times each day in the same manner as the Alcohol group (A) but received neither ethanol nor milk. This is because according to Goodlett and Johnson, (1997) IC pups gain more weight than C pups when intubated with milk. Besides the IC group, there was a Control group (C) weighed daily with no additional treatment. The pups were intubated at the same time each morning.

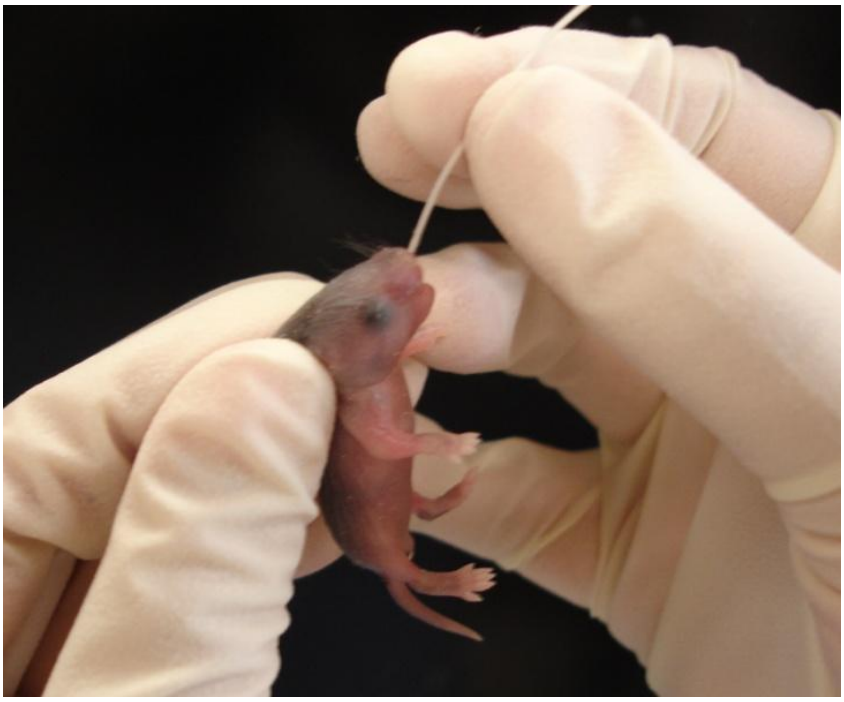

Figure 2.1 The moment of intragastric intubation

2.5. Diet

An artificial enriched milk and milk/ethanol solutions were prepared according to a method applied by Kelly and Lawrence (2008). Sterile conditions were used to prepare this solution. A mineral mix which contains 1.2 g of ZnSO4, 1.2 g of CuSO4, 1.2 g of FeSO4, 20 g of MgCl, 20 g of KCl was added into 500 ml of sterile H2O. Because this mixture is a slurry one, it had to be stirred prior to its combination with the milk solution. A vitamin mix specially formulated and listed as the custom mix for the University of Iowa was ordered from BioServ. In order to prepare the milk solution 50 ml of the mineral mix as described above, 10 g of vitamin mix ordered from BioServ, 70 g of Supro 710 protein power, 130 ml of corn oil, 2 g of methionine, 1 g of tryptophan, 11 g of calcium phosphate dibasic, and 0.2 g of deoxycholic acid were combined and added to the 1500 ml of evaporated milk dissolved in 450 ml of sterile H2O. This final mixture was homogenized. In this work, it is referred to as the milk solution. 50 ml portions of the milk solution were put into small bottles which were then sealed with a rubber topper. To pasteurize the milk solution, the bottles were heated in an oven to 60 - 65°C for 30 minutes and then cooled very fast. These bottles were stored −60°C, that provides stability to the milk solution for a very long time. In the alcohol group, prior to the intubation, a bottle of milk was thawed and a required amount of ethanol was added. To determine the amount of ethanol added to each 50 ml of the stock milk solution, calculations were done taking as the basis the known density of 100% ethanol equal to 0.7893 g/ml, the ethanol dose to be applied equal to 3.0 g/kg body weight, and the to be applied fluid volume equal to 0.02 ml/g body weight. Accordingly, the amount of ethanol in per ml of the stock milk solution should be 0.15 g. The volume of 100% ethanol that should be added to the 50 ml of the stock milk solution in order to reach the above ethanol concentration was calculated as follows:

$$\frac{0.15\ \text{g}}{1\ \text{ml}} = \frac{\frac{0.7893\text{g}}{\text{ml}} * \text{X ml (100 \% EtOH)}}{50\text{ml (milk)} + \text{X ml (100 \% EtOH)}}$$

$$0.15 * 50\ \text{g ml} + 0.15 * \text{X g ml} = 1\ \text{ml} * \left(\frac{0.7893\text{g}}{\text{ml}} * \text{X ml}\right)$$

$$0.75\ \text{g ml} + 0.15\ \text{X g ml} = 0.7893\text{X g ml}$$

$$0.75\ \text{g ml} = 0.7893\text{X g ml} - 0.15\text{X g ml}$$

$$0.75\ \text{g ml} = 0.6393\text{X g ml}$$

$$\text{X} = \frac{0.75\ \text{g ml}}{0.6393\ \text{g ml}}$$

X= 11.731 ml of 100% EtOH to a 50 ml bottle of milk solution.

2.6. Experiment 1: Retina Ganglion Cell Morphology

2.6.1. Retina Collection

On PD20, after the last intubation, the pups from A, IC, and C groups were euthanized with a lethal i.p. dose (0.1 ml) of Fatal Plus (Vortech Pharmaceuticals). After enucleation, the cornea and lens were removed. Before removing the retina from the sclera, a notch was made to identify the nasal retina. Retina was dissected out and vitreous removed using paint brushes. The eyecup was fixed for 2 h in 4% PFA in PBS then washed and stored in PBS until processed for immunohistochemistry.

2.6.2. Immunohistochemistry

Fixed retinas were blocked for 2 h in a blocking solution containing 10% normal donkey serum (Jackson Immuno Research), 2% bovine serum albumen (Jackson Immuno Research), 0.3% Triton X-100 in PBS (Fisher Chemicals). The following primary antibodies were diluted in fresh blocking solution: rabbit anti-green fluorescent protein (GFP) (1:500; Invitrogen, Carlsbad, CA) and a goat anti-choline acetyltransferase (1:50; Chemicon International, Temecula, CA). The retinas were incubated in the primary antibody for 3–4 days at 4 °C. After washing three times in PBS, the retinas were incubated for 2 h at room temperature in secondary antibodies Alexa-488 and Alexa 568 (1:500; Invitrogen, Carlsbad, CA) diluted in PBS. Finally, retinas were rinsed three times in PBS and incubated overnight in DAPI (1:500; KPL, Gaithersburg, MD). Radial cuts were made to flatten the retina (see Fig. 2.19), with careful note taken to the nasal identifying notch. Flattened retinas were then mounted on a glass slide, coverslipped with PBS as the mounting media and sealed with Depex (Electron Microscopy Sciences, Washingtion, PA).

2.6.3. Imaging and Morphometric Measures

The retinal ganglion cells that had obvious axons were chosen for imaging (Figure 2.2). High-resolution three-dimensional images were taken using an Olympus Fluoview 500 confocal microscope with the following parameters; x and y =1024 x 1024 pixels, and two images averaged at each focal plane.

Confocal microscopy has advantages of the ability to control depth of field, elimination or reduction of background information away from the focal plane, and the capability to serially produce thin (0.5 to 1.5 micrometer) optical sections from thick materyal. With most confocal microscopy software packages, optical sections are not restricted to the perpendicular lateral (x-y) plane, but can also be collected and displayed in transverse

planes. Vertical sections in the x-z and y-z planes can be readily generated by confocal software programs (www.olympusmicro.com).

A broad range of lasers such as UV laser (351-405 nm) for "UV-signals" i.e, DAPI, Argon Blue (458/488/515 nm) for "green or yellow" signals i.e, AlexaFluor-488, Green Helium Neon (543nm) for "red" signals i.e, AlexaFluor-546/568 Yellow Krypton (568nm), Red Helium Neon (633nm) and Helium Cadmium (442nm) lasers are available to suit most fluorescence applications. In the present study, each confocal image stack of individual retinal ganglion cells was traced using Neurolucida software (Microbrightfield, Williston, VT).

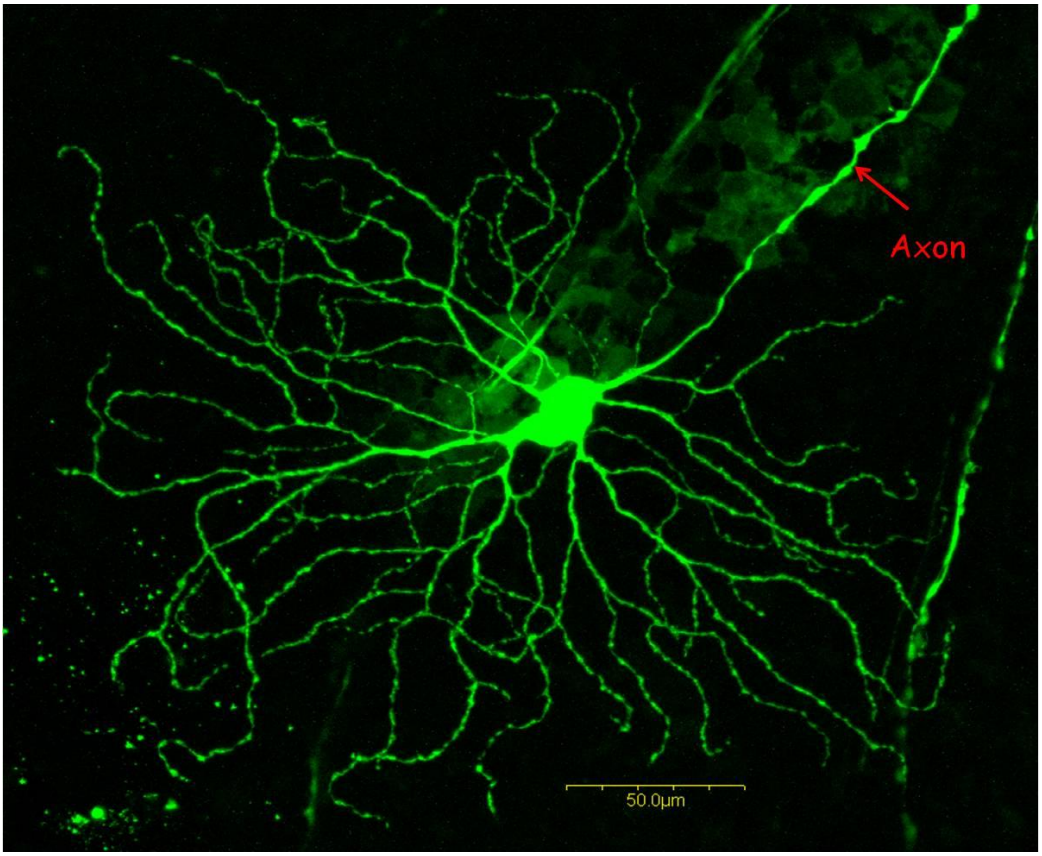

Figure 2.2 Confocal image of retina ganglion cell. Scale bar: 250 µm

Thirteen parameters were measured and analyzed as described by Coombs *et al.,* (2006). The measured parameters are described beneath.

1- Somal size: A topographic series of contour lines were drawn around each soma to outline the shape in three-dimensions with the largest contour used to calculate the area (Fig.2.3).

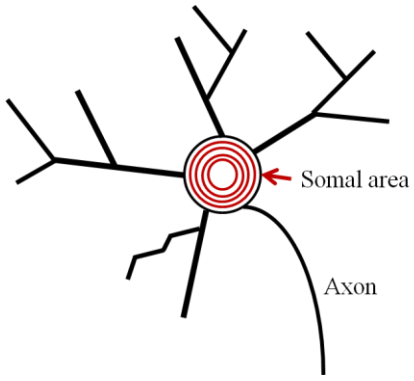

Figure 2.3 Schematic diagram of somal area

2- Dendritic field area: A line was drawn connecting the outermost tips of the dendrites around the edge of the arbor with dendritic field area defined as the area within this contour (Figure 2.4).

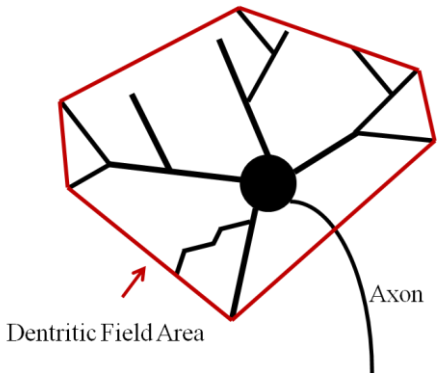

Figure 2.4 Schematic diagram of dentritic field area

3- Total dendrite length: The sum of the lengths of all the dendrites, a+b+c+d+e+……. (Figure 2.5).

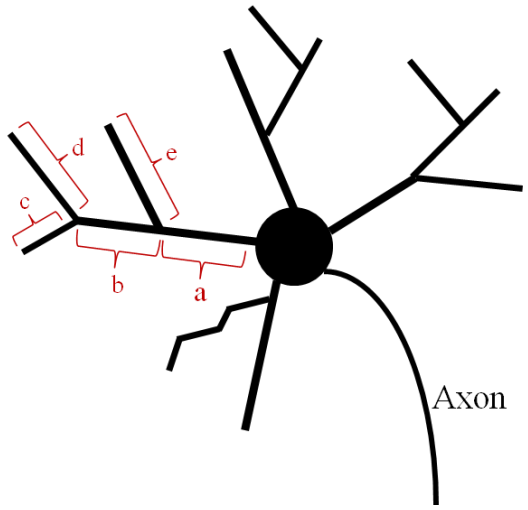

Figure 2.5 Schematic diagram of total dendrite length

4- Number of dendritic branches: all branches of all dendrites per cell (Figure 2.6 1,2,3,4,5,6,7,……).

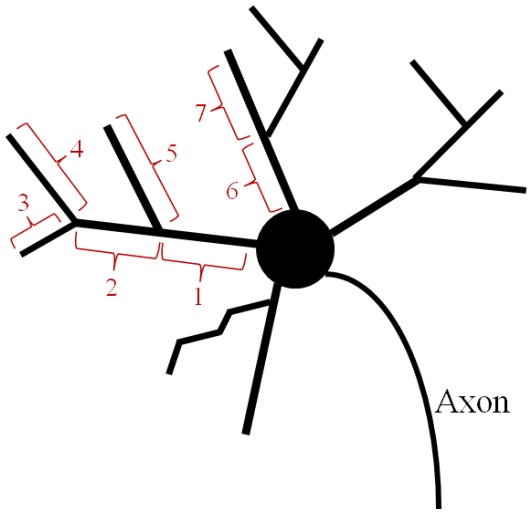

Figure 2.6 Schematic diagram of number of dendritic branches

5- Branch order: The largest number of times a dendrite branches, with the primary branch emerging from the soma defined as branch order 1 (Figure 2.7).

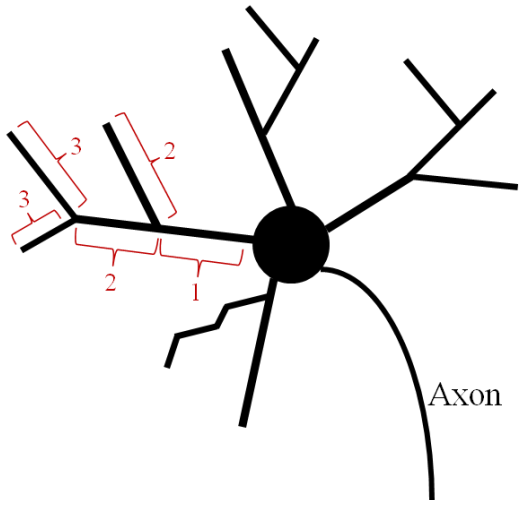

Figure 2.7 Schematic diagram of branch order

6- Mean internal branch length: average distance along the dendrite between the soma and the first branch point and between branch points (Figure 2.8).

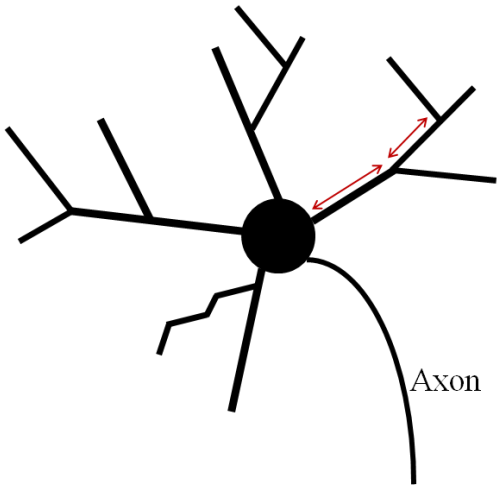

Figure 2.8 Schematic diagram of mean internal branch length

7- Mean terminal branch length: Average distance along the dendrite from the last branch point to the end of the dendrite (Figure 2.9).

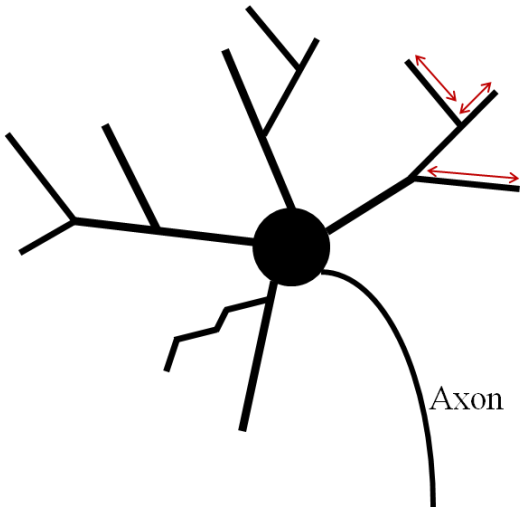

Figure 2.9 Schematic diagram of mean terminal branch length

8- Branch angle: The angle (in three-dimensions) formed by two lines that each pass through the branch point and the two subsequent branch points (Figure 2.10).

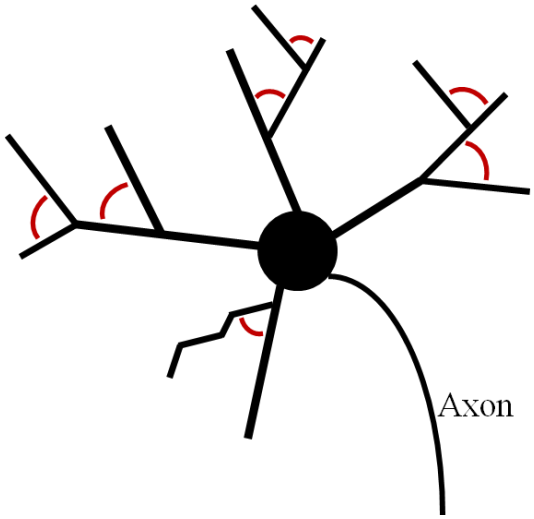

Figure 2.10 Schematic diagram of branch angle

9- Number of dendrites: Number of primary dendrites emerging from the soma (Figure 2.11).

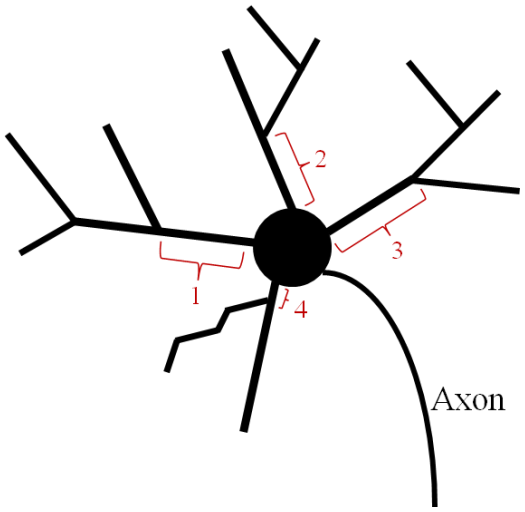

Figure 2.11 Schematic diagram of number of dendrites

10- Spine density: The total number of spines divided by the total dendrite length (Figure 2.12). Spines were defined as terminal dendritic projections less than 5 μm long.

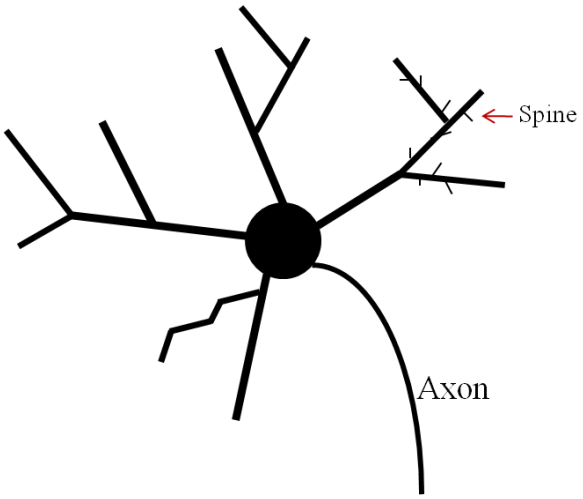

Figure 2.12 Schematic diagram of spine density

11- Dendrite diameter: The mean diameter of the three branch orders closest to the soma (Figure 2.13).

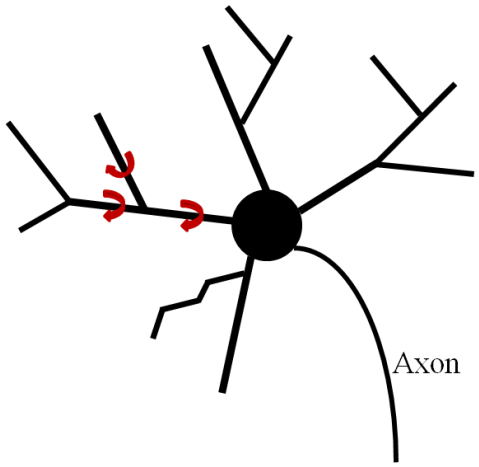

Figure 2.13 Schematic diagram of dendrite diameter

12-Tortuosity: The ratio (a/b) of the length along each dendritic branch (a) and the length of the straight line drawn between the two nodes (b) that define the branch (Figure 2.14).

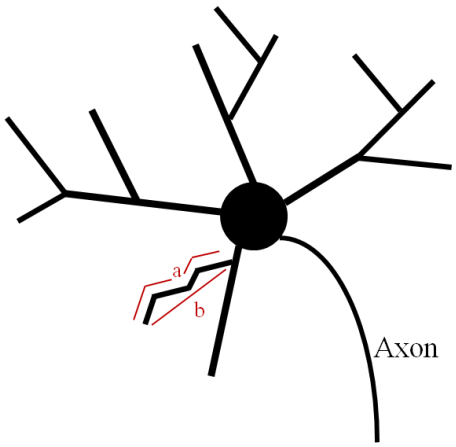

Figure 2.14 Schematic diagram of tortuosity

13- Symmetry: Location of the soma in relation to the dendritic field from a bird's-eye view, expressed as a percentage of the radius of the dendritic field and the distance of the soma from the closest edge of the dendritic field (Figure 2.15).

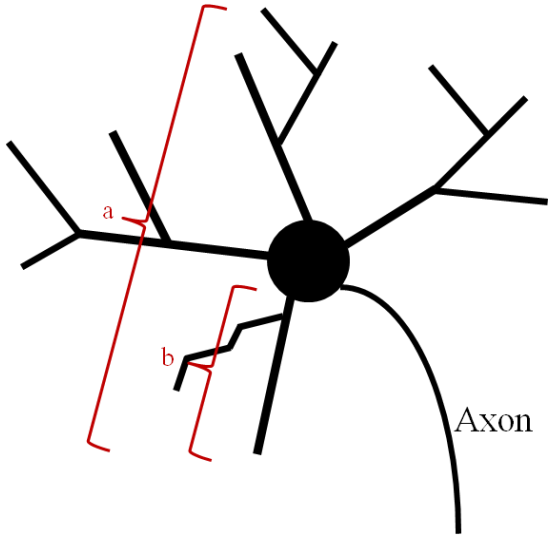

Figure 2.15 Schematic diagram of symmetry ((a/2)-b / (a-2))

2.7. Experiment 2: Anterograde Labeling of Retinogeniculate Projections

As earlier mentioned, in this study, the male and female C57BL/6 mice from Charles River Laboratories (Wilmington, MA) were used. The C57BL/6 mice were assigned to one of the three experimental groups: the alcohol treated (A), intubation control (IC), and pure control (C) group. The groups were treated as described in the Section 2.4. except that the treatment was carried out from PD3 throughout PD 10 only.

2.7.1. Tissue Collection

On PD9, pups in each group were anesthetized with a cocktail containing 3.5 mg/kg ketamine and 2.1 mg/kg xylazine in 0.9% sterile sodium chloride saline solution.

Borosilicate glass micropipettes (Sutter Instrument Co., Novato, CA, USA) were pulled on a Flaming/Brown micropipette puller (Sutter Instrument Co.) and filled with 1-1.5 µl cholera toxin-β (CTB) either conjugated to Alexa 488 or Alexa 594 (Invitrogen, Carlsbad, CA). The eyelids were opened and intraocular injections of CTB conjugated to Alexa 488 (green) or 594 (red) were administrated to the left and right eye, respectively. The excitation and emission spectra of the Alexa Fluor dyes cover the visible spectrum and extend into the infrared frequency band (Panchuk–Voloshina *et al.,* 1999). Each eye was injected with a different fluorescent conjugate with projections from both eyes visualized at the same time in the LGN sections. After the intraocular dye injections, eyes were treated with a triple antibiotic ophthalmic ointment and the animal was placed on a heating pad maintained at 37 °C until full movement has been restored. On PD10, pups received the same regime as on the previous days and 24 hours after CTB injection, lethal IP dose (0.05-0.1ml) of Fatal Plus (Vortech Pharmaceuticals; Dearborn, MI) was administered. The brains were removed from the skull, fixed for 2 days in 4% paraformaldehyde (PFA, Sigma, St. Louis, MO) in 0.1M phosphate buffered saline (PBS, EMD Chemicals Inc. Gibbstown, NJ). Then, the brains were embedded in 3.5% agar (Sigma, St. Louis, MO). The resulting agarose block containing the tissue piece was then glued to a metal block, submerged in a 0.1 M PBS bath and sectioned at 50 µm in the coronal plane using a vibratome (Leica Microsystems; Bannockburn, IL). Individual sections were then collected with a fine brush, transferred to multiwell plates filled with 0.1 M PBS, and eventually mounted on slides. The sectioning of brain with vibratome has some advantages when doing immunohistochemistry. The vibratome is similar to a microtome but uses a vibrating razor blade to cut through tissue. The vibration amplitude, the speed, and the angle of the blade can all be regulated. With this method the structure of tissue sections is not disrupted due to freezing and thawing.

2.7.2. Imaging and Morphometric Measures

Images of the dLGN slices from pups treated with CTB were taken on a Nikon Eclipse E600 upright microscope equipped with an CCD digital camera (Hamamatsu Photonics) using a 10X objective lens. Imaging and quanitification of retinogenicular projections was carried using similar procedures to those described previously (Huberman *et al.*, 2003). Images were pseudocolored (Figure 2.16) using the Wasabi software (Hamamatsu, Japan). Raw images of green (Alexa 488) or red (Alexa 594) fluorescently labeled retinal ganglion cell input to the dLGN were imported to the Photoshope (Adobe) and Illustrator for the montages and removal of unwanted areas. Images were converted to gray scale (Figure 2.17) and cropped to virtually dissect the dorsal part of LGN and to exclude the optic tract and medial intralaminar nucleus (Figure 2.18). Image intensity was set to 30% above background, and pixel intensities less than 30% above background were set to black, and intensities greater than 30% above background were set to white. The 30% above background value is adopted from previous studies (Penn *et al.*, 1998; Huberman *et al.*, 2002). Measurements of the dLGN areas receiving projections from the contralateral and ipsilateral eye, respectively, were determined by selecting all white pixels within the image frame using Image J (Image J, NIH). Three sections from the middle portion of the dLGN per animal were used for analysis.

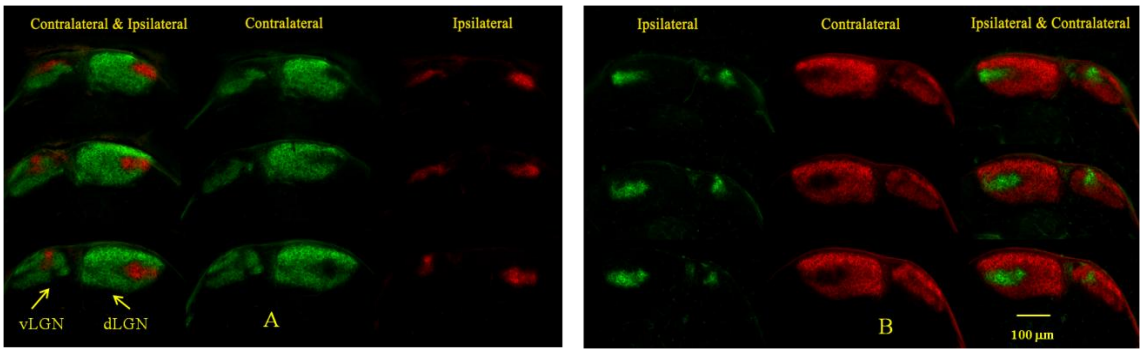

Figure 2.16 Visualization of retino geniculate afferent in mice at P10 showing the merged representations of contralateral and ipsilateral retinal inputs to the LGN. Axons from the left eye are shown in green (A). Axons from the right eye are shown in red (A). Scale bar: 100 µm

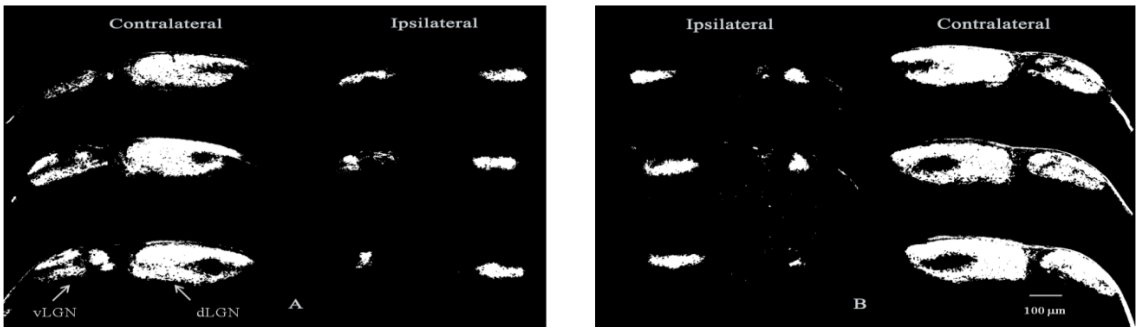

Figure 2.17 Gray scaled images. Scale bar: 100 µm

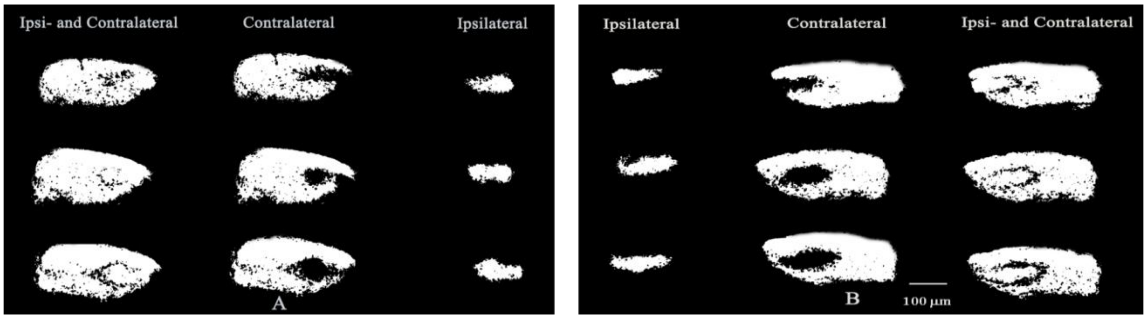

Figure 2.18 Virtually dissected dorsal parts of gray scaled images. Scale bar: 100 µm

2.8. Experiment 3: Cell Count

2.8.1. Cell Count in the Retina

In this study, retinas were dissected out as described in the Section 2.6. Free-floating whole retina tissues were stained with 0.1% cresyl violet for 6 minutes then rinsed twice with the PBS, 20 seconds each time. Stained wholemount retinas were mounted on a glass slide in PBS, coverslipped, and sealed with Depex (Figure 2.19). Using a Nikon E600 microscope, with a 20X objective, a contour line was drawn around each retina. A 100X oil-immersion lens was used for cell counting (Figure 2.20). The unbiased stereological method employing StereoInvestigator software (Microbrightfield, Williston, VT) was used for counting the neurons within the retina ganglion cell layer. The counting frame was set at 25μm with a grid size of 500μm. The total numbers of neurons estimated by optical fractionators were used for statistical analysis.

Figure 2.19 Picture of cresyl violet stained whole mount retina

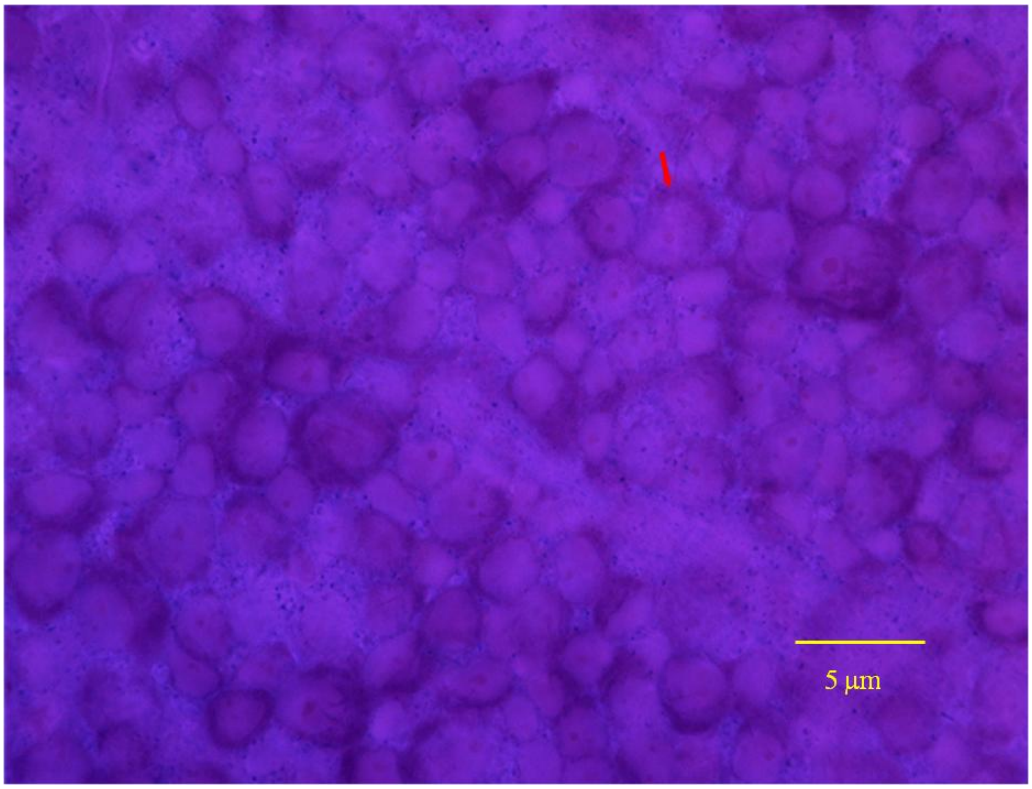

Figure 2.20 The microphotograph of the Nissl stained fragment of retina visualized under X100 magnification. The arrow points one of the neurons within the retina ganglion cell layer. Scale bar: 5 µm

2.9. Cell Count in the dorsal Lateral Geniculate Nucleus (dLGN)

For the neuron counts within the dLGN, mice were sacrificed with the lethal dose of IP Fatal plus either on PD 10 or on PD 20. The brains were perfused *in situ* with 0.1M phosphate buffer solution (PBS, pH 7.4) followed by 4% paraformaldehyde in 0.1M sodium phosphate buffer. Soon after, the brains were removed, post-fixed for 1h in 4% paraformaldehyde, cryoprotected in 10% sucrose solution for 1h, and in 30% sucrose solution for the following 24h, and then frozen in 30% sucrose until the histological analysis was performed. For the histological examination, brains were coronally sectioned on a sliding microtome (AO model 860) at 50µm. Individual sections were

then collected with a fine brush and transferred to multiwell plates filled with 0.1 M PBS with 0.1 % Na Azide and mounted on 1% gelatin coated slides. Before staining, the tissue sections were allowed to dry on the slides overnight at room temperature. The protocol of Cresyl Violet staining was adopted from Dr. Jurgen Wenzel (personal communication) and is given below.

Step 1: Dehydration

(0. 50% EtOH	2 min, optional use if necessary)
1. 70% EtOH	2 min
2. 95% EtOH I	2 min
3. 95% EtOH II	2 min
4. 100% EtOH I	2 min
5. 100% EtOH II	2 min

Step 2: Defatting

(If dehydration is good, then the tissue in xylene should change from an opaque white (as in EtOH) to a translucent appearance –clear like glass. If it remains opaque, then the xylene is not penetrating the tissue because of too much residual water, redo steps #1-5 with longer times for each.)

6. Xylene I	5 min
7. Xylene II	10 min
8. Xylene I	1 min

Step 3: Rehydration

9. 100% EtOH II	1 min
10. 100% EtOH I	1 min
11. 95% EtOH II	1 min
12. 95% EtOH I	1 min

13. 70% EtOH 1 min
14. dH_2O I 30 sec
15. dH_2O II 30 sec

Step 4: Staining

16. Cresyl Violet Acetate 0.1% 2-10 min (dependent on tissue thickness and stain freshness)
17. dH_2O II 15 sec
18. dH_2O I 15 sec

Step 5: Differentiation

19. 95% EtOH w/Acetic Acid 2-10 min (Time varies: thickness, CV time, etc.)
(150μm Acetic Acid per 100ml 95% EtOH)

Step 6: Dehydration

20. 95% EtOH I 30 sec (In 95%, check stain with microscope, restain if light or
21. 95% EtOH II 30 sec (different longer if too dark or the background is not clear.)
22. 100% EtOH I 30 sec
23. 100% EtOH II 30 sec
24. Xylene I 5 min
25. Xylene II 5 min
26. From xylene, coverslip with Permount mounting media
27. Let Permount dry at least 3+ days before cleaning off excess coverslipping media.

The number of neurons within the dLGNwere counted in an unbiased manner using the StereoInvestigator software (Microbrightfield, Williston, VT). Images were captured using Nikon E600 microscope connected to a color video camera. A motorized stage controller attached to the microscope will encode and transmitted the *X*-, *Y*-, and *Z*-stage movements to the computer program. The *Z*-axis encoder attached to the fine-focus of the microscope allows for optical scanning of nuclei. This method uses a three-dimensional disector probe to optically section the sample in the *Z*-axis. Counting was performed according to the rules of the unbiased stereology with the optical dissector (West *et al.*, 1991). On each section, the dLGN were outlined under low power magnification (10X magnification), and neurons were counted under oil immersion magnification (100X objective) (see, Figure 2.22 and Figure 2.23). The counting frame was set at 20μm with a grid size of 100μm. The first focal plane of the dissector was placed 2 μm below the top of the section (i.e., guard height setting). Counting was then carried out through a depth of 10 μm (dissector height). Neurons were counted if their nuclei first came into focus within the dissector height (10μm), were within the dissector frame or touching the inclusion lines, and did not touch any exclusion lines. If nuclei were in focus within the guard height setting of 2 μm they were not included in the count (Figure 2.21). Every 2nd tissue section was counted, and the tissue thickness was measured for each counting frame, separately. Stereological analysis were carried out to a high degree of sampling stringency (coefficient of error [CE] < 0.6, shape factor m=1). A fixed dissector height of 10 μm was used in each counting step. A guard volume of 2 μm was applied to avoid artifacts at the sectioning surface. The total estimation of cell numbers (N) was calculated by the following equation:

$$N = [\Sigma Q^{-}.(1/ssf).(1/asf).(1/tsf)]$$

where ssf is the section sampling fraction, asf is the area sampling fraction, tsf is the thickness-sampling fraction (where the measured thickness of the tissue is divided by the disector height), and ΣQ^{-} is the total number of cells counted within a disector. In order

to estimate the average thickness of a single section ([t]), the local section thicknesses were estimated and all the thickness data obtained from a set of sampled sections were averaged. Then, the section thickness sampling fraction were estimated (thickness sampling fraction=tsf=10/[t]). An unbiased estimate of the total number of neurons was calculated as the total number of sampled dissector particles (Q^-) within optical dissectors multiplied by the reciprocals of the sampling fractions used. Statistical evaluation and error determination of obtained estimates were determined by coefficient of error (CE) and coefficient of variation (CV) estimates described by Gundersen and Jensen (1987). The coefficient of error (CE) was calculated for each measure (points, cell number, dissector frame number, and density) within each region. All CEs should be below 10%. The number of neurons estimated by number weighted section thickness was used for statistical analysis. Estimated Total by Number Weighted Section Thickness means that the section thickness measurements from counting sites where contain markers. These measured thicknesses were then weighted by the number of objects associated with them to produce a weighted average.

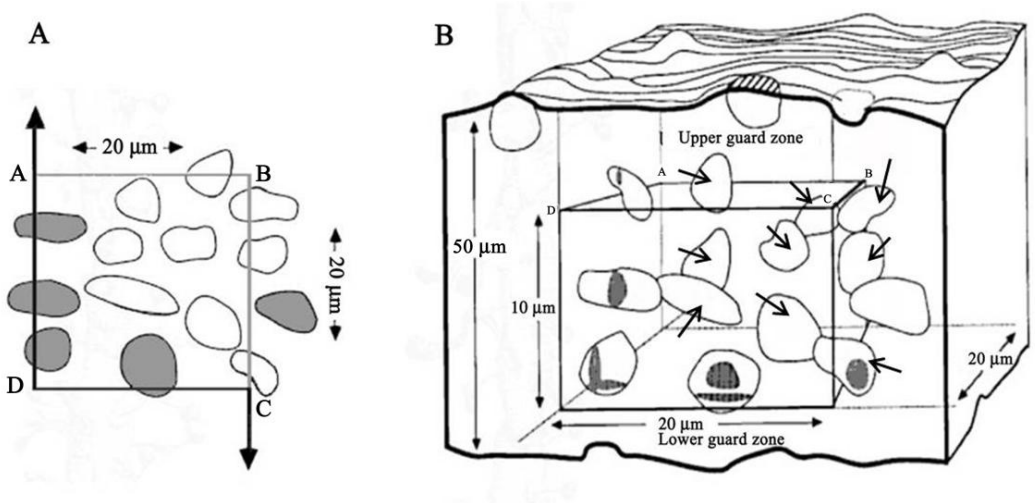

Figure 2.21 A representation of a counting frame (A) and a small piece of brain. Arrows indicate countable cells corresponding to white cells on the left (Modified after Williams and Rakic, 1988).

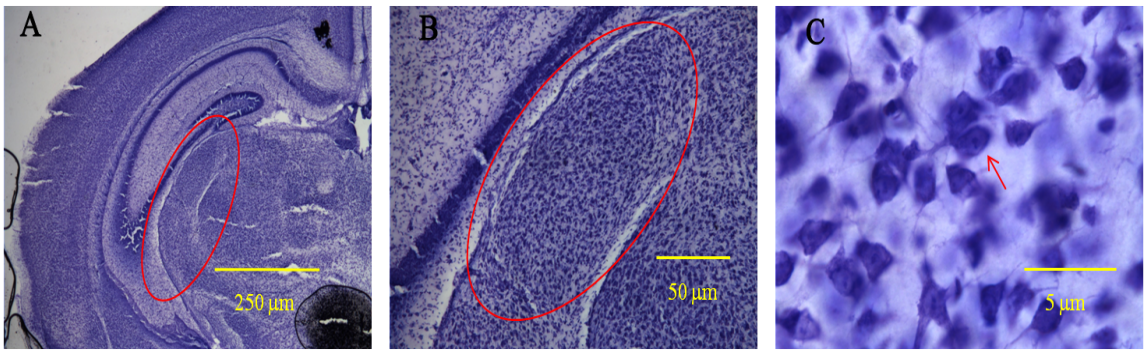

Figure 2.22 Microphotographs of the mice brain slices stained with cresyl violet at three different magnifications: 2.5 X (A), 10X (B), and 100 X (C) on PN10. The dLGN is circumvented by a red line. Scale bars: 250 µm, 50 µm, and 5 µm for A, B, and C, respectively.

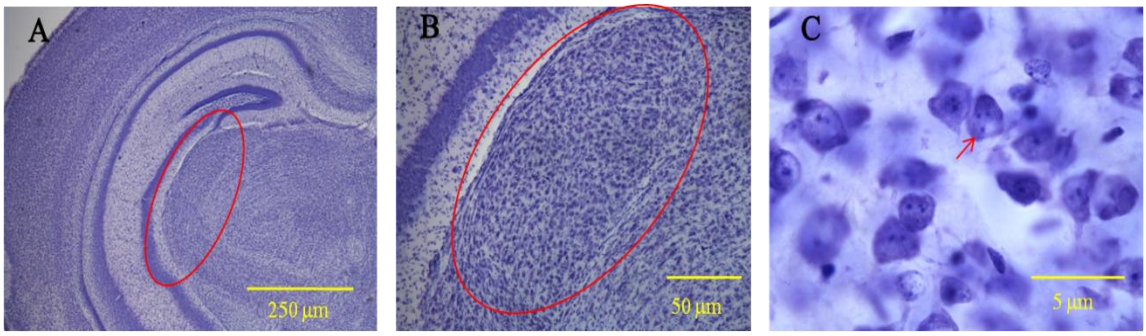

Figure 2.23 Microphotographs of the mice brain slices stained with cresyl violet at three different magnifications: 2.5 X (A), 10X (B), and 100 X (C) on PN10. The dLGN is circumvented by a red line. Scale bars: 250 µm, 50 µm, and 5 µm for A, B, and C, respectively.

2.10. Blood Alcohol Concentration

Blood alcohol concentration (BAC) was measured in a separate group of pups on PD3, PD10, and PD20 at 4 different time points, 1, 1.5, 2 and 3 h after the second ethanol intubation. On PD3 and PD10, pups were anesthetized in an ice bath until movement stop then decapitated and blood collected in a heparinized capillary tubes. On P20, 10 µl

of blood was collected into a heparinized capillary tube from a small nick in the tail at the same time points. Blood samples were centrifuged at 10000 rpm, 4 °C for 5 minutes (Ependorf Centrifuge 5804 R, Brinkmann Instruments Inc, Westbury, NY). Blood plasma was taken and kept on at -70 °C. Blood Alcohol Concentrations (BACs) were analyzed using an oximetric procedure (Helfer *et al.*, 2009) with an Analox GL5 Alcohol Analyzer (Analox Instruments, Lunenburg, MA). Between 2 and 4 different pups were sampled for each PD and each time point.

2.11. Statistical Analyses

Group means ± SEM were calculated from all the measures. The data were analyzed with treatment (i.e., A, IC, and C) as the independent factor. A one way ANOVA for the number of neurons in the retina and dLGN, and a repeated measure ANOVA for body weight were carried out. A conditional hierarchical linear model was employed for analysis of morphometric parameters of RGCs. The three-level hierarchical linear model consisted of three variance components parameters: the treatment-to-treatment variability (fixed effects part), retina-to-retina variability (random effects part), and cell-to-cell variability (random effects part). The Tukey HSD test and the Differences of Least Squares Means were used for post hoc analysis of the data. For the statistical analysis of the data the statistical packages SAS and SPSS 16 (Chicago, IL) were used.

CHAPTER 3

RESULTS

3.1. Results of Retina Ganglion Cells Morphology

3.1.1. Changes in the YFP Pups' Body Weights between PD 3–20

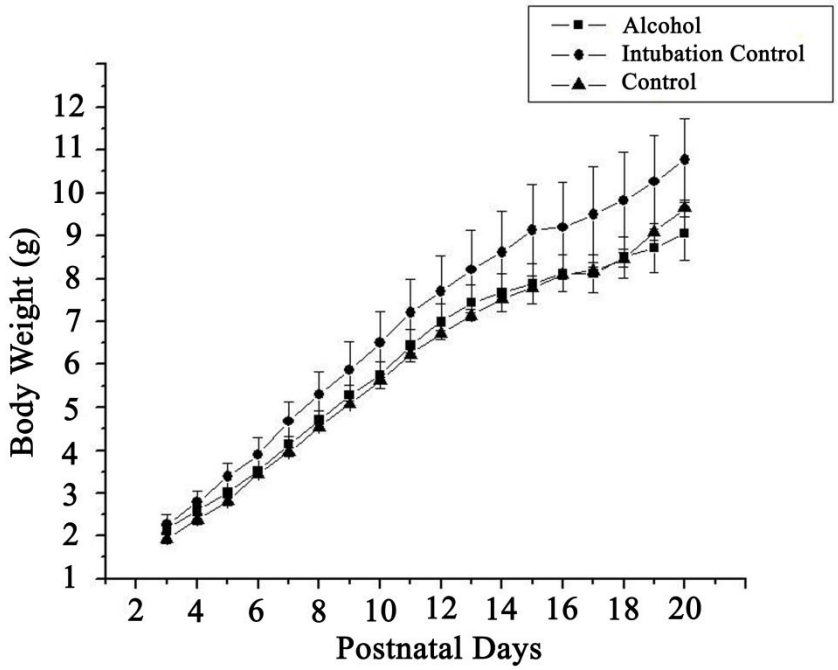

Figure 3.1 Growth rates of the three treatment groups, A, IC, and C, with daily body weights averaged across male and female pups in each group. Error bars denote SEM.

The pups' mean body weight (± SEM) was recorded throughout PD3-PD20 for A (n=10), IC (n=7), and C (n=8) groups. A two-way repeated measures ANOVA (treatment x days) applied to this data yielded significant day effect ($F_{(17:374)} = 374.68$, $p<0.00$) confirming a steady increase in the pups' body weight throughout the first 20 postnatal days. There was no significant effect of alcohol treatment on body weight.

3.1.2. Morphometric Analyses of Retina Ganglion Cells

The numbers of traced ganglion cells were as follows: Alcohol group: n=104, Intubation Control group: n=81, Control group: n=108. The average number of RGCs per animal in alcohol and control groups was as follow: A group (n=4) -26, IC group (n=5)-16,2 and C group (n=5)-21,6.

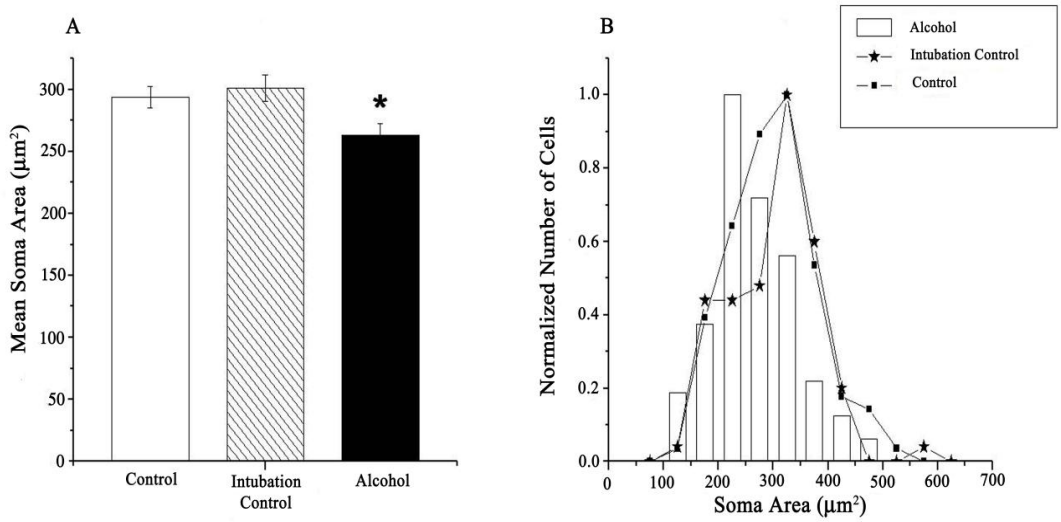

Figure 3.2 Morphometric measures of Soma Area (A) and the normalized number of ganglion cells (B) estimated for each group independently. The degree of significance is denoted as $p<0.05$* and error bars denote SEM.

As seen from Fig. 3.2A, alcohol treatment significantly affected the mean soma area of retinal ganglion neurons ($F_{(2:16)}$= 4.25, p=0.033). Individual group comparisons showed that mean soma area for Group A was significantly smaller compared to both control groups (p=0.017 and p=0.031, for IC and C group, respectively). The two control groups did not differ significantly. In all three groups, ganglion cell soma area showed normal frequency distribution with a peak at 250 μm^2 for alcohol-treated pups and 350 μm^2 for control subjects (Fig. 3.2B).

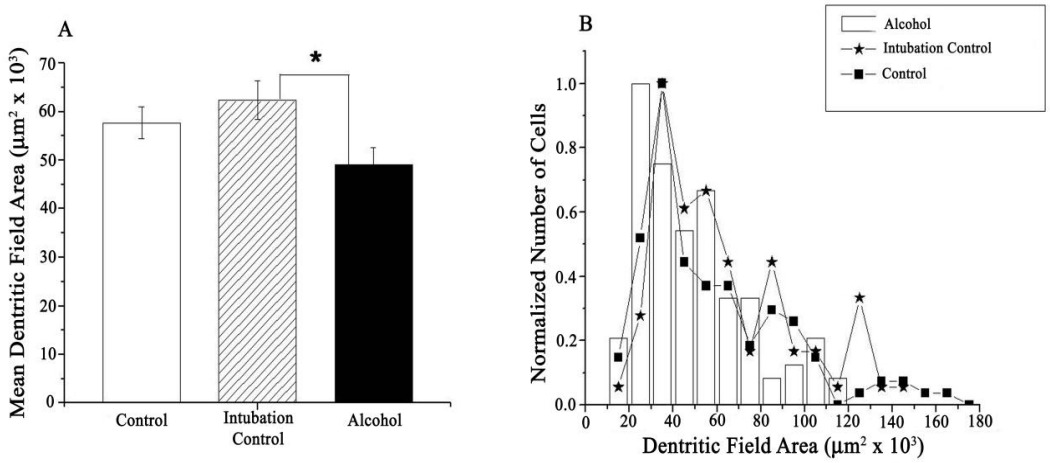

Figure 3.3 Morphometric measures of Dentritic Field Area (A) and the normalized number of ganglion cells (B) estimated for each group independently. The degree of significance is denoted as p<0.05* and error bars denote SEM.

In the alcohol group, the mean dendritic field area was smaller as compared to IC group (Fig. 3.3A). This difference between A and IC groups closely approached the accepted level of statistical significance ($F_{(2,16)}$=3.30, p=0.06). On the other hand, there was no difference in the mean dendritic field area between the control and each of the two remaining groups. As seen from Fig. 3.3B, in the ethanol-exposed pups, neurons with dendritic fields within the range between 20000 - 30000 μm^2 constituted the largest group of ganglion cells. In contrast, in the control groups, the largest group of ganglion cells had dendritic fields within the range between 30000 - 40000 μm^2.

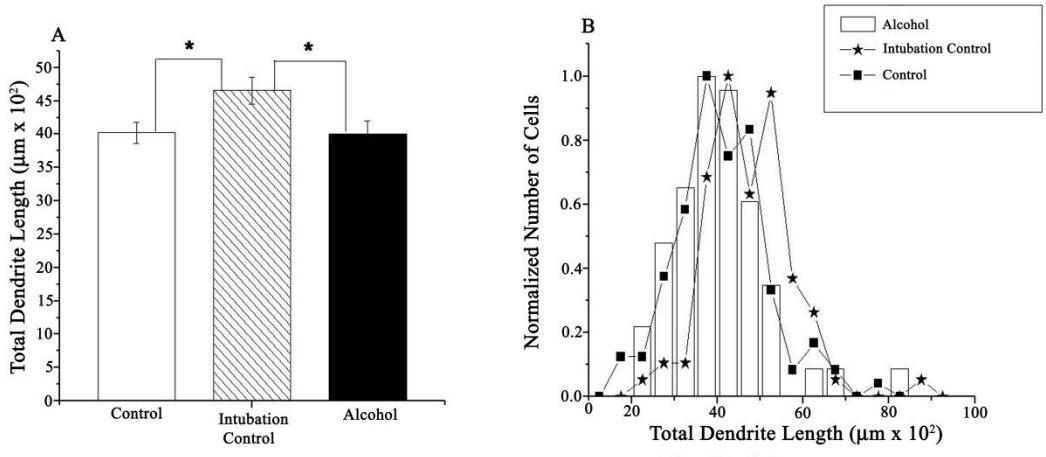

Figure 3.4 Morphometric measures of Total Dentritic Length (A) and the normalized number of ganglion cells (B) estimated for each group independently. The degree of significance is denoted as $p<0.05$* and error bars denote SEM.

Statistical analysis of dendritic length yielded the main group effect significant ($F_{(2:16)}=3.64$, $p=0.05$). Post hoc analysis showed that the mean dendrite length in the IC group was significantly greater than that in either the A or C group ($p=0.034$ and $p=0.026$, respectively). The difference between C and A groups was insignificant. Differences were found between treatment groups for the dendrite length frequency distribution. In control pups, the predominant dendrite length was between 3500 and 4000 µm. In alcohol group, the typical dendritic length fell within the broader range of values, between 3500 and 4500 µm. In contrast, in the IC group of pups the distribution of dendritic length showed two peaks, one at 4000-4500 and the second at 5500-6000 µm (see Fig.3.4B).

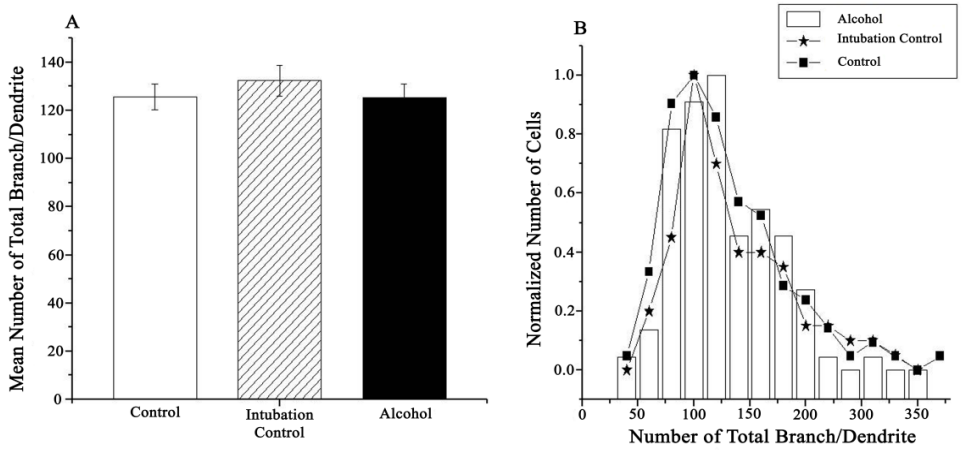

Figure 3.5 The mean (± SEM) number of branches/dendrite (A) and the normalized number of ganglion cells (B) for each treatment group independently. Error bars denote SEM.

The number of branches/dendrite in A group did not differ from those in IC and C groups. In all three groups, the frequency distribution for this score was normal with a peak value between 100-125 branches/dendrite (see Fig.3.5).

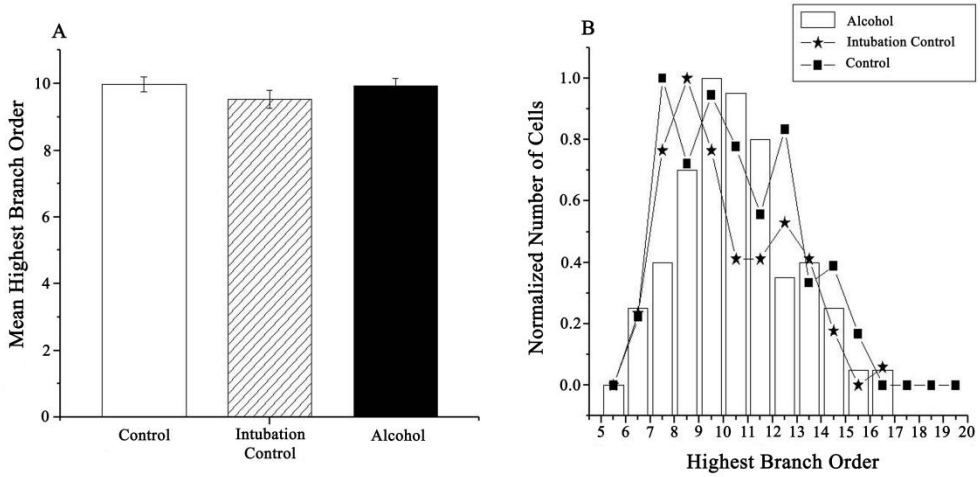

Figure 3.6 The mean (± SEM) highest branch order (A) and the normalized number of ganglion cells (B) for each treatment group independently. Error bars denote SEM.

The branch order also did not show a significant between-group difference. In all three groups, the score values showed normal distribution with the highest mean branch order between 9-11 (see Fig.3.6).

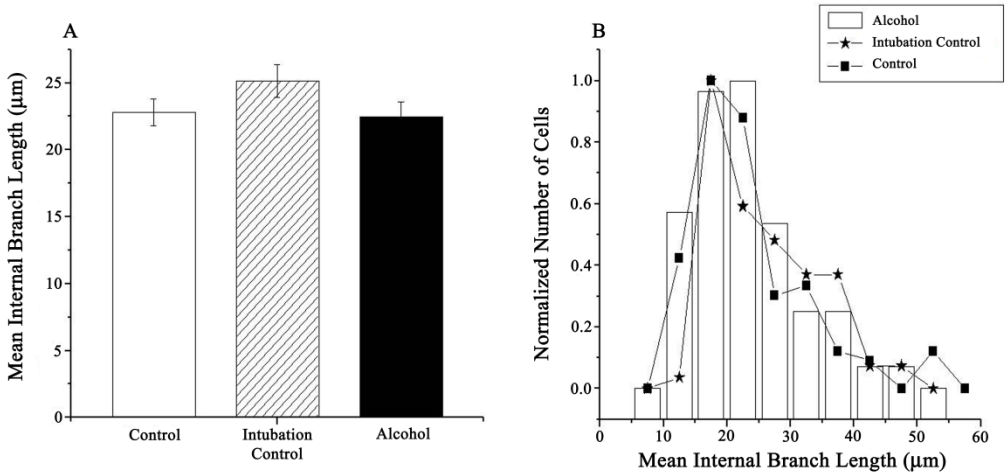

Figure 3.7 The mean (± SEM) internal branch length (A) and the normalized number of ganglion cells (B) for each treatment group independently. Error bars denote SEM.

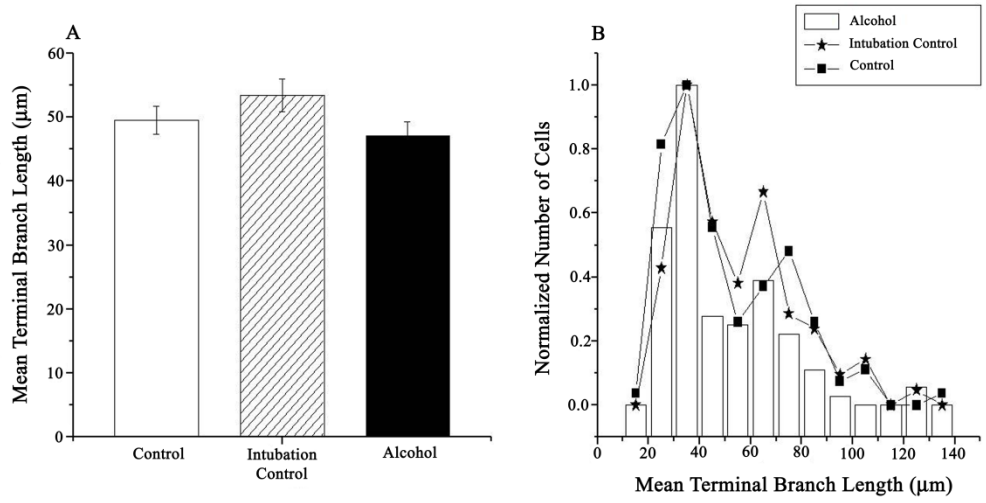

Figure 3.8 The mean (± SEM) terminal branch length (A) and the normalized number of ganglion cells (B) for each treatment group independently. Error bars denote SEM.

The main effect of the treatment on the mean internal branch length and mean terminal branch length was also yielded insignificant. The peak average internal branch length varied between 15 - 25 μm, while the peak average terminal branch length was between 30 - 40 μm (Fig 3.7 and Fig.3.8, respectively).

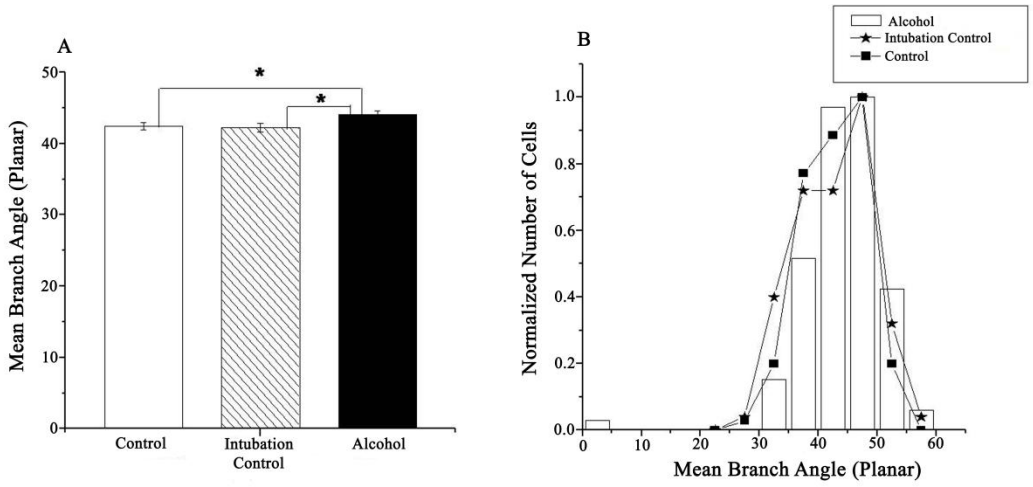

Figure 3.9 Morphometric measures of the branch angle (A) and the normalized number of ganglion cells (B) estimated for each group idependently. The degree of significance is denoted as $p<0.05$* and error bars denote SEM.

Another parameter affected by postnatal ethanol administration was the dendritic branch angle (Fig 3.9A). For this parameter, the main group effect was marginally significant ($F_{(2:16)}= 3.34$, $p=0.06$) with the mean branch angle larger in A group as compared to controls. In all three groups, the branch angle frequency distribution was normal with a peak at 40 to 50 degrees.

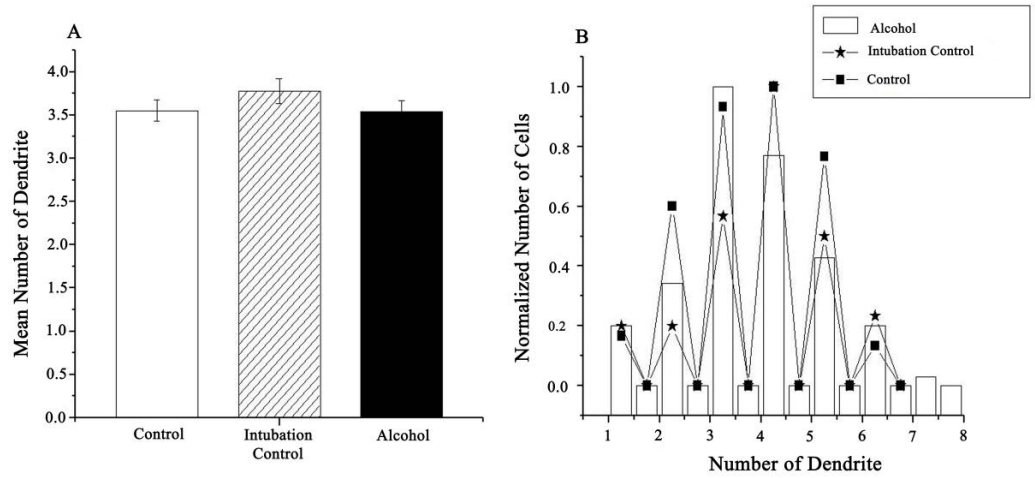

Figure 3.10 The mean (± SEM) number of dendrites (A) and the normalized number of ganglion cells (B) for each treatment group independently. Error bars denote SEM.

There was no significant main effect of postnatal alcohol treatment on dendrite number (p=0.4). The two largest cluster of neurons had as an average 3-3,5 and 4-4,5 dendrites (Fig 3.10B).

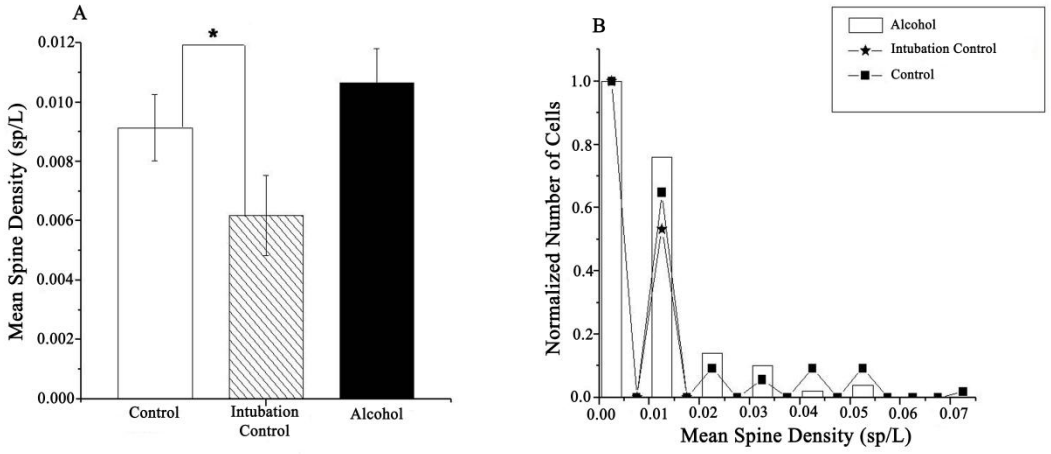

Figure 3.11 Morphometric measures of spine density (A) and the normalized number of ganglion cells (B) estimated for each group independently. The degree of significance is denoted as $p<0.05$*.

The effects of treatment on dendritic spine density of the retinal ganglion cells approached but did not reach the accepted level of statistical significance ($F_{(2,16)}$= 3.22 , p=0.07). Interestingly, it was the IC group that showed relatively lower spine density when compared to the untreated control group (Fig 3.11A). As shown in Fig. 3.11B, the A and C groups appeared to have a bimodal distribution of spine densities, with peaks within the range between 0-0.005 and 0.01-0.015, respectively (Fig 3.11B). In IC group, the largest cluster of cells had spine density in the range of 0.01-0.015.

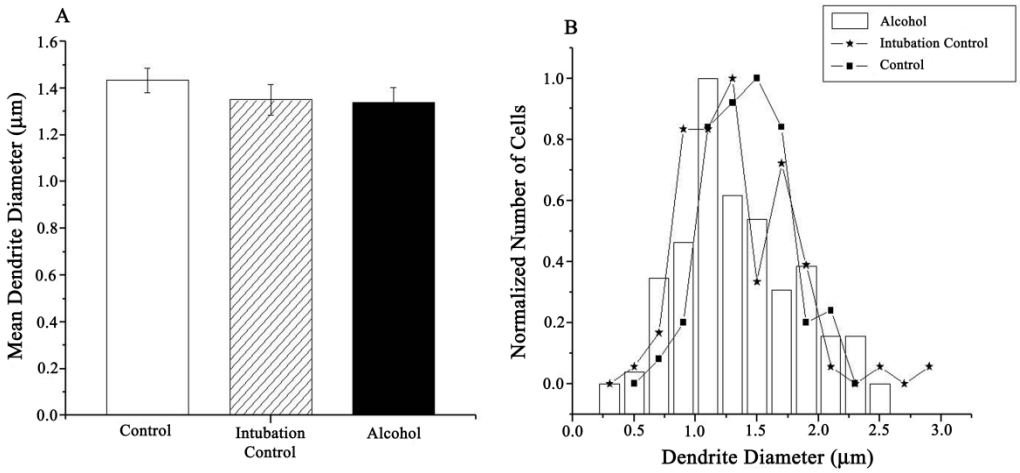

Figure 3.12 The mean (± SEM) dendrite diameter (A) and the normalized number of ganglion cells (B) for each treatment group independently. Error bars denote SEM.

As seen Figure 3.12., postnatal alcohol treatment had no effect on dendrite diameter. In all three groups, the dendrite diameter distribution was normal with a peak at 1 to 1,5 µm.

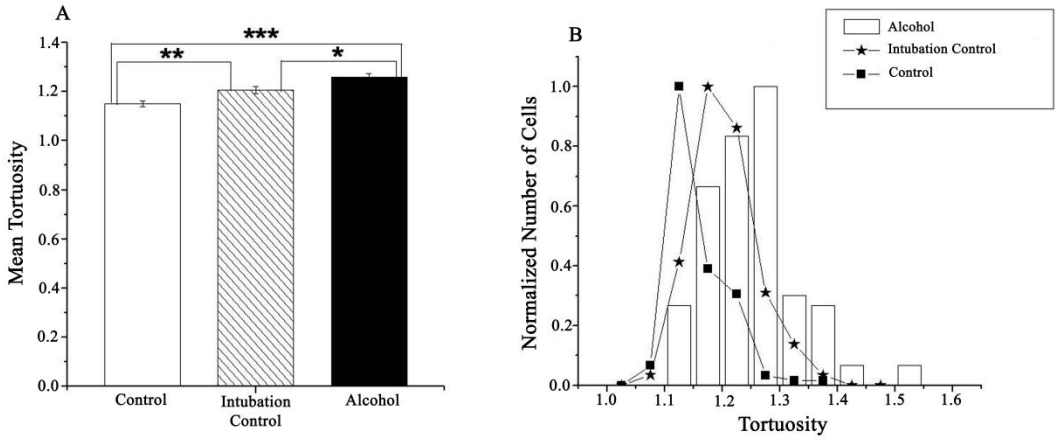

Figure 3.13 Morphometric measures of dendritic tortuosity (A) and the normalized number of ganglion cells (B) estimated for each treatment group independently. The degree of significance is denoted as $p<0.05$*, $p<0.01$**, $p<0.001$*** and error bars denote SEM.

Dendrite tortuosity was estimated as the ratio of the length along each dendritic branch and the length of the straight line drawn between the two nodes that define the branch. The overall group effect was highly significant ($F_{(2,16)}=16.76$, $p=0.0001$). As seen in Fig. 3.13A, the dendritic tortuosity was larger for both the IC and A groups compared to untreated group ($p=0.01$ and $p=0.0001$, respectively). In the control group, the tortuosity index manifested by the largest cluster of the retinal ganglion cells was 1.1-1.15, in IC group, it was 1.15-1.25, while in the ethanol-exposed group it was 1.25-1.3 (Fig.3.13B).

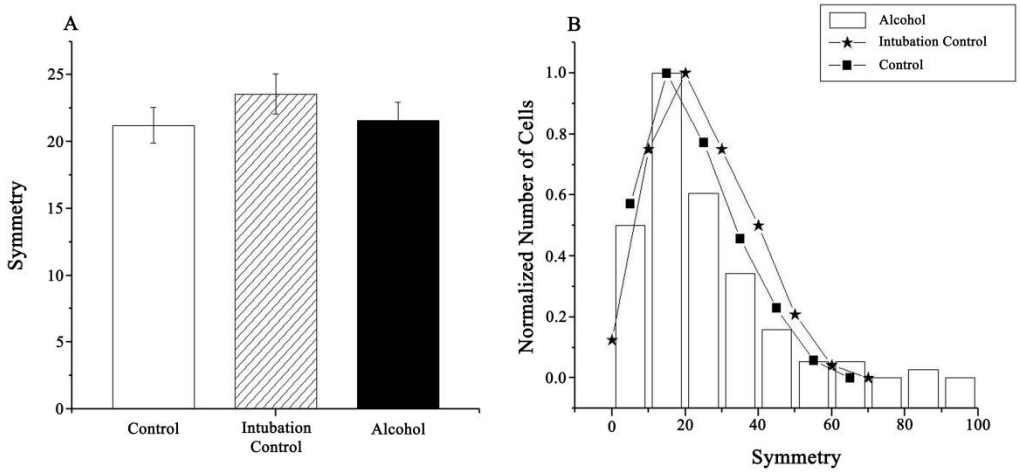

Figure 3.14 The mean (± SEM) symmetry index (A) and the normalized number of ganglion cells (B) for each treatment group independently. Error bars denote SEM.

There were no significant between-group differences in the symmetry index showing peak at the score of 10 to 20 (Fig 3.14).

3.2. Results of Anterograde Labeling of Retinogeniculate Projections

3.2.1. Changes in the C57BL/6 Pups' Body Weights between PD 3–10

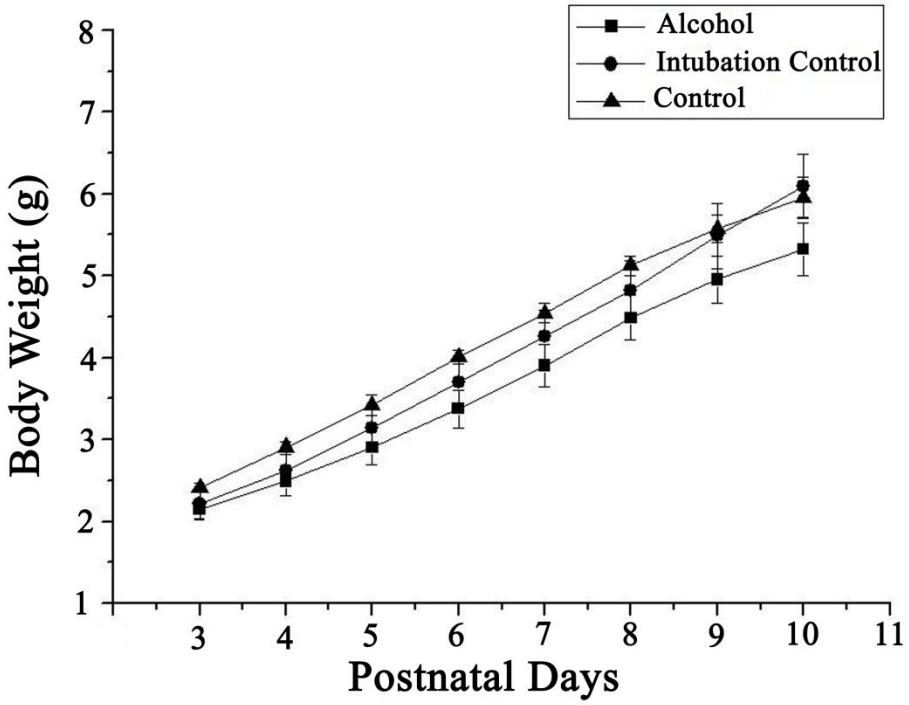

Figure 3.15 The gain of the body weight across the PD3–PD10 in control and ethanol-treated C57BL/6 mice pups. Error bars denote SEM.

The pups' mean body weight (± SEM) was calculated throughout PD3-PD10 for A (n=13), IC (n=7), and C (n=9) group, separately. As seen from the Fig. 3.15, in all three groups, a steady gain the body weight was observed throughout the first 10 postnatal days. The gain of the body weight was slower in the pups subjected to ethanol treatment , however, two-way repeated measure ANOVA yielded significant day effect ($F_{(7:259)}$ = 751.69, $p<0.00$) and did not yield the main effect of treatment significant.

3.2.2. The total and the percentage areas occupied by contra- and ipsilateral retinal projections

The numbers of pups used for anterograde labeling of retinogeniculate projections were as follows: A group: n=6, IC group: n=3, and C group: n=5.

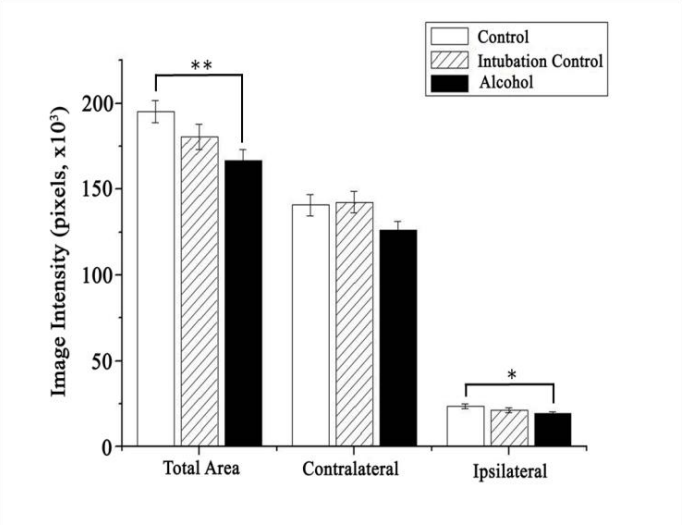

Figure 3.16 The dLGN area (pixel) occupied by, respectively, total, contralateral, and ipsilateral retinal projections as estimated at P10. The degree of significance is denoted as p=0.06*, p=0.015** and error bars denote SEM.

One-way ANOVA performed for the total size of the CTB positive area revealed the main group effect significant ($F_{(2:27)}$= 5.00 , p=0.015) According to the results of the Tukey post hoc group comparisons the mean total area of retino-genuculate projection in the A group was significantly smaller as compared to the C group (p=0.01), however, it did not significantly differed from that in IC group (p=0.4). A marginal significance of the main group effect was also observed for the area of the minor, ipsilateral projection ($F_{(2,27)}$= 2.95, p = 0.07). In the group A as compared to the control, the mean area of the ipsilateral projection was smaller (Fig 3.16) although this difference was also yielded only marginally significant (p = 0.06). The main group effect for the area of the contralateral projection was insignificant.

3.3. The total area of retina and the cell counts in the retina ganglion cell layer and the dorsal Lateral Geniculate Nucleus (dLGN)

Cell counting was done on retinas obtained from three different animal groups: A (n=7), IC (n=7), and C (n=6).

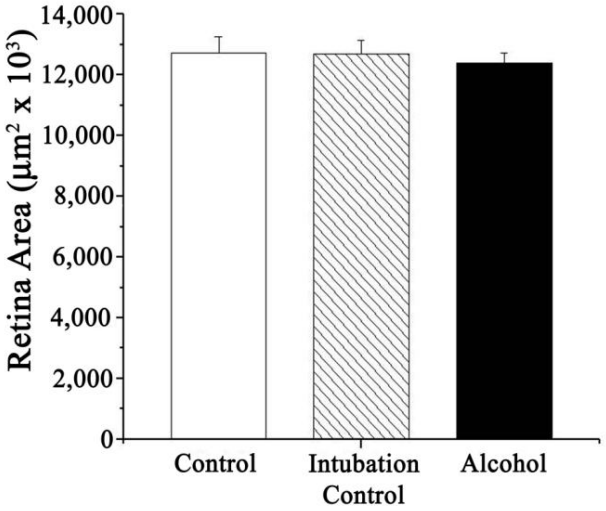

Figure 3.17 The total area of retina at P20. Error bars denote SEM.

As seen from Fig. 3.17, and confirmed by one way ANOVA analysis, there were no significant between-group differences in the size of the retina.

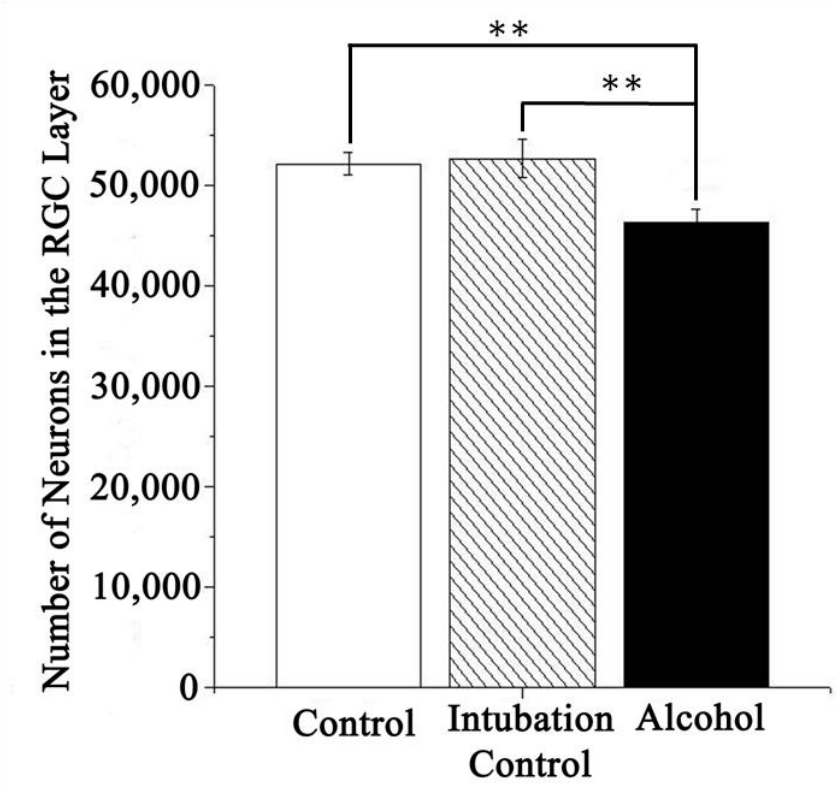

Figure 3.18 Mean number (± SEM) of neurons in the retina ganglion cell layer at PD20. The degree of significance is denoted as p<0.01** and error bars denote SEM.

Numbers of cells in the retinal ganglion cell layer from different groups at PD 20, assessed by unbiased stereological methods, were presented in Fig.3.18. The statistical analysis of these data carried out using one way ANOVA yielded the main group effect significant ($F_{(2:18)}$= 5.86 , p=0.012). The post hoc individual group comparisons confirmed that there were significantly fewer neurons in group A compared to the IC and C groups (p=0.02 and p=0.03, respectively). The difference between two control groups was not statistically significant.

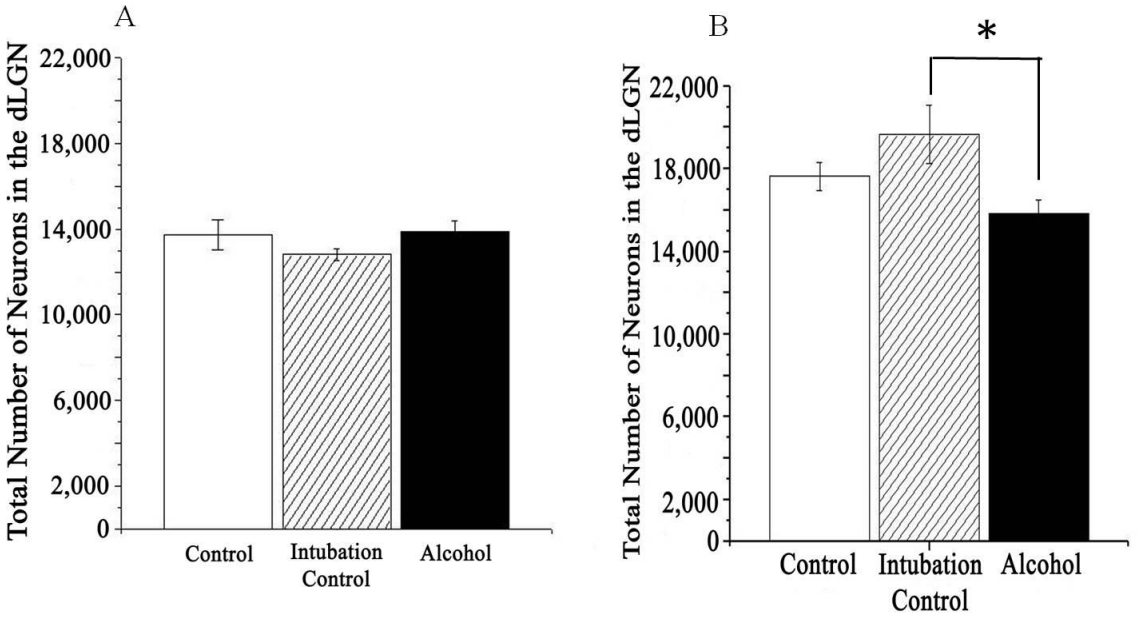

Figure 3.19 Mean number (± SEM) of neurons in the dLGN at PD10 (A) and at PN 20 (B). The degree of significance is denoted as $p<0.05$* and error bars denote SEM.

Counts of neurons within dLGN at PD10 were performed for the three animal groups: A (n=5), IC (n=6), and C (n=5). The results are presented in Fig 3.19A One way ANOVA applied to statistically evaluate the cell counts within dLGN at PD10 confirmed the lack of a significant between-group differences, $F_{(2:15)}= 1.38$, $p=0.28$.

Counts of neurons within dLGN at PD20 were performed for the three animal groups as follows: A (n=7), IC (n=7), and C (n=6). The results are presented in Fig.3.19B. One-way ANOVA applied for statistical evaluation of these data yielded the main group effect significant ($F_{(2:19)}= 3.76$, $p=0.044$). However, the post hoc comparisons revealed statistically significant ($p=0.035$). The difference between A and IC groups only with significantly higher number of neurons in IC group as compared to A group.

An univariate analysis of variance (treatment x age) was applied to compare number of neurons on dLGN between PN10 and P20. It revealed the significant main effect of age

($F_{(1:36)}$=35.37, p=0.00) and a significant age x treatment interaction ($F_{(2:36)}$=4.21, p=0.024), however, the main effect of treatment remained insignificant. Student t-test performed for each age and treatment group independently confirmed that the number of neurons in the dLGN in all P10 treatment groups was significantly lower than in the corresponding PD20 (PD10 A versus PD20 A p=0.059, PD10A versus PD20 IC p=0.008, PD10 A versus PD20 C p=0.002, PD10 IC versus PD20 A p=0.003, PD10 IC versus PD20 IC p=0.001, PD10 IC versus PD20 C p=0.00, PD10 versus PD20 A p=0.06, PD10 C versus PD20 IC p=0.008, PD10 C versus PD20 C p=0.003).

3.4. Blood Alcohol Concentration

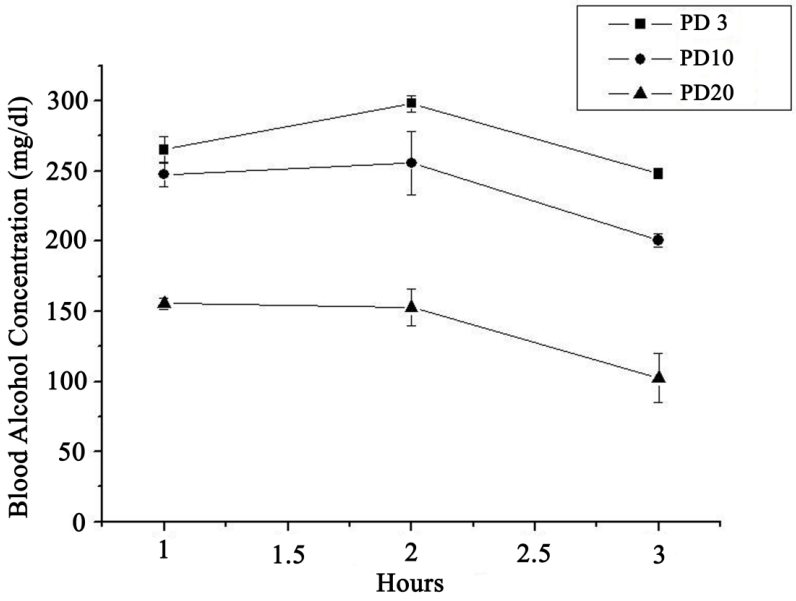

Figure 3.20 Mean of blood alcohol concentration measured 1, 1.5, 2, 3 hour following last intubation with alcohol containing milk on PD3, PD10 and PD20. Error bars denote SEM.

As seen from figure 3.20, the peak BAC was observed 1-1.5 h after the second intubation, at 298 ±5.9, 256±22.67, and 156±5.73 mg/dl for PD3, PD10, and PD20,

respectively. BAC decreased within time, however, the overall blood alcohol levels were lower on PD20 than on PD3 and PD10.

CHAPTER 4

DISCUSSION

The present study shows that in mice, early postnatal (PD3-20) exposure to a low dose of ethanol (3 g/kg body weight/day) affected the developing visual system, significantly decreasing the neuron numbers in both the retinal ganglion cell layer and dorsolateral geniculate nucleus, and changing some morphological parameters of retinal output neurons, the retinal ganglion cells.

In this study, with ethanol administered at relatively low daily dose in enriched milk formula, pups body weight gain was not affected by ethanol exposure. The ethanol dose of 3 g/kg/day delivered just like in the present study: during early postnatal period by intragastric intubation was reported also by other authors not to compromise the body weight gain in new born pups (Serbus *et al.,* 1986).

The BAC was reaching its peak value 1-1.5 h after the last ethanol administration and remained within the range between 156-298 mg/dl (PD3, 10 and 20). These BACs were above the toxic level shown by other authors to produce damage to the brain and visual system in rodents (Pierce and West, 1986; Bonthius and West, 1990; Ikonomidou *et al.,* 2000; Livy *et al.,* 2003; Tenkova *et al.,* 2003). The amplitude of the BAC was inversely proportional to the pups' age (Figure 3.20), likely due to the increase in the efficiency of liver alcohol dehydrogenase and microsomal ethanol oxidizing system and thus, an increase in metabolic tolerance to alcohol with maturation (Bhalla *et al.,* 2005; Krasner *et al.,* 1974).

In this study, the 3 g/kg/day ethanol dose given to mice during the extended postnatal period between PD 3-20 resulted in a significant loss of neurons in the ganglion cell layer with no change in the total retinal area. Loss of RGCs after ethanol exposure during the early postnatal period has been reported previously in different animal species such as chick (Aguilera *et al.,* 2004; Chmielewski *et al.,* 1997), rat (Pinoza-Duran *et al.,* 1997), the macaque monkey (Clarren *et al.,* 1990), and also in humans (Pinoza-Duran *et al.,* 1997; Strömland and Pinazo-Duran, 2002). Our results are consistent with ethanol-induced reduction in the number of optic nerve fibers and decrease in the optic nerve cross-sectional area reported earlier in mice (Ashwell and Zang,1994; Dangata and Kaufman, 1997; Kennedy and Elliott, 1986; Parnell *et al.,* 2006; Parson and Sojita, 1995; Parson *et al.,* 1995), rats (Harris *et al.,* 2000; Pinazo-Duran *et al.,* 1993; Philips *et al.,* 1991; Samoraski *et al.,* 1986), chicks (Tufan *et al.,* 2007) and zebrafish (Dlugos and Rabin,2007; Kashyap *et al.,* 2007). Ethanol-induced cell loss has been shown to be caused by apoptotic cell death due to ethanol toxicity (Ikonomidou *et al.,* 2000; Tenkova *et al.,* 2003). Exposure to ethanol during development may also alter neurotrophin levels and/or function (Climent *et al.,* 2002; Heaton *et al.,* 1999: 2000(a); 2000(b); Parks *et al.,* 2008), and change expression of neurotropic receptors (Dohrman *et al.,* 1997; Light *et al.,* 2002). Neurotrophins and their receptors were shown to be important for the survival and differentiation of neurons in the chick retina (Frade *et al.,* 1999). In the present study, in parallel to the significant loss of retinal output neurons, a decrease in the neuron number was found in the lateral geniculate nucleus of thalamus, the major target area of RGCs. This observation is consistent with the results by Tenkova *et al.,* (2003) pointing towards high susceptibility of dLGN neurons to ethanol toxicity at postnatal days PD4 to PD7 in mice. Our results confirm the generalized neurotoxic effect of early postnatal ethanol administration shown earlier in other brain regions including the hippocampus (Barnes and Walker, 1981; Miller, 1995; Miki *et al.,* 2000, 2003, 2004, 2008; Moulder *et al.,* 2002; Gonzales-Burgos *et al.,* 2006; Tran and Kelly, 2003), cerebellum (Goodlett *et al.,* 1990, 1997, 1998; Goodlett and Eilers, 1997; Miki *et al.,* 1999; Thomas *et al.,* 1998), and cerebral cortex (Climent *et al.,* 2002; Tenkova *et al.,*

2003; Han *et al.,* 2005; Money and Napper, 2005; Jiang *et al.,* 2007). However, it is not possible based on the present results to determine whether the loss of neurons in the dLGN is due to direct neurotoxic effects of ethanol, or whether it may be secondary to a reduction in axonal projections from the retina.

Retinas were collected on PD20 when RGCs are reported to display adult cell morphological characteristics (Diao *et al.,* 2004; Coombs *et al.,* 2007; Chalupa and William, 2008, pp 194). For the quantitative analysis of ganglion cell morphologies in control and ethanol-exposed mice, 13 different structural parameters were considered. These parameters have been previously used to classify RGCs (Coombs *et al.,* 2006). In the present study, irrespective of the RGC type, two conventional size measurements, soma area and dendritic field diameter, were affected by neonatal ethanol exposure. In normal mice, these two parameters show a steady growth during the early postnatal retina development, and so the effects of alcohol exposure are particularly striking (Coombs *et al.,* 2007). Another parameter showing a similar developmental trajectory, dendritic branch length, remained unaffected by early postnatal ethanol administration. The reduced size of both soma and dendritic field area support the idea that within a neuron population, soma size may be a good predictor of the volume occupied by the cell's dendritic tree. These results are in accord with findings by other authors reporting reduction of soma size and dendritic fields of the neurons in the rat oculomotor nucleus (Burrows *et. al.,* 1995), Bergmann glial cells (Perez-Torrero *et al.,* 1997), and cerebellar granule cells (Smith *et al.,* 1986) due to perinatal alcohol exposure.

Two other morphological measurements appeared to be affected by the ethanol intoxication: dendrite tortuosity and the dendritic branch angle. In contrast to soma size and the dendritic field area which were reduced in ethanol-exposed subjects, ethanol administration increased dendrite tortuosity and appeared to increase branch angles. In mice, these two latter features reach adult values shortly after birth, and remain relatively unchanged throughout postnatal development (Coombs *et al.,* 2007). A similar

developmental pattern is seen in the kitten cerebellar Purkinje cells (Calvet and Calvet, 1984). However, in postnatal dendritic development of Y-like geniculocortical relay neurons in cat (Coleman and Friedlander, 2002), both the branch angle and dendrite tortuosity have been reported to decrease in the course of postnatal development. During normal development of these dLGN relay neurons, these two changes in the dendritic architecture were negatively correlated with the changes in the size of the soma and dendritic field. Similarly, in the present study the changes in the values of these two pairs of parameters show opposite trends. A decrease in the branch angle has also been observed for hippocampal pyramidal neurons during human fetal development (Paldino and Purpura, 1979). The decrease in the branch angle occurring during neural development would be expected to contribute to an increase in the distance between the dendrite terminal tips and the soma. The straightening of dendritic segments associated with reduced tortuosity would have a similar effect. However, during early stages of retinal development, the meandering of growing fibers may facilitate finding the specific cellular targets, which would be more difficult if dendrite elongation took place along a straight trajectory. It has been postulated by some authors that tortuosity might reflect a search for specific inputs or targets (Stepanyants *et al.,* 2004). It has been also suggested that increased tortuosity represents a morphologic marker of nerve regeneration (Kallinikos *et al.,* 2004). On the other hand, ethanol-induced hypoplasia of the RGCs could result in the delayed reduction in both the branch angle and dendrite tortuosity. The increased dendrite tortuosity in RGCs of ethanol-exposed mice may also explain why the dendritic field area of these neurons was significantly smaller despite no changes recorded in the total dendrite length, number of branches and the highest branch order. The lack of ethanol effects on the RGCs' dendrite length and branch number observed in the present study is consistent with the absence of the significant difference in these two parameters in the rat prefrontal cortex after similar neonatal ethanol intoxication, however, in the latter study, spine density was lower in ethanol treated group as compared to control (Whitcher and Klintsova, 2008). In mice, perinatal ethanol exposure covering late pregnancy and the first postpartum week (the time window

coinciding with growth and development of dendritic arbors in hippocampus) was reported to cause a marked reduction in the extent of basilar dendrites in CA1 pyramidal neurons as assessed by PD14 (Davies and Smith, 1981). In rat hippocampal pyramidal neuronal cultures, six days of ethanol exposure in the medium (i.e., 200, 400 or 600 mg/dl), beginning at the time of plating, was also shown to decrease the total dendrite number and dendritic length (Yanni and Lindsley, 2000). The changes in the dendritic arbor towards a reduction in the number of dendritic branches, and a reduction in the arbor complexity were also observed in the rat oculomotor nucleus on P15 (Burrows *et al.*, 1995) and in the mouse cerebellar granular cells on PD14 (Smith *et al.*, 1986) following a prenatal ethanol exposure. In contrast to these findings, Qiang and colleagues (2002) found an increase in the number and length of apical and basilar dendritic branches in the corpus callosum that project to neurons in the rat visual cortex after prenatal alcohol exposure restricted to the second trimester equivalent. These differing results reported in the literature may be due to regional differences in ethanol susceptibility and different timing of ethanol administration. Interestingly, in the present study, RGC dendrite elongation and the decrease in the spine density were observed in the IC group, as compared to both ethanol-exposed and pure control subjects. The change in the morphology of RGC parameters in the intubation control group may be related to the repeated intubation stress the newborn pups were subjected to. In the alcohol group, intubation stress could be attenuated by the sedative action of ethanol. Retrospective studies on human and animals suggest that even chronic maternal stress during pregnancy, associated with raised plasma levels of CRH, ACTH and cortisol, may increase the likelihood of morphological and functional abnormalities in the nervous system of ethanol exposed offspring (Weinstock, 2001). It has been demonstrated that corticosteroid receptors are distributed widely throughout the central nervous system and are also present in the developing retina (Koehler and Moscona, 1975; Gremo and Vernadakis, 1981; Zhang *et al.*, 1993**).** There are, however, relatively few studies examining the effect of perinatal stress on brain morphology and none on the development of visual system in rodents. The available studies have been focused on the

limbic regions of the brain such as hippocampus, anterior cingulate and orbitofrontal cortices, where perinatal stress can result in dendritic atrophy manifested by reduction in spine densities, the dendrite length and complexity of the dendritic trees (Hayashi *et al.,* 1998; Bartesaghi and Severi, 2002; Andersen and Teicher, 2004; Murmu *et al.,* 2006). These results stand in contrast to the dendrite elongation recorded in the IC group in the present study.

The decrease in RGC spine density observed in IC group could be secondary to the increase in the dendrite length and thus fiber surface in this group. On the other hand, the lack of change in the spine number in the alcohol exposed group in this study differs from some earlier reports about the decrease in the spine density after perinatal ethanol administration. For example, a decrease in the spine number was found in the hippocampal pyramidal cells of 30-day-old rat pups exposed to ethanol during gestation through lactation (Gonzalez-Burgos *et. al.,* 2006). Lower spine density was also reported by Whitcher and Klintsova (2008) in the rat prefrontal cortex after a short, neonatal (PD 4-9) exposure to ethanol although in that study no between-group differences in dendritic complexity were noted. However, these discrepant findings may be related to regional differences in ethanol effects on the developing nervous system (e.g., cortex versus dLGN).

There is strong evidence that ethanol-induced brain damage including adverse changes occurring in the developing visual system is most pronounced when ethanol is delivered during the brain growth spurt, a critical period characterized by an increased susceptibility to ethanol effects (Tran *et al.,* 2000; Tenkova *et al.,* 2003). This was the reason why in the present study ethanol was administered to new born mice pups between PD 3-20. It would be interesting to compare our results with potential changes in the developing mouse retina due to fetal ethanol intoxication throughout embryonic days 11-19, the early period of RGC generation and differentiation. However, to our knowledge, there are no such data available.

One of the important means to evaluate the effects of adverse events such as visual deprivation or drug intoxication on visual system development is the investigation of ocular dominance plasticity. In the present study, to examine the potential changes in the development of ocular dominance, the immunohistochemical anterograde labeling of retinal output neurons was performed in both control and ethanol exposed mice pups at PD9, a day by which the eye-specific segregation of retino-geniculate projection is completed in this species (Godement *et al.,* 1984; Jaubert-Miazza *et al.,* 2005). The analysis of retino-geniculate projections in control and ethanol exposed mice pups confirmed the presence of highly predominant contralateral projection occupying approximately 85% of the total area in LGN. This is an expected result which proves that, in the present study, the anterograde labeling of retino-geniculate cells and estimation of the segregation of inputs from the two eyes was successful.

In addition to a significant decrease in the dLGN cell number and the total reticulo-geniculate projection area in alcohol-exposed mice pups, the separate analysis of contra- and ipsilateral retino-geniculate projections showed a significant decrease only in the ipsilateral projection area originating from the temporal and ventral retina. Since crossed retinal fibers innervate the LGN at E16 (about 5 days before birth) while uncrossed ones arrive to the developing LGN and spread through this structure postnatally between PD0 –PD7, the obtained results suggest that the ethanol intoxication has an effect primarily on the immature, developing connections. The question, how the reduction in the ipsilateral retino-geniculate projection may affect the visual perception remains open. Since the mouse has laterally placed eyes, highly predominant contralateral retino-geniculate projection, and poor binocular vision, the adverse effect of the reduction in the ipsilateral projection field induced by neonatal ethanol intoxication may be negligible. However, it has been found that, despite of the fact that only about 3% of the total retino-geniculate pathway projects ipsilaterally, and the number of RGCs stimulated by both eyes is approximately nine times higher for contralateral than for the ipsilateral retina (Dräger and Olsen, 1980), at the level of dLGN, the proportion of

binocular segments in contra- and ipsilateral projection fields is only three-to-one (Frenkel and Bear, 2004). This reduction in the contralateral binocular input to the dLGN is due to the high convergency of contralateral axons on the target dLGN neurons (Coleman *et al.,* 2009) and results in contralateral-to-ipsilateral ratio of visually evoked responses in binocular visual cortex (V1) equal to 2:1 which obviously may increase the impact of the minor ipsilateral retino-geniculate projection on the binocular vision in mice. Therefore, it is important to correlate the ethanol-induced morphological abnormalities with functional changes in the visual system (the degree of impairment in visual perception). Reduced visual acuity in one or both eyes, diplopia, hyperopia, myopia and astigmatism has been reported in FAS children (Strömland, 2004). However, no comparative studies on visual perception have been done so far in rodent models of FAS.

CHAPTER 5

CONCLUSION

In summary, this study provides clear evidence of ethanol toxicity on the development of mouse RGCs during the early postnatal period considered to be equivalent to the human third trimester when the fetal nervous system is particularly susceptibility to the damaging effects of ethanol. The findings also show that early postnatal ethanol intoxication affected RGC development in dissimilar ways. The most affected parameters were soma size and total dendritic field area, both showing decrease, as well as dendrite branch angle and dendrite tortuosity, both showing an increase. Since during the normal retinal development, these parameters also show opposite trends, ethanol-induced changes in RGCs' morphology observed in the present study suggest developmental delay rather than a permanent damage. To confirm this notion further investigation of retinal morphology in mouse pups at more advanced ages will be required. At the level of dLGN neonatal alcohol intoxication in mice resulted in a significant decrease in the total number of dLGN neurons, a decrease in the total reticulo-geniculate projection area with a significantly greater adverse effect on the minor ipsilateral projection field. Since crossed (contralateral) retinal fibers innervate the LGN prior to birth, while uncrossed (ipsilateral) fibers arrive to the developing LGN early postnatally, the latter result may suggest that ethanol is more toxic for the developing than for the mature neural elements. Having in view the relatively high contribution of ipsilateral retino-geniculate projection to the binocular vision in mice despite of their minor anatomical representation, the potential functional deficits arising from the morphological anomalies observed in C57BL/6 mice pups neonatally exposed to ethanol should be further controlled in the behavioral tests.

REFERENCES

Aguilera Y., Ruiz-Gutiérrez V., Prada FA., Martínez JJ., Quesada A., Dorado ME. (2004) "Alcohol-Induced Lipid and Morphological Changes in Chick Retinal Development" Alcoholism: Clinical and Experimental Research 28(5): 816–823.

Andersen SL., Teicher MH. (2004) "Delayed effects of early stress on hippocampal development" Neuropsychopharmacology 29(11): 1988–1993.

Arenzana FJ., Carvan MJ., Aijón J., Sánchez-González R., Arévalo R., Porteros A. (2006) "Teratogenic effects of ethanol exposure on zebrafish visual system development" Neurotoxicology and Teratology 28(3): 342–348.

Aronson M., Olegard R. (1987) "Children of alcoholic mothers" Pediatrician 14: 57–61.

Artal P., Herreros de Tejada P., Muñoz Tedó C., Green DG. (1998) "Retinal image quality in the rodent eye" Visual Neuroscience 15(4): 597–605.

Ashwell KW., Zhang LL. (1994) "Optic nerve hypoplasia in an acute exposure model of the Fetal Alcohol Syndrome" Neurotoxicology and Teratology 16(2): 161–167.

Badea TC., Nathans J. (2004) "Quantitative analysis of neuronal morphologies in the mouse retina visualized by using a genetically directed reporter" The Journal of Comparative Neurology 480: 331–351.

Barnes DE., Walker DW. (1981) “Prenatal ethanol exposure permanently reduces the number of pyramidal neurons in the rat hippocampus” Developmental Brain Research 1: 333–340.

Bartesaghi R., Severi S. (2002) “Effects of early environment on field CA3a pyramidal neuron morphology in the guinea-pig” Neuroscience 110: 475–488.

Bayer SA., Altman J., Russo RJ., Zhang X. (1993) “Timetables of neurogenesis in the human brain based on experimentally determined patterns in the rat” Neurotoxicology 14 (1): 83–144.

Baylor DA. (1987) “Photoreceptor signal and vision” Investigative Ophthalmology and Visual Science 28: 34–49.

Beebe DC. (1986) “Development of the ciliary body: a brief review” Transactions of the Ophthalmological Societies of the United Kingdom 105 (2): 123–130.

Berman RF., Hannigan JH. (2000) “Effects of prenatal alcohol exposure on the hippocampus: Spatial behavior, Electrophysiology, and Neuroanatomy” Hippocampus 10: 94–110.

Bhalla S., Kaur K., Akhtar Mahmood A., Mahmood S. (2005) “Postnatal development of alcohol dehydrogenase in liver & intestine of rats exposed to ethanol *in utero*” The Indian Journal of Medical Research 121: 39–45.

Birch D., Jacobs GH. (1979) “Spatial contrast sensitivity in albino and pigmented rats” Vision Research 19(8): 933–937.

Block MT. (1969) “A note on the refraction and image formation of the rat's eye” Vision Research. 9(6): 705–711.

Bonthius DJ., West JR. (1990) “Alcohol-induced neuronal loss in developing rats: Increased brain damage with binge exposure” Alcoholism: Clinical and Experimental Research 14(1): 107–118.

Bowmaker JK., Dartnall HJA. (1980) “Visual pigments of rods and cones in a human retina” Journal of Physiology 298: 501–511.

Bruce BB., Biousse V., Dean AL., Newman NJ. (2009) “Neurologic and ophthalmic manifestations of fetal alcohol syndrome” Reviews in Neurological Diseases 6(1): 13–20.

Burrows RC., Shetty AK., Phillips DE. (1995) “Effects of prenatal alcohol exposure on the postnatal morphology of the rat oculomotor nucleus” Teratology 51: 318–328.

Calvet MC., Calvet J. (1984) “Computer assisted analysis of HRP labeled and Golgi stained Purkinje neurons” Progress in Neurobiology 23: 251–272.

Campbell G., So KF., Lieberman AR. (1985) “Identification of synapses formed by the aberrant, uncrossed retinogeniculate projection in the hamster after neonatal monocular enucleation” Developmental Brain Research 21: 137–140.

Carter RC., Jacobson SW., Molteno CD., Chiodo LM., Viljoen D., Jacobson JL. (2005) “Effects of prenatal alcohol exposure on infant visual acuity” The Journal of Pediatrics 147(4): 473–479.

Carones F., Brancato R., Venturi E., Bianchi S., Magni R. (1992) “Corneal endothelial anomalies in the fetal alcohol syndrome” Archives Ophthalmology 110(8): 1128–1131.

Chalupa LM., Günhan E. (2004) “Development of On and Off retinal pathways and retinogeniculate projections” Progress in Retinal and Eye Research 23(1): 31–51.

Chalupa LM., Williams RW. (2008) “Eye, Retina, and Visual System of The Mouse” The MIT press, Cambridge, Massachusetts London,England

Chan T., Bowell R., O'Keefe M., Lanigan B. (1991) “Ocular manifestations in fetal alcohol syndrome” The British Journal of Ophthalmology 75(9): 524–526.

Chan DQ. (1999) “Fetal alcohol syndrome” Optometry and Vision Science 76(10): 678–85.

Chiao CC., Masland RH. (2002) “Starburst cells nondirectionally facilitate the responses of direction-selective retinal ganglion cells” Journal of Neuroscience 22(24): 10509–10513.

Chmielewski CE., Hernandez LM., Quesada A., Pozas JA., Picabea L., Prada FA. (1997) “Effects of ethanol on the inner layers of chick retina during development” Alcohol 14(4): 313–317.

Chow RL., Lang RA. (2001) “Early eye development in vertebrate” Annual Review of Cell and Developmental Biology 17: 255–296.

Clarren SK., Alvord EC Jr., Sumi SM., Streissguth AP., Smith DW. (1978) “Brain malformations related to prenatal exposure to ethanol” The Journal of Pediatrics 92(1): 64–67.

Clarren SK., Astley SJ., Bowden DM., Lai H., Milam AH., Rudeen PK., Shoemaker WJ. (1990) “Neuroanatomic and neurochemical human primate infants exposed abnormalities in nonto weekly doses of ethanol during gestation” Alcoholism: Clinical and Experimental Research 14(5): 674–683.

Climent E., Pascual M., Renau-Piqueras J., Guerri C. (2002) “Ethanol Exposure Enhances Cell Death in the Developing Cerebral Cortex: Role of Brain- Derived Neurotrophic Factor and Its Signaling Pathways” Journal of Neuroscience Research 68: 213–225.

Coles CD., Platzman KA., Lynch ME., Freides D. (2002) “Auditory and visual sustained attention in adolescents prenatally exposed to alcohol” Alcoholism: Clinical and Experimental Research 26(2): 263–271.

Coleman LA., Friedlander MJ (2002) “Postnatal dendritic development of Y-like geniculocortical relay neurons” International Journal of Developmental Neuroscience 20: 137–159.

Coleman JE., Law K., Bear MF. (2009) “Anatomical origins of ocular dominance in mouse primary visual cortex” Neuroscience 161(2): 561–571.

Connor PD, Streissguth AP, Sampson PD, Bookstein FL, Barr HM. (1999) "Individual differences in auditory and visual attention among fetal alcohol-affected adults” Alcoholism: Clinical and Experimental Research 23(8): 1395–1402.

Cook CS., Nowotny AZ., Sulik KK. (1987) “Fetal alcohol syndrome. Eye malformations in a mouse model” Archives of Ophthalmology 105(11): 1576–1581.

Cook JE., Chalupa LM. (2000) “Retinal mosaics: New insights into an old concept”. Trends in Neurosciences 23: 26–34.

Coombs JL., Van Der List D., Wang GY., Chalupa LM. (2006) “Morphological properties of mouse retinal ganglion cells” Neuroscience 140: 123–136.

Coombs JL., Van Der List D., Chalupa LM. (2007) “Morphological properties of mouse retinal ganglion cells during postnatal development” The Journal of Comparative Neurology 503(6): 803–814.

Dacey DM. (1990) “The dopaminergic amacrine cell” The Journal of Comparative Neurology 301: 461–489.

Dacey DM. (1994) “Physiology, morphology and spatial densities of identified ganglion cell types in primate retina” Ciba Foundation Symposium 184: 63–70.

Dacey DM., Lee BB., Stafford DK., Pokorny J., Smith VC. (1996) “Horizontal cells of the primate retina: cone specificity without spectral opponency” Science 271: 656–658.

Dangata YY., Kaufman MH. (1997) “Morphometric analysis of the postnatal mouse optic nerve following prenatal exposure to alcohol” Journal of Anatomy 191: 49–56.

Davies DL., Smith DE. (1981) “A Golgi study of mouse hippocampal CA1 pyramidal neurons following perinatal ethanol exposure” Neuroscience Letters 26(1): 49–54.

De Courten C., Garey LJ. (1982) “Morphology of the neurons in the human lateral geniculate nucleus and their normal development. A Golgi study” Experimental Brain Research. 47(2): 159–171.

De Vries SH. (2000) “Bipolar cells use kainate and AMPA receptors to filter visual information into separate channels” Neuron 28: 847–856.

Diao L., Sun W., Deng Q., He S. (2004) “Development of the mouse retina: emerging morphological diversity of the ganglion cells” Journal of Neurobiology 61(2): 236–249.

Discenza CB., Karten HJ., Reinagel P. (2008). “Anatomical targets of retinal ganglion cell axons in the Long-Evans rat” SFN 2008 458.3 EE16.

Dlugos CA, Rabin RA (2007) Ocular deficits associated with alcohol exposure during zebrafish development. The Journal of Comparative Neurology 502: 497–506.

Dobbing J., Sands J. (1979) “Comparative aspects of the brain growth spurt” Early Human Development 3: 79–84.

Dohrman DP., West JR., Pantazis NJ. (1997) “Ethanol reduces expression of the nerve growth factor receptor, but not nerve growth factor protein levels in the neonatal rat cerebellum” Alcoholism: Clinical and Experimental Research 21(5): 882–893.

Dräger UC., Olsen JF. (1980) “Origins of crossed and uncrossed retinal projections in pigmented and albino mice” The Journal of Comparative Neurology 191(3): 383–412.

Driscoll CD., Streissguth AP., Riley EP. (1990) “Prenatal alcohol exposure: Comparability of effects in humans and animal models” Neurotoxicology and Teratology 12(3): 231–237.

Famiglietti EV., Kolb H. (1976) “Structural basis for ON and OFF-center responses in retinal ganglion cells” Science, 194: 193–195.

Famiglietti EV. (2002) “A structural basis for omnidirectional connections between starburst amacrine cells and directionally selective ganglion cells in rabbit retina, with associated bipolar cells” Visual Neuroscience 19(2): 145–162.

Farah MH., Easter SS Jr.(2005) “Cell birth and death in the mouse retinal ganglion cell layer” The Journal of Comparative Neurology 489(1): 120–341

Feng G., Mellow RH., Bernstein M., Keller-Peck C., Nguyen QT., Wallace M., Nerbonne JM., Lichtman JW., Sanes JR. (2000) “Imaging neuronal subsets in transgenic mice expressing multiple spectral variants of GFP” Neuron 28: 41–51.

Flanigan EY., Aros S., Bueno MF., Conley M., Troendle JF., Cassorla F., Mills JL. (2008) “Eye malformations in children with heavy alcohol exposure in utero” The Journal of Pediatrics 153(3): 391-395.

Frade JM., Bovolenta P., Rodriguez-Tebar A. (1999) “Neurotrophins and other growth factors in the generation of retinal neurons” Microscopy Research And Technique 45: 243–251.

Frenkel MY., Bear MF. (2004) “How monocular deprivation shifts ocular dominance in visual cortex of young mice” Neuron 44(6): 917–923.

Garey LJ., de Courten C. (1983) “Structural development of the lateral geniculate nucleus and visual cortex in monkey and man” Behavioural Brain Research 10(1): 3–13.

Gilpin NW., Richardson HN., Cole M., Koob GF. (2008) “Vapor inhalation of alcohol in rats” Current Protocols in Neuroscience. Chapter 9: Unit 9.29.

Godement P., Salaün J., Imbert M. (1984) “Prenatal and postnatal development of retinogeniculate and retinocollicular projections in the mouse” The Journal of Comparative Neurololgy 230(4): 552–575.

Gonzalez-Burgos I., Alejandre-Gomez M., Olvera-Cortes ME., Perez-Vega MI., Evans S., Feria-Velasco A. (2006) “Prenatal-through-postnatal exposure to moderate levels of ethanol leads to damage on the hippocampal CA1 field of juvenile rats: A stereology and golgi study” Neuroscience Research 56: 400–408.

Goodlett CR., Marcussen BL., West JR. (1990) “A Single Day of Alcohol Exposure During the Brain Growth Spurt Induces Brain Weight Restriction and Cerebellar Purkinje Cell Loss” Alcohol 7: 107–114.

Goodlett CR., Johnson RB. (1997) “Neonatal binge ethanol exposure using intubation: timing and dose effects on place learning” Neurotoxicology and Teratology 19: 435–446.

Goodlett CR., Eilers AT. (1997) “Alcohol-induced purkinje cell loss with a single binge exposure in neonatal rats: A stereological study of temporal windows of vulnerability” Alcoholism: Clinical and Experimental Research 21(4): 738–744.

Goodlett CR., Pearlman AD., Lundahl KR. (1997) “Binge-like alcohol exposure of neonatal rats via intragastric intubation induces both Purkinje cell loss and cortical astrogliosis” Alcoholism: Clinical and Experimental Research 21(6): 1010–1017.

Goodlett CR., Pearlman AD., Lundahl KR. (1998) “Binge neonatal alcohol intubations induce dose-dependent loss of Purkinje cell” Neurotoxicology and Teratology 20(3): 285–292.

Goodlett CR., Horn KH., Zhou FC. (2005) “Alcohol teratogenesis: Mechanisms of damage and strategies for intervention” Experimental Biology and Medicine (Maywood) 230: 394–406.

Gorgels TG., van Norren D. (1992) “Spectral transmittance of the rat lens” Vision Research 32(8): 1509–1512.

Graw J. (1996) “Genetic aspects of embryonic eye development in vertebrates” Developmental Genetics 18(3): 181–197.

Graw J. (2010) “Eye development” Current Topics in Developmental Biology 90:343–386.

Green DG., Powers MK., Banks MS. (1980) “Depth of focus, eye size and visual acuity” Vision Research 20: 827–835.

Green JT., Arenos JD., Dillon CJ. (2006) “The effects of moderate neonatal ethanol exposure on eyeblink conditioning and deep cerebellar nuclei neuron numbers in the rat”Alcohol 39(3): 135–150.

Gremo F., Vernadakis A. (1981) “Preferential accumulation of [^{3}H] corticosterone in chick brain during embryonic development” Neurochemical Research 6(4): 343–351.

Grieve KL. (2005) “Binocular visual responses in cells of the rat dLGN” The Journal of Physiology 566(1): 119–124.

Gundersen HJ., Jensen EB. (1987) “The efficiency of systematic sampling in stereology and its prediction” Journal of Microscopy 147: 229–263.

Han JY., Joo Y., Kim YS., Lee YK., Kim HJ., Cho GJ., Choi WS., Kang SS. (2005) "Ethanol induces cell death by activating caspase-3 in the rat cerebral cortex" Molecules and Cells 20(2): 189–195.

Harris SJ., Wilce P., Bedi KS. (2000) "Exposure of rats to a high but not low dose of ethanol during early postnatal life increases the rate of loss of optic nerve axons and decreases the rate of myelination" Journal of Anatomy 197: 477–485.

Hayashi A., Nagaoka M., Yamada K., Ichitani Y., Miake Y., Okado N. (1998) "Maternal stress induces synaptic loss and developmental disabilities of offspring maternal stress" International Society for Developmental Neuroscience 16(3-4): 209–216.

Heaton MB., Mitchell JJ., Paiva M. (1999) "Ethanol-Induced Alterations in Neurotrophin Expression in Developing Cerebellum: Relationship to Periods of Temporal Susceptibility" Alcoholism: Clinical and Experimental Research 23(10): 1637–1642.

Heaton MB., Mitchell JJ., Paiva M. (2000a) "Overexpression of NGF Ameliorates Ethanol Neurotoxicity in the Developing Cerebellum" Journal of Neurobiology 45(2): 95–104.

Heaton MB., Mitchell JJ., Paiva M., Walker DW. (2000b) "Ethanol-induced alterations in the expression of neurotrophic factors in the developing rat central nervous system" Developmental Brain Research 121: 97–107.

Helfer JL., Calizo LH., Dong WK., Goodlett CR., Greenough WT., Klintsova AY. (2009) "Binge-like postnatal alcohol exposure triggers cortical gliogenesis in adolescent rats" The Journal of Comparative Neurology 514: 259–271.

Hellström A., Svensson E., Strömland K. (1997) “Eye size in healthy Swedish children and in children with fetal alcohol syndrome” Acta Ophthalmologica Scandinavica 75(4): 423–428.

Hemmingsen EA., Douglas EL. (1970) “Ultraviolet radiation thresholds for corneal injury in antarctic and temporate-zone animals” Comparative Biochemistry and Physiology 32: 539–600.

Hirasawa H., Kaneko A. (2003) “pH changes in the invaginating synaptic cleft mediate feedback from horizontal cells to cone photoreceptors by modulating Ca2+ channels” The Journal of General Physiology 122: 657–671.

Hollenberg J., Spira AW. (1973) “Human retinal development. Ultrastructure of the outer retina” The American Journal of Anatomy 137: 357–386.

Hoyme HE., May PA., Kalberg WO., Kodituwakku P., Gossage JP., Trujillo PM., Buckley DG., Miller JH., Aragon AS., Khaole N., Viljoen DL., Jones KL., Robinson LK. (2005) “A practical clinical approach to diagnosis of fetal alcohol spectrum disorders: clarification of the 1996 Institute of Medicine criteria” Pediatrics 115: 39–47.

Huberman A., Stellwagen D., Chapman B. (2002) “Decoupling eye-specific segregation from lamination in the lateral geniculate nucleus” Journal of Neuroscience 22(21): 9419–9429.

Huberman A., Wang GY., Liets LC., Collins OA., Chapman B., Chalupa LM. (2003) “Eye-specific retinogeniculate segregation independent of normal neuronal activity” Science 300: 994–998.

Hug TE., Fitzgerald KM., Cibis GW. (2000) “Clinical and electroretinographic findings in fetal alcohol syndrome” Journal of AAPOS 4(4): 200–204.

Ikonomidou C., Bittigau P., Ishimaru MJ., Wozniak DF., Koch C., Genz K. (2000) “Ethanol-induced apoptotic neurodegeneration and fetal alcohol syndrome” Science 287: 1056–1060.

Ilia M., Jeffery G. (2000) “Retinal cell addition and rod production depend on early stages of ocular melanin synthesis” Journal of Comparative Neurology 420(4): 437–444.

Iwai L., Kawasaki H. (2009) “Molecular development of the lateral geniculate nucleus in the absence of retinal waves during the time of retinal axon eye-specific segregation” Neuroscience 159(4): 1326–1337.

Jacobs GH., Fenwick JA., Williams GA. (2001) “Cone-based vision of rats for ultraviolet and visible lights” The Journal of Experimental Biology 204(14): 2439–2446.

Jaubert-Miazza L., Green E., Lo FS., Bui K., Mills J., Guido W. (2005) “Structural and functional composition of the developing retinogeniculate pathway in the mouse” Visual Neuroscience 22(5): 661–676.

Jeffery G., Cowey A., Kuypers HG. (1981) “Bifurcating retinal ganglion cell axons in the rat, demonstrated by retrograde double labelling” Experimental Brain Research 44(1): 34–40.

Jeon CJ., Strettoi E., Masland RH. (1998) “The major cell populations of the mouse retina. Journal of Neuroscience 18(21): 8936–8946.

Jiang Q., Hu Y., Wu P., Cheng X., Li M., Yu D., Deng J. (2007) “Prenatal alcohol exposure and the neuroapoptosis with long-term effect in visual cortex of mice”. Alcohol and Alcoholism 42(4): 285–290.

Jones KL., Smith DW. (1973) “Recognition of the fetal alcohol syndrome in early infancy” Lancet 2 (7836): 999–1001.

Jones KL., Smith DW., Ulleland CN., Streissguth P. (1973) “Pattern of malformation in offspring of chronic alcoholic mothers” Lancet :1(7815): 1267–1271.

Jones KL., Smith DW., Streissguth AP., Myrianthopoulos NC. (1974) “Outcome in offspring of chronic alcoholic women” Lancet 1(7866): 1076–1078.

Joselevitch C., Kamermans M. (2007). “Interaction between rod and cone inputs in mixed-input bipolar cells in goldfish retina” Journal of Neuroscience Research 85: 1579–1591.

Kallinikos P., Berhanu M., O’Donnell C., Boulton AJM., Efron N., Malik RA. (2004) “Corneal Nerve Tortuosity in Diabetic Patients with Neuropathy” Investigative Ophthalmology and Visual Science 45(2): 418–422.

Kamermans M., Fahrenfort I., Schultz K., Janssen-Bienhold U., Sjoerdsma T., Weiler R. (2001) “Hemichannel-mediated inhibition in the outer retina” Science 292: 1178–1180.

Karanian J., Yergey J., Lister R., D'Souza N., Linnoila M., Salem N., Jr. (1986) “Characterization of an automated apparatus for precise control of inhalation chamber ethanol vapor and blood ethanol concentrations” Alcoholism: Clinical and Experimental Research 10: 443–447.

Kashyap B., Frederickson LC., Stenkamp DL. (2007) “Mechanisms for persistent microphthalmia following ethanol exposure during retinal neurogenesis in zebrafish embryos” Visual Neuroscience 24(3): 409–421.

Keane B., Leonard B. (1989) “Rodent models of alcoholism: A review” Alcohol and Alcoholism, 24 (4): 299–309.

Kelly SJ., Lawrence CR. (2008) “Intragastric intubation of alcohol during the perinatal period” Methods in Molecular Biology 447: 101–110.

Kelly SJ., Goodlett CR., Hannigan JH. (2009) “Animal Models Of Fetal Alcohol Spectrum Disorders: Impact of the Social Environment” Developmental Disabilities Research Reviews 15: 200–208.

Kennedy LA, Elliott MJ (1986) “Ocular changes in the mouse embryo following acute maternal ethanol intoxication” International Journal of Developmental Neuroscience 4(4): 311–317.

Kiianmaa K., Tabakoff B. (1983) “Neurochemical correlates of tolerance and strain differences in the neurochemical effects of ethanol” Pharmacology, Biochemistry and Behavior 18 (1): 383–383.

Koehler DE., Moscona AA. (1975) “Corticosteroid receptors in the neural retina and other tissues of the chick embryo” Archives of Biochemistry and Biophysics. 170(1): 102–113.

Kolb H. (1979) “The inner plexiform layer in the retina of the cat: electron microscopic observations” Journal of Neurocytology 8: 295–329.

Kondo Y., Tanaka M., Honda Y., Mizuno N. (1993) “Bilateral projections of single retinal ganglion cells to the lateral geniculate nuclei and superior colliculi in the albino rat” Brain Research 608: 204–215.

Kong JH., Fish DR., Rockhill RL., Masland RH. (2005) “Diversity of ganglion cells in the mouse retina: Unsupervised morphological classification and its limits” The Journal of Comparative Neurology 489: 293–310.

Kraaij DA., Spekreijse H., Kamermans M. (2000) “The open- and closed-loop gain-characteristics of the cone/horizontal cell synapse in goldfish retina” Journal of Neurophysiology 84: 1256–1265.

Krasner J., Eriksson M., Yaffe SJ. (1974) “Developmental changes in mouse liver alcohol dehydrogenase” Biochemical Pharmacology 23(3): 519–522.

Kuma H, Miki T, Matsumoto Y. (2004) “Early maternal deprivation induces alterations in brain-derived neurotrophic factor expression in the developing rat hippocampus” Neuroscience Letters 372: 68–73.

Langmann T. (2007) “Microglia activation in retinal degeneration” Journal of Leukocyte Biology 81: 1345–1351.

Lashley KS. (1932) “The mechanism of vision. V. The structure and image-forming power of the rat's eye” The Journal of Comparative Physiology 13: 173–200.

Lemoine P., Harousseau H., Borteyru JP., Menuet JC. (1968) “Children of alcoholic parents: Abnormalities observed in 127 cases” Ouest Medical 8: 476–482.

Leskov IB., Klenchin VA., Handy JW., Whitlock GG., Govardovskii VI., Bownds MD., Lamb TD., Pugh Jr EN., Arshavsky VY. (2000) “The gain of rod phototransduction: Reconciliation of biochemical and electrophysiological measurements” Neuron 27: 525–537.

Light KE., Brown DP., Newton BW., Belcher SM., Kane CJM. (2002) “Ethanol-induced alterations of neurotrophin receptor expression on Purkinje cells in the neonatal rat cerebellum” Brain Research 924: 71–81.

Linden R., Perry VH. (1983) “Retrograde and anterograde-transneuronal degeneration in the parabigeminal nucleus following tectal lesions in developing rats” The Journal of Comparative Neurology 218(3): 270–281.

Little BB., Snell LM., Rosenfeld CR., Gilstrap LC., Gant NF. (1990) “Failure to recognize fetal alcohol syndrome in newborn infants” American Journal of Diseases of Children 144(10): 1142–1146.

Livy DJ., Miller EK., Maier SE., West JR. (2003) “Fetal alcohol exposure and temporal vulnerability: effects of binge-like alcohol exposure on the developing rat hippocampus” Neurotoxicology and Teratology 25: 447–458.

Luo DG., Xue T., Yau KW. (2008) “How vision begins: An odyssey” Proceedings of the National Academy of Sciences of the United States of America 105: 9855–9862.

Marc RE., Sperling HG. (1977) “Chromatic organization of primate cones” Science 196: 454–456.

Martin PR. (1986) “The projection of different retinal ganglion cell classes to the dorsal lateral geniculate nucleus in the hooded rat” Experimantal Brain Research 62(1): 77–88.

Masland RH. (2001) “Neuronal diversity in the retina” Current Opinion Neurobiology 11(4): 431–436.

Matsui JI., Egana AL., Sponholtz TR., Adolph AR., Dowling JE. (2006) **“**Effects of ethanol on photoreceptors and visual function in developing zebrafish” Investigative Ophthalmology and Visual Science *47*(10): 4589–4597.

Miki T., Harris S., Wilce PA., Takeuchi Y., Bedi KS. (1999) “The effect of the timing of ethanol exposure during early postnatal life on total number of Purkinje cells in rat cerebellum” Journal of Anatomy 194: 423–431.

Miki T., Harris SJ., Wilce PA., Takeuchi Y., Bedi KS. (2000) “Neurons in the hilus region of the rat hippocampus are depleted in number by exposure to alcohol during early postnatal life” Hippocampus 10: 284–295.

Miki T., Harris SJ., Wilce PA, Takeuchi Y., Bedi KS. (2003) “Effects of alcohol exposure during early life on neuron numbers in the rat hippocampus. I.Hilus Neurons and Granule Cells” Hippocampus 13: 388–398.

Miki T., Harris SJ., Wilce PA., Takeuchi Y., Bedi KS. (2004) “Effects of age and alcohol exposure during early life on pyramidal cell numbers in the CA1-CA3 region of the rat hippocampus” Hippocampus 14: 124–134.

Miki T., Yokoyama T., Sumitani K., Kusaka T., Warita K., Matsumoto Y., Wang Z., Wilce PA., Bedi SK., Itoh S., Takeuchi Y. (2008) “Ethanol neurotoxicity and dentate gyrus development” Congenital Anomalies 48: 110–117.

Miller M., Israel J., Cuttone J. (1981) “Fetal alcohol syndrome” Journal of Pediatric Ophthalmology Strabismus 18(4): 6–15.

Miller MT., Epstein RJ., Sugar J., Pinchoff BS., Sugar A., Gammon JA., Mittelman D., Dennis RF., Israel J. (1984) "Anterior segment anomalies associated with the fetal alcohol syndrome" Journal of Pediatric Ophthalmology Strabismus. 21(1): 8–18.

Miller MW. (1995) "Generation of neurons in the rat dentate gyrus and hippocampus: Effects of prenatal and postnatal treatment with ethanol". Alcoholism: Clinical and Experimental Research 19(6): 1500–1509.

Mooney SM., Napper RM. (2005) "Early postnatal exposure to alcohol reduces the number of neurons in the occipital but not the parietal cortex of the rat" Alcoholism: Clinical and Experimental Research 29(4): 683–691.

Moulder KL., Fu T., Melbostad H., Cormier RJ., Isenberg KE., Zorumski CF., Mennerick S. (2002) "Ethanol-induced death of postnatal hippocampal neurons" Neurobiology of Disease 10: 396–409.

Murmu MS., Salomon S., Biala Y., Weinstock M., Braun K., Bock J. (2006) "Changes of spine density and dendritic complexity in the prefrontal cortex in offspring of mothers exposed to stress during pregnancy" European Journal of Neuroscience 24: 1477–1487.

Muir-Robinson G., Hwang BJ., Feller MB. (2002) "Retinogeniculate axons undergo eye-specific segregation in the absence of eye-specific layers" Journal of Neuroscience 22(13): 5259–5264.

Nakajima Y., Iwakabe H., Akazawa C., Nawa H., Shigemoto R., Mizuno N., Nakanishi S. (1993) "Molecular characterization of a novel retinal metabotropic glutamate receptor mGluR6 with a high agonist selectivity for L-2-amino-4- phosphonobutyrate" Journal of Biological Chemistry 268: 11868–11873.

Nelson R., Famiglietti EVJ., Kolb H. (1978) “Intracellular staining reveals different levels of stratification for on- and off-center ganglion cells in the cat retina” Journal of Neurophysiology 41: 472–483.

Nelson R., Kolb H. (1985) “A17: a broad-field amacrine cell in the rod system of the cat retina” Journal of Neurophysiology 54: 592–614.

Newman EA., Reichenbach A. (1996) “The Muller cell: A functional element of the retina” Trends in Neurosciences 19: 307–312.

Newman EA. (2003) “New roles for astrocytes: Regulation of synaptic transmission” Trends in Neurosciences 26: 536–542.

Nikonov SS., Kholodenko R., Lem J., Pugh, E.N. Jr. (2006) “Physiological features of the S- and M-cone photoreceptors of wild type mice from single cell recordings” The Journal of General Physiology 127(4): 359–374.

Nomura A., Shigemoto R., Nakamura Y., Okamoto N., Mizuno N., Nakanishi S. (1994) “Developmentally regulated postsynaptic localization of a metabotropic glutamate receptor in rat rod bipolar cells” Cell 77: 361–369.

Olney JW., Ishimaru MJ., Bittigau P., Ikonomidou C. (2000) “Ethanol-induced apoptotic neurodegeneration in the developing brain” Apoptosis 5: 515–521.

O’Malley DM., Sandell JH., Masland RH. (1992) “Corelease of acetylcholine and GABA by the starburst amacrine cells” Journal of Neuroscience 12: 1394–1408.

Paldino AM., Purpura DP. (1979) “Branching patterns of hippocampal neurons of human fetus during dendritic differentiation” Experimental Neurology 64(3): 620–631.

Panchuk–Voloshina N., Haugland RP., Bishop–Stewart J., Bhalgat MK., Millard PJ., Mao F., Leung WY., Haugland RP. (1999) “Alexa Dyes, a series of new fluorescent dyes that yield exceptionally bright, photostable conjugates” The Journal of Histochemistry and Cytochemistry 47 (9): 1179–1188.

Papia MF., Burke MW., Zangenehpour S., Palmour RM., Ervin FR., Ptito M. (2010) “Reduced soma size of the M-neurons in the lateral geniculate nucleus following foetal alcohol exposure in non-human primates” Experimental Brain Research 205(2): 263–271.

Parks EA., McMechan AP., Hannigan JH., Berman RF. (2008) “Environmental enrichment alters neurotrophins levels after fetal alcohol exposure in rats” Alcoholism:Clinical and Experimental Research 32(10): 1741–1751.

Parnell SE., Dehart DB., Wills TA., Chen S, Hodge CW, Besheer J, Waage-Baudet HG, Charness ME, and Sulik KK (2006) “Maternal oral intake mouse model for fetal alcohol spectrum disorders: Ocular defects as a measure of effect” Alcoholism:Clinical and Experimental Research 30(10):1791–1798.

Parson SH., Dhillon B., Findlater GS., Kaufman MH. (1995) “Optic nerve hypoplasia in the fetal alcohol syndrome: a mouse model” Journal of Anatomy 186:313–320.

Parson SH., Sojitra NM. (1995) “Loss of myelinated axons is specific to the central nervous system in a mouse model of the fetal alcohol syndrome” Journal of Anatomy 187:739–748.

Patel S., Marshall J., Fitzke FW. (1995) “Refractive index of the human corneal epithelium and stroma” Journal of Refractive Surgery 11(2): 100–105.

Peichl L., González-Soriano J. (1994) “Morphological types of horizontal cell in rodent retinae: a comparison of rat, mouse, gerbil, and guinea pig” Visual Neuroscience 11(3): 501–517.

Penn AA., Riquelme PA., Feller MB., Shatz CJ. (1998) “Competition in retinogeniculate patterning driven by spontaneous activity” Science 279(5359): 2108–2112.

Perez-Torrero E., Duran P., Granados P., Gutierrez-Ospina G., Cintra L., Diaz-Cintra S. (1997) “Effects of acute prenatal ethanol exposure on Bergmann glia cells early postnatal development” Brain Research 746: 305–308.

Perry VH., Walker M. (1980) “Amacrine cells, displaced amacrine cells and interplexiform cells in the retina of the rat” Proceedings the Royal Society London; Biological Sciences 208: 415–431.

Peters BN., Masland RH. (1996) “Responses to light of starburst amacrine cells” Journal of Neurophysiology 75(1): 469–480.

Phillips DE. (1989) “Effects of limited postnatal ethanol exposure on the development of myelin and nerve fibers in rat optic nerve” Experimental Neurology 103(1): 90–100.

Phillips DE., Krueger SK. (1990) “Effects of postnatal ethanol exposure on glial cell development in rat optic nerve” Experimental Neurology 107(1): 97–105.

Phillips DE., Krueger SK., Rydquist JE. (1991) “Short- and long-term effects of combined pre- and postnalal ethanol exposure (three trimester equivalency) on the development of myelin and axons in rat optic nerve” International Journal of Developmental Neuroscience 9: 631–647.

Phillips DE., Krueger SK. (1992) “Effects of combined pre- and postnatal ethanol exposure (three trimester equivalency) on glial cell development in rat optic nerve” International Journal of Developmental Neuroscience 10(3): 197–206.

Pie YF., Rhodin JA. (1970) “The prenatal development of the mouse eye” The anatomical record 168(1): 105–125.

Pierce DR., West JR. (1986) “Alcohol-induced microencephaly during the third trimester equivalent: relationship to dose and blood alcohol concentration” Alcohol 3(3): 185–191.

Pinazo-Duran MD., Renau-Piqueras J., Guerri C. (1993) “Developmental changes in the optic nerve related to ethanol consumption in pregnant rats: Analysis of the ethanol-exposed optic nerve” Teratology 48: 305–322.

Pinazo-Duran MD., Renau-Piqueras J., Guerri C., Strömland K. (1997) “Optic nerve hypoplasia in fetal alcohol syndrome: an update” European Journal of Ophthalmology 7(3): 262–270.

Polyak SL. (1941) “The Retina” University of Chicago Press, Chicago.

Prusky GT., West PW., Douglas RM. (2000) “Behavioral assessment of visual acuity in mice and rats” Vision Research 40 (16): 2201-2209.

Prusky GT., Harker KT., Douglas RM., Whishaw IQ. (2002) “Variation in visual acuity within pigmented, and between pigmented and albino rat strains” Behaviuoral Brain Research 136(2): 339–348.

Qiang M., Wang MW., Elberger AJ. (2002) “Second trimester prenatal alcohol exposure alters development of rat corpus callosum” Neurotoxicology and Teratology 24: 719–732.

Rachel RA., Dolen G., Hayes NL., Lu A., Erskine L., Nowankowski RS. Mason CA. (2002) “Spatiotemporal features of early neurongenesis differ in wild-type and albino mouse retina” Journal of Neuroscience 22: 4249–4263.

Rakic P. (1986) “Mechanism of ocular dominance segregation in the lateral geniculate nucleus: competitive elimination hypothesis” Trends in Neurosciences 8: 11–15.

Rapaport DH., Wong LL., Wood ED., Yasumura D., LaVail MM. (2004) “Timing and topography of cell genesis in the rat retina” Journal of Comparative Neurology 474: 304–324.

Reese BE. (1988) “'Hidden lamination' in the dorsal lateral geniculate nucleus: the functional organization of this thalamic region in the rat” Brain Research 472(2): 119–137.

Ribeiro IM., Vale PJ., Tenedorio PA., Rodrigues PA., Bilhoto MA., Pereira HC. (2007) “Ocular manifestations in fetal alcohol syndrome” European Journal of Ophthalmology 17(1): 104–109.

Rice D., Barone S Jr. (2000) “Critical periods of vulnerability for the developing nervous system: evidence from humans and animal models” Environmental Health Perspectives 108 (3): 511–533.

Riley EP., Mattson SN., Sowell ER., Jernigan TL., Sobel DF., Jones KL. (1995) "Abnormalities of the corpus callosum in children prenatally exposed to alcohol" Alcoholism: Clinical and Experimental Research 19(5): 1198–1202.

Riley EP., McGee CL. (2005) "Fetal alcohol spectrum disorders: an overview with emphasis on changes in brain and behavior" Experimental Biology and Medicine (Maywood) 230 (6): 357–365.

Robson JA., Mason CA., Guillery RW. (1978) "Terminal arbors of axons that have formed abnormal connections" Science 201: 635–637.

Rodieck RW., Watanabe M. (1993) "Survey of the morphology of macaque retinal ganglion cells that project to the pretectum, superior colliculus, and parvicellular laminae of the lateral geniculate nucleus" Journal of Comparative Neurology 338: 289–303.

Roorda A., Metha AB., Lennie P., Williams DR. (2001) "Packing arrangement of the three cone classes in primate retina" Vision Research 41: 1291–1306.

Rosett H. (1980) "A clinical perspective of the fetal alcohol syndrome" Alcoholism: Clinical and Experimental Research 4: 119–122.

Saha MS., Servetnick M., Grainger RM. (1992) "Vertebrate eye development" Current opinion in genetics and development 2 (4): 582–588.

Samoraski T., Lancaster F., Wiggins RC. (1986) "Fetal Ethanol Exposure: A Morphometric Analysis of Myelination in the Optic Nerve" International Journal of Developmental Neuroscience 4(4): 369–374.

Serbus DC., Young MW., Light KE. (1986) “Blood ethanol concentrations following intragastric intubation of neonatal rat pups” Neurobehavioral Toxicology and Teratology 8(4): 403–406.

Shatz CJ. (1990) “Competitive interactions between retinal ganglion cells during prenatal development” Journal of Neurobiology 21(1): 197–211.

Skrzypek J., Werblin FS. (1983) “Lateral interactions in absence of feedback to cones” Journal of Neurophysiology 49: 1007–1016.

Smith DE., Foundas A., Canale J. (1986) “Effect of perinatally administered ethanol on the development of the cerebellar granule cell” Experimental Neurology 92: 491–501.

So KF., Woo HH., Jen LS. (1982) “Effect on segregation of retinogeniculate projections in early unilaterally enucleated or dark reared hamsters” The Society for Neuroscience. Abstracts. 8, 816.

So KF., Campbell G., Lieberman AR. (1990) “Development of the mammalian retinogeniculate pathway: target finding, transient synapses and binocular segregation” The Journal of Experimental Biology 153: 85–104.

Stanfield BB. (1984) “Postnatal reorganization of cortical projections: the role of collateral elimination. Trends in Neurosciences 7: 37–41.

Stell WK., Lightfood DO., Wheeler TG., Leeper HF. (1975) “Goldfish retina: functional polarization of cone horizontal cell dendrites and synapses” Science 190(4218): 989–990.

Stepanyants A., Tama´s G., Chklovskii DB. (2004) “Class-specific features of neuronal wiring” Neuron 43: 251–259.

Stockard CR. (1910) “The influence of alcohol and other anæsthetics on embryonic development” American Journal of Anatomy 10(1): 369–392.

Stone J., Fukuda Y. (1974) “Properties of cat retinal ganglion cells: Comparison of W-cells with X- and Y-cells” Journal of Neurophysiology 37: 722–748.

Stratton K., Howe C., Battglia F. (1996) “Fetal alcohol syndrome: Diagnosis, epidemiology, prevention and treatment” National Academy Press, Washington, DC

Streissguth AP., Landesman-Dwyer S., Martin JC., Smith DW. (1980) “Teratogenic effects of alcohol in humans and laboratory animals” Science 209 (4454): 353–361.

Streissguth AP., Clarren SK., Jones KL. (1985) “Natural history of the fetal alcohol syndrome: a 10-year follow-up of eleven patients” Lancet 2(8446): 85–91.

Strömland K. (1982) “Eyeground malformations in the fetal alcohol syndrome” Birth defects original article series 18(6): 651–655.

Strömland K. (1985) “Ocular abnormalities in the fetal alcohol syndrome” Acta Ophthalmologica Supplement 171: 1–50.

Strömland K. (1987) “Ocular involvement in the fetal alcohol syndrome” Survey of Ophthalmology. 31(4): 277–284.

Strömland K. (1990) “Contribution of ocular examination to the diagnosis of foetal alcohol syndrome in mentally retarded children” Journal of Mental Deficiency Research 34 (5): 429–435.

Strömland K., Pinoza-Duran MD. (1994) “Optic nerve hypoplasia: Comparative effects in children and rats exposed to alcohol during pregnancy” Teratology 50: 100–111.

Strömland K., Hellström A. (1996) “Fetal alcohol syndrome– an ophthalmological and socioeducational prospective study” Pediatrics 97: 845–850.

Strömland K., Sundelin K. (1996) “Paediatric and ophthalmologic observations in offspring of alcohol abusing mothers” Acta Paediatrica 85(12): 1463–1468.

Strömland K., Pinoza-Duran MD. (2002) “Ophthalmic involvement in Fetal Alcohol Syndrome: Clinical and Animal model studies” Alcohol and Alcoholism 37(1): 2–8.

Strömland K. (2004) “Visual impairment and ocular abnormalities in children with fetal alcohol syndrome” Addiction Biology 9: 153–157.

Sulik KK., Johnston MC., Webb MA. (1981) “Fetal alcohol syndrome: embryogenesis in a mouse model” Science 214(4523): 936–938.

Sulik KK., Johnston MC. (1983) “Sequence of developmental alterations following acute ethanol exposure in mice: craniofacial features of the fetal alcohol syndrome” The American Journal of Anatomy 166(3): 257–269.

Sun W., Li N., He S. (2002a) “Large-scale morphological survey of rat retinal ganglion cells” Visual Neuroscience 19: 483–493.

Sun W., Li X., He S. (2002b) “Large-scale morphological survey of mouse retinal ganglion cells” Journal of Comparative Neurology 451: 115–126.

Szél A., Röhlich P., Caffé AR., Juliusson B., Aguirre G., Van Veen T. (1992) “Unique topographic separation of two spectral classes of cones in the mouse retina” Journal of Comparative Neurology: 325(3): 327–342.

Tachibana M., Kaneko A. (1987) “Gamma-aminobutyric acid exerts a local inhibitory action on the axon terminal of bipolar cells: Evidence for a negative feedback from amacrine cells” Proceedings of the National Academy of Sciences of the United States of America 84: 3501–3505.

Tenkova T., Young C., Dikranian K., Labruyere J., Olney JW. (2003) “Ethanol induced apoptosis in the developing visual system during synaptogenensis. Investigative Ophthalmology and Visual Science 44(7): 2809–2817.

Thomas JD., Goodlett CR., West JR. (1998) “Alcohol-induced Purkinje cell loss depends on developmental timing of alcohol exposure and correlates with motor performance” Developmental Psychobiology 29(5): 433–452.

Tran TD., Cronise K., Marino MD., Jenkins WJ., Kelly SJ. (2000) “Critical periods for the effects of alcohol exposure on brain weight, body weight, activity and investigation” Behavioural Brain Research 116: 99–110.

Tran TD., Kelly SJ. (2003) “Critical periods for ethanol-induced cell loss in the hippocampal formation” Neurotoxicology and Teratology 25: 519–528.

Trivino A., Ramirez JM., Ramirez AI., Salazar JJ., Garcia-Sanchez J. (1992) “Retinal perivascular astroglia: An immunoperoxidase study” Vision Research 32: 1601–1607.

Tufan AC., Abbana C., Akdogan I., Erdogan D., Ozogul C. (2007) "The effect of in ovo ethanol exposure on retina and optic nerve in a chick embryo model system" Reproductive Toxicology 23: 75–82.

Uzbay IT., Kayaalp SO. (1995) "A modified liquid diet of chronic ethanol administration: Validation by ethanol withdrawal syndrome in rats" Pharmacological Research 31 (1): 37–42.

Vasudevan B., Simpson TL., Sivak JG. (2008) "Regional variation in the refractive-index of the bovine and human cornea" Optometry and Vision Science 85(10): 977–981.

Vessey JP., Stratis AK., Daniels BA., Da Silva N., Jonz MG., Lalonde MR., Baldridge WH., Barnes S. (2005) "Proton-mediated feedback inhibition of presynaptic calcium channels at the cone photoreceptor synapse" The Journal of Neuroscience 25: 4108–4117.

Völgyi B., Chheda S., Bloomfield SA. (2009) "Tracer coupling patterns of the ganglion cell subtypes in the mouse retina" The Journal of Comparative Neurology 512(5): 664–687.

Waltman R., Iniquez ES. (1972) "Placental transfer of ethanol and its elimination at term" Obstetrics and Gynecology 40: 180–185.

Warren KR., Foudin LL. (2001) "Alcohol-related birth defects--the past, present, and future" Alcohol Research and Health: The Journal of the National Institute on Alcohol Abuse and Alcoholism 25(3): 153–158.

Wässle H., Boycott BB. (1991) "Functional architecture of the mammalian retina" Physiological Reviews 71: 447–480.

Wässle H. (2004) “Parallel processing in the mammalian retina” Nature *Reviews* Neuroscience 5: 747–757.

Wattendorf DJ., Muenke M. (2005) “Fetal Alcohol Spectrum Disorders” American Family Physician 72 (2): 279–285.

Web page of allaboutvision (available online at http://harcourtcarteroptical.com/pageselect.cfm?page=21, last access date: 07.02.11)

Web page of Center for Imaging Science (available online at http://www.cis.rit.edu/people/faculty/montag/vandplite/pages/chap_9/ch9p1.html, last access date: 07.02.11)

Web page of Olympus (available online at http://www.olympusmicro.com/primer/techniques/confocal/confocalintro.html, last access date: 07.02.11)

Web page of The Washington University School of Medicine Neuroscience Tutorial (available online at http://thalamus.wustl.edu/course/eyeret.html, last access date: 07.02.11

Web page of Translating Time Across Developing Mammalian Brain (available online at http://bioinformatics.ualr.edu/ttime/, last access date: 07.02.11)

Weinstock M. (2001) “Alterations induced by gestational stress in brain morphology and behaviour of the offspring” Progress in Neurobiology 65(5): 427–451.

West JR., Hamre KM., Pierce DR. (1984) “Delay in brain growth induced by alcohol in artificially reared rat pups” Alcohol 1: 83–95.

West JR., Goodlett CR., Bonthius DJ., Pierce DR. (1989) “Manipulating peak blood alcohol concentrations in neonatal rats: Review of an animal model for alcohol-related developmental effects” Neurotoxicology 10(3): 347–365.

West MJ., Slomianka L., Gundersen HJ. (1991) “Unbiased stereological estimation of the total number of neurons in thesubdivisions of the rat hippocampus using the optical fractionator” The Anatomical Record 231(4): 482–497.

Whitcher LT., Klintsova AY. (2008) “Postnatal binge-like alcohol exposure reduces spine density without affecting dendritic morphology in rat mPFC” Synapse 62(8): 566–573.

Wiesenfeld Z., Branchek T. (1976) “Refractive state and visual acuity in the hooded rat” Vision Research 16(8): 823–827.

Williams RW., Rakic P. (1988) “Three-dimensional counting: an accurate and direct method to estimate numbers of cells in sectioned material” Journal of Comparative Neurology 278(3): 344–352.

Wingate RJT., Fitzgibbon T., Thompson ID. (1992) “Lucifer Yellow, retrograde tracers, and fractal analysis characterise adult ferret retinal ganglion cells” Journal of Comparative Neurology 323: 449–474.

Witkovsky P. (2004) “Dopamine and retinal function” Documenta Ophthalmologica 108: 17–40.

Wong RL. (2006) “Introduction – from eye field to eyesight” In Sernagor E., Eglen S., Harris B., Wong RL (Eds.) Retinal development (pp. 1–7). Cambridge: Cambridge University Press.

Wong AA., Brown RE. (2006) “Visual detection, pattern discrimination and visual acuity in 14 strains of mice” Genes, Brain and Behavior 5(5): 389–403.

Wu SM. (1992) “Feedback connections and operation of the outer plexiform layer of the retina” Current Opinion in Neurobiology 2: 462–468.

Yanni PA., Lindsley TA. (2000) “Ethanol inhibits development of dendrites and synapses in rat hippocampal pyramidal neuron cultures” Developmental Brain Research 120(2): 233–243.

Young RW. (1985) “Cell differentiation in the retina of the mouse” The Anatomical Record 212: 199–205.

Zhang H., Li YC., Young AP. (1993) “Protein kinase A activation of glucocorticoid-mediated signaling in the developing retina” Proceedings of the National Academy of Sciences of the U S A 90(9): 3880–3884.

Ziburkus J., Guido W. (2006) “Loss of binocular responses and reduced retinal convergence during the period of retinogeniculate axon segregation” Journal of Neurophysiology 96(5): 2775–2784.

CURRICULUM VITAE

Name & Surname: İlknur Dursun
Nationality: Turkish (TC)
Date and Place of Birth: 14.04.1978 Pülümür-Tunceli/Turkey
Phone: +90 532 747 31 05
e-mail: ilknur_dursun@yahoo.com
Foreign Languages: English

EDUCATION

Degree	Institution	Graduation
Ph.D.	METU Dept.of Biological Sci.	2011
M.Sc.	METU Dept.of Biological Sci.	2005
B.Sc.	Ankara Uni. Biology Dept.	2000
High School	Semiha Şakir Lisesi, İstanbul	1995

EXPERIENCE

Division of Medical Genetics, Child Health Institute, Istanbul Uni. Istanbul, Turkey (October 2000-August 2001).

Research Assistant at Department of Biological Sciences, METU (2002-present)

Research Assistant at Neurophysiology Research Laboratory, METU (2002- present)

Teaching Assistantship Animal Physiology Laboratory, METU (2003-2009)

IBRO Neuroscience Course, Ege University, Izmir, Turkey (September 10-18, 2003)

Third Ege Biennial International Neuroscience Graduate Summer School, Ege University Faculty of Medicine and Center for Brain Research , Izmir, Turkey (July 5-9, 2004)

Louisiana State University, Health Science Center, Department of Cell Biology and Anatomy, Short Term Scholar in Dr. William Guido Laboratory (July 4 - September 1, 2005)

Eight National Stereology Course, Baskent University, Ankara, Turkey **(**September 14-17 2005**)**

Noldus- Ethovision 3.1 Software User Training Meeting, Ankara, Turkey (April 2006)

Visiting Researcher University of California, Davis, Department of Department of Neurobiology, Physiology, and Behavior & Center for Neuroscience (March 5 2007-July 7 2008)

Visiting Researcher University of California, Davis, Center for Neuroscience (June 25–August 16 2009)

BIO 112, BIO 501 and BIO 601 "Seminars in Biology for Freshman and Graduate Students" Assistanship (2009-2011)

FENS-IBRO Open Format School, "Looking back at Mount Ararat: Diversity and Cross-Fertilization among Approaches to Memory," took place April 5-10, 2010, in Yerevan, Armenia (April 5-10 2010)

CONGRESS PRESENTATIONS

Can B., **Dursun I.,** Uysal A.K., Canan S., Jakubowska-Dogru E., Investigation of Morphological Regeneration in The Neonatal Rat Hippocampus After Fetal Alcohol Administration, 7th FENS Forum of European of Neuroscience, FENS Abstr., vol.5, 115.19, July 2010.

Elibol-Can B., **Dursun I.,** Uysal A.K., Canan S., Jakubowska-Dogru E., The Effects of Prenatal Exposure to Ethanol on the Morphology of Developing Rat Hippocampus, 9th National Congress of Neuroscience, Turkish Journal of Neurology, 16(1), pp:239, İstanbul, April 2010.

I. Dursun, E. Jakubowska-Doğru, T. Uzbay. Prenatal Exposure to Alcohol Increases Neophobia But Does Not Affect Locomotor Activity, Motor Coordination And Memory in Rat Pups Tested as Young Adults. FENS-IBRO Open Format School,in Yerevan April 5-10,2010

I. Dursun, E., Jakubowska-Doğru, L.M.Chalupa, R.F.Berman, "Effects of Postnatal Alcohol Exposure on Developing the Dorsal Lateral Genıculate Nucleus (dLGN) in the C57bl/6 Mice" 32nd Annual Scientific Meeting of the Research Society on Alcoholism, Alcoholism Clinical & Experimental Research, June 2009, vol: 33(6), pp:165A

I. Dursun, B. Elibol , Jakubowska-Doğru E, T. Uzbay "Confounding Factors, Gender and Age, in The Research of Fetal Ethanol Effects On Animal Behavior" 32nd Annual Scientific Meeting of the Research Society on Alcoholism, Alcoholism Clinical & Experimental Research, June 2009, vol: 33(6), pp:35A

I. Dursun, B. Elibol , T. Uzbay , Jakubowska-Doğru E, "Animal's Gender And Age At Testing Are Critical Factors In Evaluation Of Fetal Ethanol Effects On Behavior" 8th National Congress of Neuroscience. Bolu – Turkey, April 2009,pp:185-186.

Dursun I. "Effects of early postnatal alcohol intoxication on retina ganglion cell morphology" Neuroscience Workshop on the Effects of Perinatal and Adult Ethanol Intake on Brain and Behavior in Animal Models Oct 20-21 2008 METU, Ankara Oral Presentation

Dursun I., E. Jakubowska-Doğru, "Effects of fetal alcohol on learning and memory are gender, age, and strain dependent." 13th World Congress of Psychophysiology, The Olympics of the Brain, Istanbul, Aug.-Sept. 2006 International Journal of Psychophysiology Abstract Book Volume 61(3) P 351

Jakubowska-Doğru E., B. Elibol, **I. Dursun,** F. Severcan, "Effects of chronic alcohol intake and withdrawal on memory and brain protein and lipid profiles assessed by FT– IR technique in young adult Wistar rats.", The 5th International Congress of Pathophysiology, Beijing, China, Chinese J. Pathophysiol. 22: 437, July 2006.

Dursun I.; Jakubowska-Dogru E. Sex-related differences in spatial learning in juvenile rats after fetal alcohol exposure. The 5th National Congress of Neuroscience. Zonguldak-Turkey, April 2006, Neuroanatomy 5 Suppl. P.17

Jakubowska-Doğru E., **I. Dursun,** T. Uzbay, "Effects of prenatal alcohol exposure on activity, anxiety and learning in young adult Wistar rats." Polish Neuroscience Society 7th International Congress Krakow, Poland, September 7–10, 2005 Acta Neurobiol. Exp.Abstract Book 65(3):345,2005 P12.12(Poster Presentation)

Jakubowska-Doğru E., **I. Dursun,** T. Uzbay, „Effects of prenatal alcohol exposure on activity, anxiety and learning in young adult Wistar rats." 4th National Congress of Neuroscience, Mersin, Turkey, March 2005, Neuroanatomy Abstract Book P22. (Poster Presentation)

PUBLICATION

I. Dursun, E. Jakubowska-Doğru**,** T. Uzbay "Effects of prenatal alcohol exposure on activity, anxiety, and memory in young adult Wistar rats." Pharmacology, Biochemistry and Behavior 2006 Oct 85(2):345-55.

I. Dursun, E. Jakubowska-Doğru, "Effects of prenatal alcohol exposure in young adult Wistar rats; impact on activity, anxiety, and memory" Lambert Academic Publishing 2010 (ISBN 978-3-8383-7058-3)

Dursun I., Jakubowska-Doğru E., van der List D., Liets LC., Coombs JL., Berman RF. "Effects of early postnatal exposure to ethanol on retina ganglion cell morphology and numbers of neurons in the dorsolateral geniculate in mice" Submitted to Alcoholism: Clinical and Experimental Research

AWARDS

Travel Award, 32nd Annual Scientific Meeting of the Research Society on Alcoholism in San Diego June 20-24

Travel Award, FENS-IBRO Open Format School, "Looking back at Mount Ararat: Diversity and Cross-Fertilization among Approaches to Memory" in Yerevan, April 5-10, 2010

RESEARCH PROJECTS

2007-2008 "The effects of early postnatal ethanol intoxication on retinal morphology, retino-geniculate projection and visual functions in mice" Supported by the National Eye Institute of the NIH EY003991 and P30EY12576 to. Prof.Dr.Leo M. Chalupa,UCDAVIS

2007-2010 "The investigation of potential regeneratory processes taking place during the postnatal period in fetal alcohol Wistar rats using stereology, morphometry and immunohistochemistry " supported by the grant from the Turkish Academy of Science SBAG 107S069 to Assoc. Prof. Dr. E. Jakubowska-Doğru, METU.

2005-2006 "Effects of chronic perinatal ethanol intoxication on learning and memory in young Wistar rats." Research Funding -08-11-DPT-2002K120510-TB-6 to Assoc. Prof.Dr. E. Jakubowska-Doğru, METU

2002-2004 "Treatment of deleterious behavioural effects induced by prenatal exposure to ethanol by chronic NGF administration." supported by the grant from the Turkish Academy of Science to TBAG – 2177 (102T064) Assoc. Prof. Dr. E. Jakubowska-Doğru, METU.